FAST ALGORITHMS FOR BIHARMONIC PROBLEMS AND APPLICATIONS TO FLUID DYNAMICS

A Dissertation

by

ADITI GHOSH

Submitted to the Office of Graduate and Professional Studies of
Texas A&M University
in partial fulfillment of the requirements for the degree of

DOCTOR OF PHILOSOPHY

Chair of Committee,	Prabir Daripa
Committee Members,	Stephen Fulling
	Francis Narcowich
	Vivek Sarin
Department Head,	Emil Straube

June 2013

Major Subject: Mathematics

ABSTRACT

Many areas of physics, engineering and applied mathematics require solutions of inhomogeneous biharmonic problems. For example, various problems on Stokes flow and elasticity can be cast into biharmonic boundary value problems. Hence the slow viscous flow problems are generally modeled using biharmonic boundary value problems which have widespread applications in many areas of industrial problems such as flow of molten metals, flow of particulate suspensions in bio-fluid dynamics, just to mention a few. In this dissertation, we derive, implement, validate, and apply fast and high order accurate algorithms to solve Poisson problems and inhomogeneous biharmonic problems in the interior of a unit disc in the complex plane.

In particular, we use two methods to solve inhomogeneous biharmonic problems: (i) the double-Poisson method which is based on transforming biharmonic problems into solving a sequence of Poisson problems (sometime also one homogeneous biharmonic problem) and then making use of the fast Poisson solver developed in this dissertation.; (ii) the direct method which uses the fast biharmoninc solver also developed in this dissertation. Both of these methods are analyzed for accuracy, complexity and efficiency. These biharmonic solvers have been compared with each other and have been applied to solve several Stokes flow problems and elasticity problems.

The fast Poisson algorithm is derived here from exact analysis of the Green's function formulation in the complex plane. This algorithm is essentially a recast of the fast Poisson algorithm of Borges and Daripa from the real plane to the complex plane. The fast biharmonic algorithms for several boundary conditions for use in the direct method mentioned above have been derived in this dissertation from

exact analysis of the representation of their solutions in terms of problem specific Green's function in the complex plane. The resulting algorithms primarily use fast Fourier transforms and recursive relations in Fourier space. The algorithms have been analyzed for their accuracy, complexity, efficiency, and subsequently tested for validity against several benchmark test problems. These algorithms have an asymptotic complexity of $\mathcal{O}(\log \mathcal{N})$ per degree of freedom with very low constant which is hidden behind the order estimate. The direct and double-Poisson methods have been applied to solving the steady, incompressible slow viscous flow problem in a circular cylinder and some problems from elasticity. The numerical results from these computations agree well with existing results on these problems.

DEDICATION

To my grandmother and my family.

ACKNOWLEDGEMENTS

LIST OF FIGURES

x

1. INTRODUCTION

The biharmonic equation arises in many fields of classical physics including complex mechanical and physical processes involving solids and fluids. For example, its applications include problems of clamped plate in elasticity, slow viscous flow of an incompressible fluid, flow of particulate suspension and bio-fluid dynamics (see [38], [25], [28]). We focus in this thesis on the inhomogeneous biharmonic equation in the complex plane inside a unit disc for several boundary conditions (see [8], [7], [6]) and its application.

We develop here fast algorithms for solving several biharmonic problems using two different methods. Both of these methods require evaluation of domain integrals involving singular integrands primarily due to Green's functions and the inhomogeneous terms of the inhomogeneous biharmonic equations. Standard quadrature methods of evaluation of these integrals result in limited accuracy and have asymptotic algorithmic complexity $\mathcal{O}(N^2)$ per degree of freedom where N is the number number of degrees of freedom. This results in prohibitive computational cost for problems of large size. In order to improve upon this complexity we develop algorithms based on the use of FFT and some recursive relations derived from exact analysis. These new algorithms have asymptotic computational complexity $\mathcal{O}(\log N)$ per degree of freedom and are also very accurate. Similar algorithms have been developed before by Daripa et. al (see([12], [15], [18])) for solving other kinds of elliptic equations. For a review of these algorithms and some of their applications see Daripa [17].

To evaluate the associated domain integrals, we first expand them in terms of Fourier series. After some analysis, we express the radius dependent Fourier coef-

ficients of the integrals (see [12],[15]) as one dimensional integrals with integrands depending on the Fourier coefficients of the inhomogeneous term of the inhomogeneous biharmonic equation. These one-dimensional integrals involve integration in the radial direction of the domain. As shown in this thesis, these one-dimensional integrals bear some recursive relations which are at the heart of the low computational cost of the full algorithm for solving these inhomogeneous biharmonic equations. To summarize,

(C.1) The fast algorithms are derived from exact analysis and properties of convolution integrals involving Green's function.

(C.2) The algorithms are easily parallelizable (see [10]).

(C.3) It is easy to implement these algorithms.

(C.4) Weak singularity in the inhomogeneous term can be easily taken care of without losing order of accuracy.

(C.5) The recursive relations allow one to define higher order integration methods in the radial direction without the inclusion of additional grid points.

The extensive theory of biharmonic problems based on complex variables in [7, 4, 5, 2, 6, 3, 9, 1, 32] has laid the analytic foundation of these fast algorithms. We solve here four important boundary value problems for the biharmonic equation using the Green's function method. Apart from using Simpson and Trapezoidal rules to compute the integrals, we also use the Euler-Maclaurin expansion for Trapezoidal approximation for higher order accuracy as in [39]. Although the direct approach (to be discussed later) for numerical solution of the biharmonic problems within a unit disc has been the thrust of this thesis, we also have developed a second approach which involves decomposition of these boundary value problems into two Poisson

2

problems and then making use of similar fast algorithms for equations. Thus some sections of this thesis focus on fast algorithms to solve Poisson problems in a unit disc in the complex plane. Numerical results for both these approaches are provided in this thesis.

There has been extensive research on the numerical solution of biharmonic problems in the real plane by various methods such as finite difference/finite element methods ([35], [13],[34], [14]) and integral equation methods (see([31], [22], [25], [28], [24])). The major difficulties associated with the finite difference and finite element methods are poor convergence rate and condition number proportional to N^4 for N^2 degrees of freedom in the domain. Thus these methods are computationally expensive and less accurate. The boundary integral methods usually based on first or second kind integral equations. The first kind integral equations are often ill posed and the very high condition number of the resulting linear system poses difficulty for constructing an efficient algorithm. The second kind integral equation most commonly used in the potential theory has been widely discussed in [31],[21],[22].

Our method differs from them in that it is analysis based and thus very accurate. It is also very fast and parallelizable by construction. We focus on four types of boundary value problems (D1), (D2), (D3), (D4) defined in sections to follow. We solve them using both the direct and the double Poisson methods. The errors in the actual implementation of these algorithm arise primarily from the numerical evaluation of one dimensional integrals and the use of FFT (truncation of the Fourier series).

We give a brief outline of the thesis in the following way. Section 2 describes the fast algorithm to solve the Poisson problems in the complex plane in a unit disc. This problem in the real plane has been treated in Borges & Daripa [12] and thus this section is very similar to their work. Numerical solutions to several Poisson problems

in the complex plane have been obtained in this section. This algorithm will be used later to solve biharmonic problems by the method of double Poisson problems.

Section 3 contains the (D1) biharmonic problem and its solution. We discuss the analytical foundation of the direct method in detail and outline the double Poisson method towards the end of this section.

Section 4 and Section 5 discuss the (D2),(D3),(D4) biharmonic problems and the mathematical foundation of the direct method. It also validates the method with an example.

Section 6 builds the recursive relations for the singular integrals associated with the Green's function method for solving the biharmonic problems and thus paves the way for the development of fast algorithms in this so-called direct approach.

Section 7 outlines the quadrature method briefly and focuses further on some aspects of fast algorithms for the biharmonic problems. It also contains the results on computational complexity of these algorithms.

Section 8 deals with biharmonic problems in an annular domain and Section 9 deals with application to steady, incompressible flow in two-dimension with low and moderate Reynolds number. Validation and numerical implementation of the algorithms have been performed in Section 10. We end this section by estimating error in the evaluation of the singular integrals using the Euler-Maclaurin formula of integration in 11 and finally conclude in Section 12.

2. THEORETICAL FOUNDATION FOR THE POISSON PROBLEM

We consider here several biharmonic problems in a unit disc in the complex plane and explore different methods using associated Green's function to solve some of these problems. Before considering the biharmonic problems we first focus on Dirichlet and Neumann problems for the Poisson equation in a unit disc $\mathbf{D}$ in the complex plane. In this section, we lay the mathematical foundation for an efficient fast algorithm to solve inhomogeneous biharmonic problems in $\mathbf{D}$ (see [8],[7],[2]). We first consider the Poisson equation with Dirichlet boundary conditions.

2.1 The Dirichlet Problem

The Dirichlet problem for the Poisson equation in a unit disc $\mathbf{D}$ in the complex plane is given by

$$\partial_z \partial_{\bar{z}} \omega = f \quad \text{in} \quad \mathbf{D}, \quad \omega = \gamma \quad \text{on} \quad \partial \mathbf{D} \tag{P1}$$

This problem is uniquely solvable for $f \in L_1(\mathbf{D}, \mathbb{C}), \gamma \in C(\partial \mathbf{D}; \mathbb{C})$ (see [7]). If u is the solution of the homogeneous problem,

$$\partial_z \partial_{\bar{z}} u = 0 \quad \text{in} \quad \mathbf{D}, \quad u = \gamma - v \quad \text{in} \quad \partial \mathbf{D}, \tag{2.1}$$

where v satisfies the equation

$$\partial_z \partial_{\bar{z}} v = f, \tag{2.2}$$

then the solution of problem (P1) is given by

$$\omega = u + v.$$

A principal solution of (2.2) is obtained using the standard Green's function method (see[2],[12],[23]) and can be written as

$$v(z) = 4 \iint\limits_{\mathbf{D}} G(z, \zeta) f(\zeta) d\xi d\eta, \tag{2.3}$$

where

$$G(z, \zeta) = \frac{1}{2\pi} \log |\zeta - z|$$

is the Green's function for the Poisson equation. Note here that f is a function of ζ and $\bar{\zeta}$. We introduce the following notations below.:

$$
\begin{aligned}
B(\sigma, r) &= \{z \in \mathbb{C} : |z - \sigma| < r\}, \\
\bar{B}(\sigma, r) &= \{z \in \mathbb{C} : |z - \sigma| \le r\}, \\
\Omega_0^r &= B(0, r), \\
\Omega_{r-\epsilon}^{r+\epsilon} &= B(0, r + \epsilon) - B(0, r - \epsilon), \\
\check{\Omega}_{r-\epsilon}^{r+\epsilon} &= \Omega_{r-\epsilon}^{r+\epsilon} - B(z, \epsilon).
\end{aligned}
$$

Hence,

$$
\begin{aligned}
v(z) &= \frac{2}{\pi} \iint_{\mathbf{D}} \log|\zeta - z| f(\zeta) d\xi d\eta \\
&= \frac{2}{\pi} \lim_{\epsilon \to 0} \iint_{\mathbf{D}-B(z,\epsilon)} \log|\zeta - z| f(\zeta) d\xi d\eta \\
&= \frac{2}{\pi} \lim_{\epsilon \to 0} \iint_{\Omega_0^{r-\epsilon}} \log|\zeta - z| f(\zeta) d\xi d\eta + \frac{2}{\pi} \lim_{\epsilon \to 0} \iint_{\check{\Omega}_{r-\epsilon}^{r+\epsilon}} \log|\zeta - z| f(\zeta) d\xi d\eta \\
&+ \frac{2}{\pi} \lim_{\epsilon \to 0} \iint_{\Omega_{r+\epsilon}^1} \log|\zeta - z| f(\zeta) d\xi d\eta.
\end{aligned}
$$

Now we see if

$$
I^\epsilon = \frac{2}{\pi} \iint_{\check{\Omega}_{r-\epsilon}^{r+\epsilon}} \log|\zeta - z| f(\zeta) d\xi d\eta,
$$

then

$$
\begin{aligned}
|I^\epsilon| &\le \frac{2}{\pi} \sup_{\zeta \in \check{\Omega}_{r-\epsilon}^{r+\epsilon}} \left(|f(\zeta) \log|\zeta - z|| \right) \left(\pi(r+\epsilon)^2 - \pi(r-\epsilon)^2 \right) \\
&\le -8 \sup_{\zeta \in \check{\Omega}_{r-\epsilon}^{r+\epsilon}} |f(\zeta)| \epsilon \log \epsilon
\end{aligned}
$$

We obtain $\frac{2}{\pi} \lim_{\epsilon \to 0} \iint_{\check{\Omega}_{r-\epsilon}^{r+\epsilon}} \log|\zeta - z| f(\zeta) d\xi d\eta = 0$. We derive here fast numerical algorithms to compute the solution of the Poisson equation in $\mathbf{D}$. For a similar algorithm in the real plane see [12]. Use of quadrature method results in limited accuracy and is computationally expensive. For a N^2 set of grid points the complexity is $\mathcal{O}(N^4)$ which is computationally very expensive when N is very large. In order to improve upon this, we develop a method which uses Fourier coefficients and recursive

relations in Fourier space and reduces the complexity to $\mathcal{O}(\log N)$ per point from N^2 per point. We expand $\omega(.)$ in terms of Fourier series and derive the Fourier coefficients of the associated singular integrals in terms of recursive relations utilizing one dimensional integrals in the radial direction. To demonstrate this, we evaluate the singular integral $v(z = re^{i\alpha}); \quad 0 < \alpha \le 2\pi$. The Fourier coefficients $v_n(r)$ of $v(z = re^{i\alpha})$ are given by

$$
v_n(r) = \frac{1}{\pi^2} \lim_{\epsilon \to 0} \int_0^{2\pi} e^{-in\alpha} \iint_{\Omega_0^{r-\epsilon}} \log|\zeta - z| f(\zeta) d\xi d\eta d\alpha
$$

$$
+ \frac{1}{\pi^2} \lim_{\epsilon \to 0} \int_0^{2\pi} e^{-in\alpha} \iint_{\Omega_{r+\epsilon}^1} \log|\zeta - z| f(\zeta) d\xi d\eta d\alpha \tag{2.4}
$$

Then it follows that

$$
v_n(r) = \iint_{\Omega_0^r} f(\zeta) Q_n(r, \zeta) d\xi d\eta + \iint_{\Omega_r^1} f(\zeta) Q_n(r, \zeta) d\xi d\eta, \tag{2.5}
$$

where

$$
Q_n(r, \zeta) = \frac{1}{\pi^2} \int_0^{2\pi} e^{-in\alpha} \log|\zeta - z| d\alpha. \tag{2.6}
$$

Let $z = re^{i\alpha}$, $\quad \zeta = \rho e^{i\theta}$, $\quad x = \frac{\rho}{r}e^{-i\tau}$ for $r > \rho$ and $\eta = \frac{\rho}{r}e^{i\tau}$ for $r < \rho$. Then

$$
\begin{aligned}
\log|\zeta - z| &= \frac{1}{2}\log|\zeta - z|^2 \\
&= \log\left|r^2 + \rho^2 - 2r\cos(\tau)\right|^{\frac{1}{2}} \\
&= \log\left|r^2\left(1 + \frac{\rho^2}{r^2} - 2\frac{\rho}{r}\cos(\tau)\right)\right|^{\frac{1}{2}} \\
&= \log\left|r^2\left(1 + \frac{\rho^2}{r^2} - \frac{\rho}{r}(e^{i\tau} + e^{-i\tau})\right)\right|^{\frac{1}{2}} \\
&= \log r + \log|1 - x| \\
&= \log r - \sum_{n\neq 0}\left(\frac{\rho}{r}\right)^{|n|}\frac{1}{2|n|}e^{in\tau}, \qquad \text{if } r > \rho.
\end{aligned}
$$

Similarly for $r < \rho$ we have

$$
\log|\zeta - z| = \log\rho - \sum_{n\neq 0}\left(\frac{r}{\rho}\right)^{|n|}\frac{1}{2|n|}e^{in\tau}, \qquad \text{if } r < \rho.
$$

Simple analysis shows that for $r > \rho$ we have

$$
\begin{aligned}
Q_n(r,\zeta) &= \frac{1}{\pi^2}\int_0^{2\pi} e^{-in\alpha}\left(\log r - \sum_{m\neq 0}\left(\frac{\rho}{r}\right)^{|m|}\frac{1}{2|m|}e^{im\tau}\right)d\alpha \\
&= \frac{1}{\pi^2}\int_0^{2\pi} e^{-in\alpha}\left(\log r - \sum_{m\neq 0}\left(\frac{\rho}{r}\right)^{|m|}\frac{1}{2|m|}e^{im(\alpha-\theta)}\right)d\alpha \\
&= \frac{1}{\pi^2}\int_0^{2\pi} e^{-in\alpha}\log r\, d\alpha - \frac{1}{\pi^2}\sum_{m\neq 0}\left(\frac{\rho}{r}\right)^{|m|}\frac{1}{2|m|}e^{-im\theta}\int_0^{2\pi} e^{i(m-n)\alpha}d\alpha.
\end{aligned}
$$

Hence for $r > \rho$ we have

$$
Q_n(r,\zeta) = \begin{cases} -\frac{1}{\pi|n|}\left(\frac{\rho}{r}\right)^{|n|}e^{-in\theta}, & \text{if } n \neq 0, \\[2mm] \frac{2}{\pi}\log r, & \text{if } n = 0. \end{cases}
$$

Similarly for $r < \rho$ we have

9

$$Q_n(r,\zeta) = \begin{cases} -\frac{1}{\pi|n|}\left(\frac{r}{\rho}\right)^{|n|} e^{-in\theta}, & \text{if } n \neq 0, \\ \frac{2}{\pi}\log\rho, & \text{if } n = 0. \end{cases}$$

For $n > 0$ we have

$$\iint\limits_{\mathbf{D}} f(\zeta)Q_n(r,\zeta)d\xi d\eta = \iint\limits_{\Omega_0^r} f(\zeta)Q_n(r,\zeta)d\xi d\eta + \iint\limits_{\Omega_r^1} f(\zeta)Q_n(r,\zeta)d\xi d\eta$$

$$= -\iint\limits_{\Omega_0^r} f(\zeta)\left(\left(\frac{\rho}{r}\right)^n \frac{1}{\pi n}e^{-in\theta}\right)d\xi d\eta$$

$$-\iint\limits_{\Omega_r^1} f(\zeta)\left(\left(\frac{r}{\rho}\right)^n \frac{1}{\pi n}e^{-in\theta}\right)d\xi d\eta$$

$$= -\frac{1}{\pi n}\int\limits_0^r\int\limits_0^{2\pi} f(\rho e^{i\theta})\left(\frac{\rho}{r}\right)^n e^{-in\theta}\rho d\theta d\rho$$

$$-\frac{1}{\pi n}\int\limits_r^1\int\limits_0^{2\pi} f(\rho e^{i\theta})\left(\frac{r}{\rho}\right)^n e^{-in\theta}\rho d\theta d\rho$$

$$= -\frac{1}{\pi n}\int\limits_0^r\int\limits_0^{2\pi}\sum_{m=-\infty}^{\infty} f_m(\rho)e^{im\theta}\left(\frac{\rho}{r}\right)^n e^{-in\theta}\rho d\theta d\rho$$

$$-\frac{1}{\pi n}\int\limits_r^1\int\limits_0^{2\pi}\sum_{m=-\infty}^{\infty} f_m(\rho)e^{im\theta}\left(\frac{r}{\rho}\right)^n e^{-in\theta}\rho d\theta d\rho$$

$$= -\frac{1}{\pi n}\int\limits_0^r\left(\frac{\rho}{r}\right)^n \rho \sum_{m=-\infty}^{\infty} f_m(\rho)\int\limits_0^{2\pi} e^{i(m-n)\theta}d\theta d\rho$$

$$-\frac{1}{\pi n}\int\limits_r^1\left(\frac{r}{\rho}\right)^n \rho \sum_{m=-\infty}^{\infty} f_m(\rho)\int\limits_0^{2\pi} e^{i(m-n)\theta}d\theta d\rho$$

$$= -2\int\limits_0^r\left(\frac{\rho}{r}\right)^n \frac{\rho}{n}f_n(\rho)d\rho - 2\int\limits_r^1\left(\frac{r}{\rho}\right)^n \frac{\rho}{n}f_n(\rho)d\rho. \qquad (2.7)$$

10

Similar calculation for $n < 0$ yields

$$
\iint\limits_{D} f(\zeta) Q_n(r, \zeta) d\xi d\eta = \frac{1}{\pi n} \int\limits_{0}^{r} \int\limits_{0}^{2\pi} f(\rho e^{i\theta}) \left(\frac{\rho}{r}\right)^{-n} e^{-in\theta} \rho d\rho d\theta
$$

$$
+ \frac{1}{\pi n} \int\limits_{r}^{1} \int\limits_{0}^{2\pi} f(\rho e^{i\theta}) \left(\frac{r}{\rho}\right)^{-n} e^{-in\theta} \rho d\rho d\theta
$$

$$
= \frac{1}{\pi n} \int\limits_{0}^{r} \int\limits_{0}^{2\pi} \sum_{m=-\infty}^{\infty} f_m(\rho) e^{im\theta} \left(\frac{\rho}{r}\right)^{-n} e^{-in\theta} \rho d\rho d\theta
$$

$$
+ \frac{1}{\pi n} \int\limits_{r}^{1} \int\limits_{0}^{2\pi} \sum_{m=-\infty}^{\infty} f_m(\rho) e^{im\theta} \left(\frac{r}{\rho}\right)^{-n} e^{-in\theta} \rho d\rho d\theta
$$

$$
= \frac{1}{\pi n} \int\limits_{0}^{r} \left(\frac{r}{\rho}\right)^{n} \rho \sum_{m=-\infty}^{\infty} f_m(\rho) \int\limits_{0}^{2\pi} e^{i(m-n)\theta} d\theta d\rho
$$

$$
+ \frac{1}{\pi n} \int\limits_{r}^{1} \left(\frac{\rho}{r}\right)^{n} \rho \sum_{m=-\infty}^{\infty} f_m(\rho) \int\limits_{0}^{2\pi} e^{i(m-n)\theta} d\theta d\rho
$$

$$
= 2 \int\limits_{0}^{r} \left(\frac{r}{\rho}\right)^{n} \frac{\rho}{n} f_n(\rho) d\rho + 2 \int\limits_{r}^{1} \left(\frac{\rho}{r}\right)^{n} \frac{\rho}{n} f_n(\rho) d\rho. \qquad (2.8)
$$

Similarly for $n = 0$ we have

$$
v_n(r) = 4 \int\limits_{0}^{r} \rho \log r f_0(\rho) d\rho + 4 \int\limits_{r}^{1} \rho \log \rho f_0(\rho) d\rho. \qquad (2.9)
$$

Therefore the Fourier coefficients of $v(z)$ are given by

$$
v_n(r) = \begin{cases} 4 \int_0^r \rho \log r f_0(\rho) d\rho + 4 \int_r^1 \rho \log \rho f_0(\rho) d\rho, & \text{if } n = 0, \\[2mm] -2 \int_0^r \left(\frac{\rho}{r}\right)^n \frac{\rho}{n} f_n(\rho) d\rho - 2 \int_r^1 \left(\frac{r}{\rho}\right)^n \frac{\rho}{n} f_n(\rho) d\rho, & \text{if } n > 0, \\[2mm] 2 \int_0^r \left(\frac{r}{\rho}\right)^n \frac{\rho}{n} f_n(\rho) d\rho + 2 \int_r^1 \left(\frac{\rho}{r}\right)^n \frac{\rho}{n} f_n(\rho) d\rho, & \text{if } n < 0. \end{cases}
$$

11

The solution $u(z = re^{i\alpha})$ of the homogeneous problem (P1) is given by

$$u(r, \alpha) = \frac{1}{2\pi} \int\limits_0^{2\pi} \phi(\theta) K(r, \alpha - \theta) d\theta,$$

where

$$\phi(\theta) = \gamma(\theta) - v(\theta) \quad \text{on} \ \ \partial\mathbf{D}.$$

The Poisson Kernel $K(\rho, \theta)$ for $\zeta = \rho e^{i\theta}$ (see[23]) is given by

$$
\begin{aligned}
K(\rho, \theta) &= \frac{1 - \rho^2}{1 + \rho^2 - 2\rho \cos\theta} \qquad 0 \le \rho \le 1, \\
&= \frac{1 - \rho^2}{(1 - \rho \cos\theta)^2 + (\rho \sin\theta)^2}, \\
&= \frac{1 - |\zeta|^2}{|1 - \zeta|^2}, \\
&= \frac{1 - \zeta\bar{\zeta}}{(1 - \zeta)(1 - \bar{\zeta})}, \\
&= Re\left(\frac{1 + \zeta}{1 - \zeta}\right), \\
&= Re\left(1 + 2(\zeta + \zeta^2 + ...)\right), \\
&= \sum_{n=-\infty}^{\infty} \rho^{|n|} e^{in\theta}.
\end{aligned}
$$

12

The Fourier coefficients $u_n(r)$ of $u(z)$ are given by,

$$
\begin{aligned}
u_n(r) &= \frac{1}{2\pi} \int_0^{2\pi} e^{-in\alpha} \left(\frac{1}{2\pi} \int_0^{2\pi} \phi(\theta) K(r, \alpha - \theta) \, d\theta \right) d\alpha \\
&= \frac{1}{2\pi} \int_0^{2\pi} \phi(\theta) \left(\frac{1}{2\pi} \int_0^{2\pi} K(r, \alpha - \theta) e^{-in(\alpha - \theta)} \, d\alpha \right) e^{-in\theta} \, d\theta \\
&= \frac{1}{2\pi} \int_0^{2\pi} K_n(r) e^{-in\theta} \, d\theta \\
&= K_n(r)\phi_n \\
&= r^{|n|}\phi_n,
\end{aligned}
$$

where ϕ_n are the Fourier coefficients of $\phi(\theta)$.

2.2   The Neumann Problem

We now consider the Poisson equation with Neumann boundary condition. We have the following theorem from [7].

Theorem 2.2.1. *The Neumann problem for the Poissoin equation in a unit disc is given by*

$$
\partial_z \partial_{\bar{z}} w = f \quad in \quad \mathbf{D}, \quad \partial_\nu w = g \quad on \quad \partial \mathbf{D} \tag{N1}
$$

$f \in L_1(\mathbf{D}; \mathbb{C}), \quad g \in (\partial \mathbf{D}; \mathbb{C}), \quad k \in \mathbb{C}, \quad \frac{1}{2\pi i} \int_{\partial \mathbf{D}} w(z)\frac{dz}{z} = k$ *is uniquely solvable if and only if*

$$
\frac{1}{4i} \int_{\partial \mathbf{D}} g(\zeta)\frac{d\zeta}{\zeta} = \int_{\mathbf{D}} f(\zeta) d\xi d\eta. \tag{2.10}
$$

13

The solution is given by

$$w(z) = k + \frac{1}{4\pi i} \int_{\partial \mathbf{D}} G_3(z,\zeta) g(\zeta) \frac{d\zeta}{\zeta} - \frac{1}{\pi} \int_{\mathbf{D}} G_3(z,\zeta) f(\zeta) d\xi d\eta, \qquad (2.11)$$

where

$$G_3(z,\zeta) = \log |(1 - z\bar{\zeta})(\zeta - z)|^{-2} \qquad (2.12)$$

is the Green function for the Neumann problem.

We expand $w(.)$ in terms of Fourier series and derive its Fourier coefficients in terms of one dimensional integrals in the radial direction.

Theorem 2.2.2. *Let $w(r,\alpha)$ is the solution of the Neumann problem in Thm. 2.2.1, $z = re^{i\alpha}$, $f(re^{i\alpha}) = \sum\limits_{n=-\infty}^{\infty} f_n(r)e^{in\alpha}$ and $g(e^{i\alpha}) = \sum\limits_{n=-\infty}^{\infty} g_n e^{in\alpha}$ then the Fourier coefficients $w_n(r)$ of $w(r,\alpha)$ can be written as*

$$w_n(r) = I_{1,n}^N(r) + I_{2,n}^N(r) + u_{1,n}^N(r),$$

where

$$I_{1,n}^N(r) = \begin{cases} -2 \int_0^1 f_n(\rho) \frac{(r\rho)^n}{n} \rho d\rho & \text{if } n > 0, \\[2mm] 2 \int_0^1 f_n(\rho) \frac{(r\rho)^{-n}}{n} \rho d\rho & \text{if } n < 0, \\[2mm] 0 & \text{if } n = 0, \end{cases}$$

$$I_{2,n}^N(r) = \begin{cases} -2 \left[\int_0^r f_n(\rho)(\frac{\rho}{r})^n \frac{\rho}{n} d\rho + \int_r^1 f_n(\rho)(\frac{r}{\rho})^n \frac{\rho}{n} d\rho \right] & \text{if } n > 0, \\[2mm] 2 \left[\int_r^0 f_n(\rho)(\frac{r}{\rho})^n \frac{\rho}{n} d\rho + \int_1^r f_n(\rho)(\frac{\rho}{r})^n \frac{\rho}{n} d\rho \right] & \text{if } n < 0, \\[2mm] 4 \left[\int_r^0 f_0(\rho)\rho \log r d\rho + \int_1^r f_0(\rho)\rho \log \rho d\rho \right] & \text{if } n = 0, \end{cases}$$

and

$$u_{1,n}^N(r) = \begin{cases} g_n \frac{r^{|n|}}{|n|} & \text{if } n \neq 0, \\[2mm] 0 & \text{if } n = 0. \end{cases}$$

Proof. Let $u(z) = u_1^N(z) + I_1^N(z) + I_2^N(z)$ where

$$u_1^N(z) = -\frac{1}{\pi i} \int_{\partial \mathbf{D}} \log|1 - z\bar{\zeta}| g(\zeta) \frac{d\zeta}{\zeta}, \tag{2.13}$$

$$I_1^N(z) = \frac{2}{\pi} \iint_{\mathbf{D}} \log|1 - z\bar{\zeta}| f(\zeta) d\xi d\eta, \tag{2.14}$$

$$I_2^N(z) = \frac{2}{\pi} \iint_{\mathbf{D}} \log|\zeta - z| f(\zeta) d\xi d\eta. \tag{2.15}$$

We recall that the singular integral $I_2^N(z)$ is same as $v(z)$. Hence we obtain the following,

$$I_{2,n}^N(r) = \begin{cases} -2\left[\int_0^r f_n(\rho)(\frac{\rho}{r})^n \frac{\rho}{n} d\rho + \int_r^1 f_n(\rho)(\frac{r}{\rho})^n \frac{\rho}{n} d\rho\right] & \text{if } n > 0, \\ 2\left[\int_r^0 f_n(\rho)(\frac{r}{\rho})^n \frac{\rho}{n} d\rho + \int_1^r f_n(\rho)(\frac{\rho}{r})^n \frac{\rho}{n} d\rho\right] & \text{if } n < 0, \\ 4\left[\int_r^0 f_0(\rho)\rho \log r d\rho + \int_1^r f_0(\rho)\rho \log \rho d\rho\right] & \text{if } n = 0. \end{cases}$$

Now we write $I_1^N(z) = \sum_{n=-\infty}^{\infty} I_{1,n}^N(r) e^{in\alpha}$ and evaluate $I_{1,n}^N(r)$ first. Let $\alpha - \theta = \tau$. Then,

$$\begin{aligned} I_{1,n}^N(r) &= \frac{1}{\pi^2} \iint_{\mathbf{D}} f(\zeta) \int_0^{2\pi} \log|1 - z\bar{\zeta}| e^{-in\alpha} d\alpha d\xi d\eta \\ &= \frac{1}{\pi^2} \int_0^1 \int_0^{2\pi} f(\rho, \theta) e^{-in\theta} \int_{-\theta}^{2\pi-\theta} \log|1 - z\bar{\zeta}| e^{-in\tau} \rho d\tau d\theta d\rho \\ &= -2 \int_0^1 f_n(\rho) G_{1,n}^{(1)}(r, \rho) \rho d\rho. \tag{2.16} \end{aligned}$$

where $f_n(r)$ are the Fourier coefficients of $f(z = re^{i\alpha})$ and

$$G_{1,n}^{(1)}(r, \rho) = \frac{1}{\pi^2} \int\limits_{-\theta}^{2\pi-\theta} \log|1 - z\bar\zeta|e^{-in\tau}d\tau$$

$$= -\frac{1}{\pi^2} \int\limits_{-\theta}^{2\pi-\theta} \left(\sum_{m\neq 0} \frac{(r\rho)^{|m|}}{2|m|}e^{im\tau}\right)e^{-in\tau}d\tau$$

$$= -\frac{1}{\pi^2} \sum_{n\neq 0} \frac{(r\rho)^{|n|}}{2|n|} \int\limits_{-\theta}^{2\pi-\theta} e^{i(m-n)\tau}d\tau$$

$$= -\frac{(r\rho)^{|n|}}{\pi|n|}, \qquad\qquad \text{if } n \neq 0. \qquad\qquad (2.17)$$

Hence substituting (2.17) in (2.16) we obtain,

$$I_{1,n}^N(r) = \begin{cases} -2\int_0^1 f_n \frac{(r\rho)^n}{n}\rho d\rho & \text{if } n > 0, \\[2mm] 2\int_0^1 f_n \frac{(r\rho)^{-n}}{n}\rho d\rho & \text{if } n < 0, \\[2mm] 0 & \text{if } n = 0. \end{cases}$$

Now for the boundary integral $u_1^N(z)$ we see,

$$\begin{aligned} u_1^N(z) &= -\frac{1}{\pi i}\int\limits_{\partial\mathbf{D}} \log|1 - z\bar\zeta|g(\zeta)\frac{d\zeta}{\zeta} \\[2mm] &= \frac{1}{\pi i}\int\limits_{\partial\mathbf{D}} \sum_{n\neq 0} \frac{|z\bar\zeta|^{|n|}}{2|n|}e^{in(\alpha-\theta)}g(e^{i\theta})\frac{d\zeta}{\zeta} \\[2mm] &= \frac{1}{\pi}\int\limits_0^{2\pi} \sum_{n\neq 0} \frac{r^{|n|}}{2|n|}g(e^{i\theta})e^{in(\alpha-\theta)}d\theta \\[2mm] &= \frac{1}{\pi}\sum_{n\neq 0} \frac{r^{|n|}}{2|n|}e^{in\alpha} \sum_{m=-\infty}^{\infty} g_m \int\limits_0^{2\pi} e^{i(m-n)\theta}d\theta \\[2mm] &= \sum_{n\neq 0} \frac{r^{|n|}}{|n|}g_n e^{in\alpha}. \end{aligned}$$

16

Therefore the Fourier coefficients of $u_1^N(z = re^{i\alpha})$ are given by

$$
u_{1,n}^N(r) = \begin{cases} g_n \dfrac{r^{|n|}}{|n|} & \text{if } n \neq 0, \\[2mm] 0 & \text{if } n = 0. \end{cases}
$$

Thus we obtain the proof for the Thm.2.2.1. $\qquad\qquad\qquad\qquad\qquad\qquad$ $\square$

3. THEORETICAL FOUNDATION: DIRICHLET-1 BIHARMONIC PROBLEM

In this section, we develop the mathematical foundation of the fast algorithm for the biharmonic equation with different boundary conditions in a unit disc $\mathbf{D}$ in the complex plane. We first consider the biharmonic equation with the Dirichlet-1 boundary condition (see [7]). We notice that this cannot be decomposed into two Poisson equations directly and hence we first use the Green's function for the biharmonic equation in a unit disc to solve it directly. Also, a second approach based on [24] is obtained but it is dependent on the direct method. In order to obtain fast algorithm for the direct approach we use following theorem from [7].

3.1 Mathematical Formulation Of Dirichlet-1 Biharmonic Problem

Theorem 3.1.1. *The Dirichlet-1 problem*

$$
\begin{cases}
(\partial_z \partial_{\bar{z}})^2 \omega = f, & in \quad \mathbf{D}, \\
\omega = h_0, & on \quad \partial\mathbf{D}, \\
\partial_{\bar{z}} \omega = h_1, & on \quad \partial\mathbf{D},
\end{cases}
\tag{D1}
$$

is uniquely solvable for $f \in L_2(\mathbf{D}; \mathbb{C})$, $h_0 \in C^2(\partial\mathbf{D}, \mathbb{C})$, $h_1 \in C(\partial\mathbf{D}, \mathbb{C})$. Its solution is given by

$$
\begin{aligned}
\omega(z) = {} & \frac{1}{2\pi i} \int_{\partial\mathbf{D}} g_1(z, \zeta) h_0(\zeta) \frac{d\zeta}{\zeta} + \frac{(1 - |z|^2)}{2\pi i} \int_{\partial\mathbf{D}} \frac{z\bar{\zeta}}{(1 - z\bar{\zeta})^2} h_0(\zeta) \frac{d\zeta}{\zeta} \\
& + \frac{(1 - |z|^2)}{2\pi i} \int_{\partial\mathbf{D}} g_1(z, \zeta) h_1(\zeta) d\bar{\zeta} - \frac{1}{\pi} \iint_{\mathbf{D}} G_2(z, \zeta) f(\zeta) d\xi d\eta.
\end{aligned}
\tag{3.1}
$$

18

where

$$G_2(z, \zeta) \ = \ |\zeta - z|^2 \log \left| \frac{1 - z\bar{\zeta}}{\zeta - z} \right|^2 - (1 - |z|^2)(1 - |\zeta|^2),$$

is the Green's function for the biharmonic equation in a unit disc with (D1) *boundary condition and*

$$g_1(z, \zeta) \ = \ \partial_\nu G_1(z, \zeta) = \frac{1}{1 - z\bar{\zeta}} + \frac{1}{1 - \bar{z}\zeta} - 1.$$

Next we prove the following theorem.

Theorem 3.1.2. *If* $\omega(r, \alpha)$ *is the solution of the* (D1) *biharmonic problem,* $z = re^{i\alpha}$,
$f(re^{i\alpha}) = \sum\limits_{n=-\infty}^{\infty} f_n(r)e^{in\alpha}$, $h_0(e^{i\alpha}) = \sum\limits_{n=-\infty}^{\infty} a_n e^{in\alpha}$, *and* $h_1(e^{i\alpha}) = \sum\limits_{n=-\infty}^{\infty} b_n e^{in\alpha}$, *then the Fourier coefficients* $\omega_n(r)$ *can be written as*

$$\omega_n(r) = I_{3,n}(r) + I_{4,n}(r) + I_{5,n}(r) + u_{2,n}(r) + v_{2,n}(r) + r_{2,n}(r),$$

where

$$u_{2,n}(r) \ = \ \begin{cases} a_n r^{|n|}, & \text{if} \quad n \neq 0, \\ a_0, & \text{if} \quad n = 0, \end{cases} \tag{3.2}$$

$$v_{2,n}(r) \ = \ \begin{cases} (1 - r^2)\frac{(2)_{n-1}}{(n-1)!}r^n a_n, & \text{if} \quad n \geq 1, \\ 0, & \text{if} \quad n < 1, \end{cases} \tag{3.3}$$

19

where $(x)_n = \frac{\Gamma(x+n)}{\Gamma(x)}$,

$$
r_{2,n}(r) = \begin{cases} -b_{1+n} r^{|n|}(1 - r^2), & if \quad n \neq 0, \\[2mm] -b_1(1 - r^2), & if \quad n = 0, \end{cases} \tag{3.4}
$$

$$
I_{3,n}(r) = \begin{cases} 2(1 - r^2) \int_0^1 \rho(1 - \rho^2) f_0(\rho) d\rho, & if \quad n = 0, \\[2mm] 0, & if \quad n \neq 0. \end{cases} \tag{3.5}
$$

Now we write $I_{4,n}(r) = I_{4,n}^{(1)} + I_{4,n}^{(2)} + I_{4,n}^{(3)} + I_{4,n}^{(4)}$ *where,*

$$
I_{4,n}^{(1)}(r) = \begin{cases} 2r^2 \int_0^1 f_n(\rho) \frac{(r\rho)^n}{n} \rho d\rho, & if \quad n > 0, \\[2mm] -2r^2 \int_0^1 f_n(\rho) \frac{(r\rho)^{-n}}{n} \rho d\rho, & if \quad n < 0, \\[2mm] 0, & if \quad n = 0, \end{cases} \tag{3.6}
$$

$$
I_{4,n}^{(2)}(r) = \begin{cases} 2 \int_0^1 f_n(\rho) \frac{(r\rho)^n}{n} \rho^3 d\rho, & if \quad n > 0, \\[2mm] -2 \int_0^1 f_n(\rho) \frac{(r\rho)^{-n}}{n} \rho^3 d\rho, & if \quad n < 0, \\[2mm] 0, & if \quad n = 0, \end{cases} \tag{3.7}
$$

$$
I_{4,n}^{(3)}(r) = \begin{cases} -\frac{2}{(n+1)} \int_0^1 f_n(\rho)(r\rho)^{n+2} \rho d\rho, & if \quad n > -1, \\[2mm] \frac{2}{(n+1)} \int_0^1 f_n(\rho)(r\rho)^{-n} \rho d\rho, & if \quad n < -1, \\[2mm] 0, & if \quad n = -1, \end{cases} \tag{3.8}
$$

20

$$I_{4,n}^{(4)}(r) = \begin{cases} -\frac{2}{(n-1)} \int_0^1 f_n(\rho)(r\rho)^n \rho d\rho, & \text{if } n > 1, \\ \frac{2}{(n-1)} \int_0^1 f_n(\rho)(r\rho)^{2-n} \rho d\rho, & \text{if } n < 1, \\ 0, & \text{if } n = 1. \end{cases} \tag{3.9}$$

Now we write $I_{5,n}(r) = I_{5,n}^{(1)} + I_{5,n}^{(2)} + I_{5,n}^{(3)} + I_{5,n}^{(4)}$ where

$$I_{5,n}^{(1)}(r) = \begin{cases} -2r^2 \left[\int_0^r f_n(\rho)(\frac{\rho}{r})^n \frac{\rho}{n} d\rho + \int_r^1 f_n(\rho)(\frac{r}{\rho})^n \frac{\rho}{n} d\rho \right], & \text{if } n > 0 \\ 2r^2 \left[\int_0^r f_n(\rho)(\frac{r}{\rho})^n \frac{\rho}{n} d\rho + \int_r^1 f_n(\rho)(\frac{\rho}{r})^n \frac{\rho}{n} d\rho \right], & \text{if } n < 0 \\ 4r^2 \left[\int_0^r f_0(\rho)\rho \log r d\rho + \int_r^1 f_0(\rho)\rho \log \rho d\rho \right], & \text{if } n = 0, \end{cases} \tag{3.10}$$

$$I_{5,n}^{(2)}(r) = \begin{cases} \frac{-2}{n} \left[\int_0^r f_n(\rho)(\frac{\rho}{r})^n \rho^3 d\rho + \int_r^1 f_n(\rho)(\frac{r}{\rho})^n \rho^3 d\rho \right], & \text{if } n > 0 \\ \frac{2}{n} \left[\int_0^r f_n(\rho)(\frac{r}{\rho})^n \rho^3 d\rho + \int_r^1 f_n(\rho)(\frac{\rho}{r})^n \rho^3 d\rho \right], & \text{if } n < 0 \\ 4 \left[\int_0^r f_0(\rho)\rho^3 \log r d\rho + \int_r^1 f_0(\rho)\rho^3 \log \rho d\rho \right], & \text{if } n = 0, \end{cases} \tag{3.11}$$

$$I_{5,n}^{(3)}(r) = \begin{cases} \frac{2r}{(n+1)} \left[\int_0^r f_n(\rho)(\frac{\rho}{r})^{(n+1)} \rho^2 d\rho + \int_r^1 f_n(\rho)(\frac{r}{\rho})^{(n+1)} \rho^2 d\rho \right], & \text{if } n > -1 \\ \frac{-2r}{(n+1)} \left[\int_0^r f_n(\rho)(\frac{r}{\rho})^{(n+1)} \rho^2 d\rho + \int_r^1 f_n(\rho)(\frac{\rho}{r})^{(n+1)} \rho^2 d\rho \right], & \text{if } n < -1 \\ -4r \left[\int_0^r f_{-1}(\rho)\rho^2 \log r d\rho + \int_r^1 f_{-1}(\rho)\rho^2 \log \rho d\rho \right], & \text{if } n = -1, \end{cases} \tag{3.12}$$

$$I_{5,n}^{(4)}(r) = \begin{cases} \frac{2r}{(n-1)} \left[\int_0^r f_n(\rho)(\frac{\rho}{r})^{(n-1)} \rho^2 d\rho + \int_r^1 f_n(\rho)(\frac{r}{\rho})^{(n-1)} \rho^2 d\rho \right], & \text{if } n > 1 \\ \frac{-2r}{(n-1)} \left[\int_0^r f_n(\rho)(\frac{r}{\rho})^{(n-1)} \rho^2 d\rho + \int_r^1 f_n(\rho)(\frac{\rho}{r})^{(n-1)} \rho^2 d\rho \right], & \text{if } n < 1 \\ -4r \left[\int_0^r f_1(\rho)\rho^2 \log r d\rho + \int_r^1 f_1(\rho)\rho^2 \log \rho d\rho \right], & \text{if } n = 1, \end{cases} \tag{3.13}$$

Proof. From (3.1) we rewrite $\omega(z)$ as

$\omega(z) = u_2(z) + v_2(z) + r_2(z) + I_3(z) + I_4(z) + I_5(z)$ where

$$u_2(z) = \frac{1}{2\pi i}\int_{\partial \mathbf{D}} g_1(z,\zeta)h_0(\zeta)\frac{d\zeta}{\zeta}, \tag{3.14}$$

$$v_2(z) = \frac{(1-|z|^2)}{2\pi i}\int_{\partial \mathbf{D}} \frac{z\bar{\zeta}}{(1-z\bar{\zeta})^2}h_0(\zeta)\frac{d\zeta}{\zeta}, \tag{3.15}$$

$$r_2(z) = \frac{(1-|z|^2)}{2\pi i}\int_{\partial \mathbf{D}} g_1(z,\zeta)h_1(\zeta)d\bar{\zeta}, \tag{3.16}$$

$$I_3(z) = \frac{(1-|z|^2)}{\pi}\iint_{\mathbf{D}} f(\zeta)(1-|\zeta|^2)d\xi d\eta, \tag{3.17}$$

$$I_4(z) = -\frac{2}{\pi}\iint_{\mathbf{D}} |\zeta - z|^2 \log|1 - z\bar{\zeta}|f(\zeta)d\xi d\eta, \tag{3.18}$$

$$I_5(z) = \frac{2}{\pi}\iint_{\mathbf{D}} |\zeta - z|^2 \log|\zeta - z|f(\zeta)d\xi d\eta. \tag{3.19}$$

We evaluate first,

$$\begin{aligned}
I_4(z) &= -\frac{2}{\pi}\iint_{\mathbf{D}} |\zeta - z|^2 \log|1 - z\bar{\zeta}|f(\zeta)d\xi d\eta \\
&= -\frac{2}{\pi}\iint_{\mathbf{D}} (|\zeta|^2 + |z|^2 - \zeta\bar{z} - \bar{\zeta}z)\log|1 - z\bar{\zeta}|f(\zeta)d\xi d\eta \\
&= I_4^{(1)}(z) + I_4^{(2)}(z) + I_4^{(3)}(z) + I_4^{(4)}(z)
\end{aligned}$$

22

where

$$I_4^{(1)}(z) = -\frac{2r^2}{\pi} \iint\limits_{\mathbf{D}} \log|1 - z\bar{\zeta}| f(\zeta) d\xi d\eta,$$

$$I_4^{(2)}(z) = -\frac{2}{\pi} \iint\limits_{\mathbf{D}} \rho^2 \log|1 - z\bar{\zeta}| f(\zeta) d\xi d\eta,$$

$$I_4^{(3)}(z) = \frac{2}{\pi} \iint\limits_{\mathbf{D}} \bar{z}\zeta \log|1 - z\bar{\zeta}| f(\zeta) d\xi d\eta,$$

$$I_4^{(4)}(z) = \frac{2}{\pi} \iint\limits_{\mathbf{D}} z\bar{\zeta} \log|1 - z\bar{\zeta}| f(\zeta) d\xi d\eta.$$

Let $I_4^{(1)}(z) = \sum\limits_{n=-\infty}^{\infty} I_{4,n}^{(1)}(r)e^{in\alpha}$ and $\alpha - \theta = \tau$. Then

$$I_{4,n}^{(1)}(r) = -\frac{r^2}{\pi^2} \iint\limits_{\mathbf{D}} f(\zeta) \int\limits_0^{2\pi} \log|1 - z\bar{\zeta}| e^{-in\alpha} d\alpha d\xi d\eta$$

$$= -\frac{r^2}{\pi^2} \int\limits_0^1 \int\limits_0^{2\pi} f(\rho, \theta)e^{-in\theta} \int\limits_{-\theta}^{2\pi-\theta} \log|1 - z\bar{\zeta}| e^{-in\tau} \rho d\tau d\theta d\rho$$

$$= 2r^2 \int\limits_0^1 f_n(\rho)G_{4,n}^{(1)}(r, \rho)\rho d\rho. \tag{3.20}$$

where,

$$G_{4,n}^{(1)}(r,\rho) = -\frac{1}{\pi} \int\limits_{-\theta}^{2\pi-\theta} \log|1 - z\bar{\zeta}|e^{-in\tau}d\tau$$

$$= \frac{1}{\pi} \int\limits_{-\theta}^{2\pi-\theta} (\sum_{m\neq 0} \frac{(r\rho)^{|m|}}{2|m|}e^{im\tau})e^{-in\tau}d\tau$$

$$= \frac{1}{\pi} \sum_{n\neq 0} \frac{(r\rho)^{|m|}}{2|m|} \int\limits_{-\theta}^{2\pi-\theta} e^{i(m-n)\tau}d\tau$$

$$= \begin{cases} \frac{(r\rho)^{|n|}}{|n|}, & \text{if } n \neq 0 \\ 0. & \text{if } n = 0. \end{cases} \tag{3.21}$$

Substituting (3.21) in (3.20) we recover the Fourier coefficients of $I_4^{(1)}(z)$. Similarly we obtain the Fourier coefficients of $I_4^{(2)}(z)$. Let $I_4^{(3)}(z) = \sum\limits_{n=-\infty}^{\infty} I_{4,n}^{(3)}(r)e^{in\alpha}$. Then,

$$I_{4,n}^{(3)}(r) = \frac{1}{\pi^2} \iint\limits_{\mathbf{D}} f(\zeta) \int\limits_0^{2\pi} \zeta\bar{z} \log|1 - z\bar{\zeta}|e^{-in\alpha}d\alpha d\xi d\eta$$

$$= \frac{1}{\pi^2} \int\limits_0^1 \int\limits_0^{2\pi} f(\rho,\theta)e^{-in\theta} \int\limits_{-\theta}^{2\pi-\theta} \zeta\bar{z} \log|1 - z\bar{\zeta}|e^{-in\tau}\rho d\tau d\theta d\rho$$

$$= 2\pi \int\limits_0^1 f_n(\rho)G_{4,n}^{(3)}(r,\rho)\rho d\rho. \tag{3.22}$$

24

where $f_n(\rho)$ is the Fourier coefficient of f and

$$
\begin{aligned}
G_{4,n}^{(3)}(r,\rho) &= \frac{1}{\pi} \int_{-\theta}^{2\pi-\theta} \zeta\bar{z} \log|1-z\bar{\zeta}| e^{-in\tau} d\tau \\
&= \frac{1}{2\pi} \int_{-\theta}^{2\pi-\theta} -\sum_{m\neq 0} \frac{(\rho r)^{|m|+1}}{2|m|} e^{i(m-1)\tau} e^{-in\tau} d\tau \\
&= -\frac{1}{2\pi} \sum_{m\neq 0} \frac{(\rho r)^{|m|+1}}{2|m|} \int_{-\theta}^{2\pi-\theta} e^{i(m-1-n)\tau} d\tau \\
&= \begin{cases} -\frac{(\rho r)^{|n+1|+1}}{|1+n|}, & \text{if } n \neq -1 \\ 0, & \text{if } n = -1. \end{cases}
\end{aligned}
\tag{3.23}
$$

The Fourier coefficients of $I_4^{(3)}(z)$ are given by (3.8). Let $I_4^{(4)}(z) = \sum_{n=-\infty}^{\infty} I_{4,n}^{(4)}(r)e^{in\alpha}$. Then,

$$
\begin{aligned}
I_{4,n}^{(4)}(r) &= \frac{1}{\pi^2} \iint_{\mathbf{D}} f(\zeta) \int_0^{2\pi} z\bar{\zeta} \log|1-z\bar{\zeta}| e^{-in\alpha} d\alpha\, d\xi\, d\eta \\
&= \frac{1}{\pi^2} \int_0^1 \int_0^{2\pi} f(\rho,\theta) e^{-in\theta} \int_{-\theta}^{2\pi-\theta} z\bar{\zeta} \log|1-z\bar{\zeta}| e^{-in\tau} \rho\, d\tau\, d\theta\, d\rho \\
&= 2\pi \int_0^1 f_n(\rho) G_{4,n}^{(4)}(r,\rho)\rho\, d\rho,
\end{aligned}
\tag{3.24}
$$

25

where $f_n(\rho)$ is the Fourier coefficient of f and

$$
\begin{aligned}
G_{4,n}^{(4)}(r,\rho) &= \frac{1}{\pi} \int_{-\theta}^{2\pi-\theta} z\bar{\zeta} \log|1 - z\bar{\zeta}| e^{-in\tau} d\tau \\
&= \frac{1}{\pi} \int_{-\theta}^{2\pi-\theta} -\sum_{m\neq 0} \frac{(\rho r)^{|m|+1}}{2|m|} e^{i(m+1)\tau} e^{-in\tau} d\tau \\
&= -\frac{1}{\pi} \sum_{m\neq 0} \frac{(\rho r)^{|m|+1}}{2|m|} \int_{-\theta}^{2\pi-\theta} e^{i(m+1-n)\tau} d\tau \\
&= \begin{cases} -\frac{(\rho r)^{|n-1|+1}}{|1-n|}, & \text{if} \quad n \neq 1 \\[2ex] 0, & \text{if} \quad n = 1. \end{cases}
\end{aligned}
\tag{3.25}
$$

Substituting (3.25) in (3.24) we recover the Fourier coefficients of $I_4^4(z)$. Now we evaluate the singular integral $I_5(z)$ given by (3.19).

$$
\begin{aligned}
I_5(z) &= \frac{2r^2}{\pi} \iint_{\mathbf{D}} \log|\zeta - z| f(\zeta) d\xi d\eta - \frac{2}{\pi} \iint_{\mathbf{D}} \bar{z}\zeta \log|\zeta - z| f(\zeta) d\xi d\eta \\
&\quad + \frac{2}{\pi} \iint_{\mathbf{D}} |\zeta|^2 \log|\zeta - z| f(\zeta) d\xi d\eta - \frac{2}{\pi} \iint_{\mathbf{D}} z\bar{\zeta} \log|\zeta - z| f(\zeta) d\xi d\eta \tag{3.26} \\
&= I_5^{(1)}(z) + I_5^{(2)}(z) + I_5^{(3)}(z) + I_5^{(4)}(z), \tag{3.27}
\end{aligned}
$$

26

where

$$I_5^{(1)}(z) = \frac{2r^2}{\pi} \iint_{\mathbf{D}} \log |\zeta - z| f(\zeta) d\xi d\eta, \qquad (3.28)$$

$$I_5^{(2)}(z) = \frac{2}{\pi} \iint_{\mathbf{D}} |\zeta|^2 \log |\zeta - z| f(\zeta) d\xi d\eta, \qquad (3.29)$$

$$I_5^{(3)}(z) = -\frac{2}{\pi} \iint_{\mathbf{D}} \bar{z} \log |\zeta - z| \zeta f(\zeta) d\xi d\eta, \qquad (3.30)$$

$$I_5^{(4)}(z) = -\frac{2}{\pi} \iint_{\mathbf{D}} z \log |\zeta - z| \bar{\zeta} f(\zeta) d\xi d\eta. \qquad (3.31)$$

Notice the singular integral associated with $I_5^{(1)}(z)$ is same as $I_2^N(z)$ (see (2.15)) except a r^2 term and hence the analysis is similar. Now we focus on $I_5^{(2)}(z)$. Let $I_5^{(2)}(z) = \sum_{n=-\infty}^{\infty} I_{5,n}^{(2)}(r) e^{in\alpha}$. As in (2.5), $I_{5,n}^{(2)}(r)$ is given by

$$I_{5,n}^{(2)}(r) = \iint_{\Omega_0^r} |\zeta|^2 f(\zeta) Q_n(r, \zeta) d\xi d\eta + \iint_{\Omega_r^1} |\zeta|^2 f(\zeta) Q_n(r, \zeta) d\xi d\eta,$$

where $Q_n(r, \zeta)$ has been evaluated in Section.2. For $n > 0$ we have the following.

$$\iint_{\mathbf{D}} |\zeta|^2 f(\zeta) Q_n(r, \zeta) d\xi d\eta = \iint_{\Omega_0^r} |\zeta|^2 f(\zeta) Q_n(r, \zeta) d\xi d\eta + \iint_{\Omega_r^1} |\zeta|^2 f(\zeta) Q_n(r, \zeta) d\xi d\eta$$

$$= -\iint_{\Omega_0^r} |\zeta|^2 f(\zeta) \left(\left(\frac{\rho}{r}\right)^n \frac{1}{\pi n} e^{-in\theta} \right) d\xi d\eta$$

$$- \iint_{\Omega_r^1} |\zeta|^2 f(\zeta) \left(\left(\frac{r}{\rho}\right)^n \frac{1}{\pi n} e^{-in\theta} \right) d\xi d\eta$$

27

$$= -\frac{1}{\pi n} \int\limits_0^r \int\limits_0^{2\pi} \rho^2 f(\rho e^{i\theta}) \left(\frac{\rho}{r}\right)^n e^{-in\theta} \rho \, d\theta \, d\rho$$

$$- \frac{1}{\pi n} \int\limits_r^1 \int\limits_0^{2\pi} \rho^2 f(\rho e^{i\theta}) \left(\frac{r}{\rho}\right)^n e^{-in\theta} \rho \, d\theta \, d\rho.$$

$$= -\frac{1}{\pi n} \int\limits_0^r \int\limits_0^{2\pi} \sum_{m=-\infty}^{\infty} f_m(\rho) e^{im\theta} \rho^3 \left(\frac{\rho}{r}\right)^n e^{-in\theta} \, d\theta \, d\rho$$

$$- \frac{1}{\pi n} \int\limits_r^1 \int\limits_0^{2\pi} \sum_{m=-\infty}^{\infty} f_m(\rho) e^{im\theta} \rho^3 \left(\frac{r}{\rho}\right)^n e^{-in\theta} \, d\theta \, d\rho$$

$$= -\frac{1}{\pi n} \int\limits_0^r \left(\frac{\rho}{r}\right)^n \rho^3 \sum_{m=-\infty}^{\infty} f_m(\rho) \int\limits_0^{2\pi} e^{i(m-n)\theta} \, d\theta \, d\rho$$

$$- \frac{1}{\pi n} \int\limits_r^1 \left(\frac{r}{\rho}\right)^n \rho^3 \sum_{m=-\infty}^{\infty} f_m(\rho) \int\limits_0^{2\pi} e^{i(m-n)\theta} \, d\theta \, d\rho$$

$$= -2 \int\limits_0^r \left(\frac{\rho}{r}\right)^n \frac{\rho^3}{n} f_n(\rho) d\rho - 2 \int\limits_r^1 \left(\frac{r}{\rho}\right)^n \frac{\rho^3}{n} f_n(\rho) d\rho. \qquad (3.32)$$

Similar calculation for $n < 0$ yields,

$$\iint\limits_{\mathbf{D}} |\zeta|^2 f(\zeta) Q_n(r,\zeta) d\xi d\eta = \frac{1}{\pi n} \int\limits_0^r \int\limits_0^{2\pi} f(\rho e^{i\theta}) \left(\frac{\rho}{r}\right)^{-n} e^{-in\theta} \rho^3 \, d\rho \, d\theta$$

$$+ \frac{1}{\pi n} \int\limits_r^1 \int\limits_0^{2\pi} f(\rho e^{i\theta}) \left(\frac{r}{\rho}\right)^{-n} e^{-in\theta} \rho^3 \, d\rho \, d\theta$$

$$= \frac{1}{\pi n} \int\limits_0^r \int\limits_0^{2\pi} \sum_{m=-\infty}^{\infty} f_m(\rho) e^{im\theta} \left(\frac{\rho}{r}\right)^{-n} e^{-in\theta} \rho^3 d\rho d\theta$$

$$+ \frac{1}{\pi n} \int\limits_r^1 \int\limits_0^{2\pi} \sum_{m=-\infty}^{\infty} f_m(\rho) e^{im\theta} \left(\frac{r}{\rho}\right)^{-n} e^{-in\theta} \rho^3 d\rho d\theta$$

$$= + \frac{1}{\pi n} \int\limits_0^r \left(\frac{r}{\rho}\right)^n \rho^3 \sum_{m=-\infty}^{\infty} f_m(\rho) \int\limits_0^{2\pi} e^{i(m-n)\theta} d\theta d\rho$$

$$+ \frac{1}{\pi n} \int\limits_r^1 \left(\frac{\rho}{r}\right)^n \rho^3 \sum_{m=-\infty}^{\infty} f_m(\rho) \int\limits_0^{2\pi} e^{i(m-n)\theta} d\theta d\rho$$

$$= 2 \int\limits_0^r \left(\frac{r}{\rho}\right)^n \frac{\rho^3}{n} f_n(\rho) d\rho + 2 \int\limits_r^1 \left(\frac{\rho}{r}\right)^n \frac{\rho^3}{n} f_n(\rho) d\rho. \qquad (3.33)$$

Similarly, for $n = 0$ yields,

$$I_{5,n}^{(2)}(r) = 4 \int\limits_0^r \rho^3 \log r f_0(\rho) d\rho + 4 \int\limits_r^1 \rho^3 \log \rho f_0(\rho) d\rho. \qquad (3.34)$$

From (3.32), (3.33), (3.34) we recover (3.11).

Let $I_5^{(3)}(z) = \sum_{n=-\infty}^{\infty} I_{5,n}^{(3)}(r) e^{in\alpha}$ where $I_{5,n}^{(3)}(r)$ is similarly given by

$$I_{5,n}^{(3)}(r) = \iint\limits_{\Omega_0^r} \bar{z} \zeta f(\zeta) Q_n^1(r, \zeta) d\xi d\eta + \iint\limits_{\Omega_r^1} \bar{z} \zeta f(\zeta) Q_n^1(r, \zeta) d\xi d\eta. \qquad (3.35)$$

where

$$Q_n^1(r, \zeta) = \frac{1}{\pi^2} \int\limits_0^{2\pi} e^{-in\alpha} \bar{z} \log |\zeta - z| d\alpha.$$

For $r > \rho$, we have

$$Q_n^1(r, \zeta) = \frac{1}{\pi^2} \int_0^{2\pi} e^{-in\alpha} r e^{-i\alpha} \left(\log r - \sum_{m \neq 0} \left(\frac{\rho}{r}\right)^{|m|} \frac{1}{2|m|} e^{im\tau} \right) d\alpha$$

$$= \frac{r}{\pi^2} \int_0^{2\pi} e^{-i(n+1)\alpha} \left(\log r - \sum_{m \neq 0} \left(\frac{\rho}{r}\right)^{|m|} \frac{1}{2|m|} e^{im(\alpha-\theta)} \right) d\alpha$$

$$= \frac{r}{\pi^2} \int_0^{2\pi} e^{-i(n+1)\alpha} \log r \, d\alpha - \frac{1}{\pi^2} \sum_{m \neq 0} \left(\frac{\rho}{r}\right)^{|m|} \frac{1}{2|m|} e^{-im\theta} \int_0^{2\pi} e^{i(m-n+1)\alpha} d\alpha$$

$$= \begin{cases} \frac{r}{\pi|n+1|} \left(\frac{\rho}{r}\right)^{|n+1|} e^{-i(n+1)\theta} & \text{if } n \neq -1, \\ \frac{-2}{\pi} r \log r & \text{if } n = -1. \end{cases} \tag{3.36}$$

Similarly we obtain for $r < \rho$,

$$Q_n^1(r, \zeta) = \begin{cases} +\frac{r}{\pi|n+1|} \left(\frac{r}{\rho}\right)^{|n+1|} e^{-i(n+1)\theta}, & \text{if } \quad n \neq -1, \\ -\frac{2}{\pi} r \log \rho, & \text{if } \quad n = -1. \end{cases} \tag{3.37}$$

30

Substituting (3.36), (3.37) in (3.35) we have for $n > -1$,

$$
\begin{aligned}
I_{5,n}^{(3)}(r) &= \iint_{\Omega_0^r} \zeta f(\zeta) Q_n^1(r, \zeta) d\xi d\eta + \iint_{\Omega_r^1} \zeta f(\zeta) Q_n^1(r, \zeta) d\xi d\eta \\
&= \iint_{\Omega_0^r} \zeta f(\zeta) \left(\left(\frac{\rho}{r} \right)^{(n+1)} \frac{r}{\pi(n+1)} e^{-i(n+1)\theta} \right) d\xi d\eta \\
&\quad + \iint_{\Omega_r^1} \zeta f(\zeta) \left(\left(\frac{r}{\rho} \right)^{(n+1)} \frac{r}{\pi(n+1)} e^{-i(n+1)\theta} \right) d\xi d\eta \\
&= \frac{r}{\pi(n+1)} \int_0^r \int_0^{2\pi} \rho e^{i\theta} f(\rho e^{i\theta}) \left(\frac{\rho}{r} \right)^{(n+1)} e^{-i(n+1)\theta} \rho \, d\theta d\rho \\
&\quad + \frac{r}{\pi(n+1)} \int_r^1 \int_0^{2\pi} \rho e^{i\theta} f(\rho e^{i\theta}) \left(\frac{r}{\rho} \right)^{(n+1)} e^{-i(n+1)\theta} \rho \, d\theta d\rho \\
&= \frac{r}{\pi(n+1)} \int_0^r \int_0^{2\pi} \sum_{m=-\infty}^{\infty} f_m(\rho) e^{im\theta} \rho^2 \left(\frac{\rho}{r} \right)^{(n+1)} e^{i\theta} e^{-i(n+1)\theta} d\theta d\rho \\
&\quad + \frac{r}{\pi(n+1)} \int_r^1 \int_0^{2\pi} \sum_{m=-\infty}^{\infty} f_m(\rho) e^{im\theta} \rho^2 \left(\frac{r}{\rho} \right)^{(n+1)} e^{-in\theta} d\theta d\rho \\
&= \frac{r}{\pi(n+1)} \int_0^r \left(\frac{\rho}{r} \right)^{(n+1)} \rho^2 \sum_{m=-\infty}^{\infty} f_m(\rho) \int_0^{2\pi} e^{i(m-n)\theta} d\theta d\rho \\
&\quad + \frac{r}{\pi(n+1)} \int_r^1 \left(\frac{r}{\rho} \right)^{(n+1)} \rho^2 \sum_{m=-\infty}^{\infty} f_m(\rho) \int_0^{2\pi} e^{i(m-n)\theta} d\theta d\rho \\
&= 2r \int_0^r \left(\frac{\rho}{r} \right)^{n+1} \frac{\rho^2}{(n+1)} f_n(\rho) d\rho + 2r \int_r^1 \left(\frac{r}{\rho} \right)^{(n+1)} \frac{\rho^2}{(n+1)} f_n(\rho) d\rho. \quad (3.38)
\end{aligned}
$$

Similarly we evaluate for $n < -1$ and $n = -1$ and obtain (3.12).

Again let $I_5^{(4)}(z) = \sum\limits_{n=-\infty}^{\infty} I_{5,n}^{(4)}(r)e^{in\alpha}$ where $I_{5,n}^{(4)}(r)$ is similarly given by

$$I_{5,n}^{(4)}(r) = \iint\limits_{\Omega_0^r} z\bar\zeta f(\zeta)Q_n^{(2)}(r,\zeta)d\xi d\eta + \iint\limits_{\Omega_r^1} z\bar\zeta f(\zeta)Q_n^2(r,\zeta)d\xi d\eta.$$

where,

$$Q_n^{(2)}(r,\zeta) = \frac{1}{\pi^2}\int\limits_0^{2\pi} e^{-in\alpha}z\log|\zeta - z|d\alpha.$$

For $r > \rho$ we have,

$$Q_n^{(2)}(r,\zeta) = \frac{1}{\pi^2}\int\limits_0^{2\pi} e^{-in\alpha}re^{i\alpha}\left(\log r - \sum_{m\neq 0}\left(\frac{\rho}{r}\right)^{|m|}\frac{1}{2|m|}e^{im\tau}\right)d\alpha$$

$$= \frac{r}{\pi^2}\int\limits_0^{2\pi} e^{i(1-n)\alpha}\left(\log r - \sum_{m\neq 0}\left(\frac{\rho}{r}\right)^{|m|}\frac{1}{2|m|}e^{im(\alpha-\theta)}\right)d\alpha$$

$$= \frac{r}{\pi^2}\int\limits_0^{2\pi} e^{i(1-n)\alpha}\log r\,d\alpha - \frac{r}{\pi^2}\sum_{m\neq 0}\left(\frac{\rho}{r}\right)^{|m|}\frac{1}{2|m|}e^{-im\theta}\int\limits_0^{2\pi} e^{i(m-n+1)\alpha}d\alpha$$

$$= \begin{cases} \frac{r}{\pi|n-1|}\left(\frac{\rho}{r}\right)^{|n-1|}e^{-i(n-1)\theta}, & \text{if } n \neq 1, \\ \frac{-2}{\pi}r\log r, & \text{if } n = 1. \end{cases} \tag{3.39}$$

Similarly for $r < \rho$,

$$Q_n^{(2)}(r,\zeta) = \begin{cases} +\frac{r}{\pi|n-1|}\left(\frac{r}{\rho}\right)^{|n-1|}e^{-i(n-1)\theta}, & \text{if } n \neq -1, \\ -\frac{2}{\pi}r\log\rho, & \text{if } n = -1. \end{cases} \tag{3.40}$$

For $n > 1$ we have,

$$
I_{5,n}^{(4)}(r) = \iint\limits_{\Omega_0^r} \bar{\zeta} f(\zeta) \left(\left(\frac{\rho}{r} \right)^{(n-1)} \frac{r}{\pi(n-1)} e^{-i(n-1)\theta} \right) d\xi d\eta
$$

$$
+ \iint\limits_{\Omega_r^1} \bar{\zeta} f(\zeta) \left(\left(\frac{r}{\rho} \right)^{(n-1)} \frac{r}{\pi(n-1)} e^{-i(n-1)\theta} \right) d\xi d\eta
$$

$$
= \frac{r}{\pi(n-1)} \int_0^r \int_0^{2\pi} \rho e^{-i\theta} f(\rho e^{i\theta}) \left(\frac{\rho}{r} \right)^{(n-1)} e^{-i(n-1)\theta} \rho d\theta d\rho
$$

$$
+ \frac{r}{\pi(n-1)} \int_r^1 \int_0^{2\pi} \rho e^{-i\theta} f(\rho e^{i\theta}) \left(\frac{r}{\rho} \right)^{(n-1)} e^{-i(n-1)\theta} \rho d\theta d\rho
$$

$$
= \frac{r}{\pi(n-1)} \int_0^r \int_0^{2\pi} \sum_{m=-\infty}^{\infty} f_m(\rho) e^{im\theta} \rho^2 \left(\frac{\rho}{r} \right)^{(n-1)} e^{-i\theta} e^{-i(n-1)\theta} d\theta d\rho
$$

$$
+ \frac{r}{\pi(n-1)} \int_r^1 \int_0^{2\pi} \sum_{m=-\infty}^{\infty} f_m(\rho) e^{im\theta} \rho^2 \left(\frac{r}{\rho} \right)^{(n-1)} e^{-in\theta} d\theta d\rho
$$

$$
= \frac{r}{\pi(n-1)} \int_0^r \left(\frac{\rho}{r} \right)^{(n-1)} \rho^2 \sum_{m=-\infty}^{\infty} f_m(\rho) \int_0^{2\pi} e^{i(m-n)\theta} d\theta d\rho
$$

$$
+ \frac{r}{\pi(n-1)} \int_r^1 \left(\frac{r}{\rho} \right)^{(n-1)} \rho^2 \sum_{m=-\infty}^{\infty} f_m(\rho) \int_0^{2\pi} e^{i(m-n)\theta} d\theta d\rho
$$

$$
= 2r \int_0^r \left(\frac{\rho}{r} \right)^{n-1} \frac{\rho^2}{(n-1)} f_n(\rho) d\rho + 2r \int_r^1 \left(\frac{r}{\rho} \right)^{(n-1)} \frac{\rho^2}{(n-1)} f_n(\rho) d\rho. \quad (3.41)
$$

Similarly we evaluate for $n < 1$ and $n = 1$ and obtain (3.13).

Let $I_3(z) = \sum\limits_{n=-\infty}^{\infty} I_{3,n}(r)e^{in\alpha}$. Then,

$$I_{3,n}(r)(r) = \frac{(1-r^2)}{\pi} \int\limits_0^1 (1-\rho^2) \sum\limits_{m=-\infty}^{\infty} f_m(\rho) \int\limits_0^{2\pi} e^{im\theta} \rho\, d\theta\, d\rho, \qquad m = 0$$

$$= 2(1-r^2) \int\limits_0^1 \rho(1-\rho^2) f_0(\rho)\, d\rho$$

$$= \begin{cases} 2(1-r^2) \int_0^1 \rho(1-\rho^2) f_n(\rho)\, d\rho, & \text{if } n = 0 \\ 0, & \text{if } n \neq 0. \end{cases} \qquad (3.42)$$

Thus we recover (3.5). Now for the boundary integrals $u_2(z)$ is same as $u_1(z)$ and $r_2(z)$ can be similarly evaluated. For $v_2(z)$ we have,

$$v_2(z) = \frac{(1-|z|^2)}{2\pi i} \int\limits_{\partial D} h_0(\zeta) \sum\limits_{k=0}^{\infty} \frac{(2)_k}{k!} (z\bar\zeta)^{k+1} \frac{d\zeta}{\zeta}$$

$$= \frac{(1-r^2)}{2\pi} \int\limits_0^{2\pi} h_0(e^{i\theta}) \sum\limits_{k=0}^{\infty} \frac{(2)_k}{k!} r^{k+1} e^{i(\alpha-\theta)(k+1)}\, d\theta$$

$$= \frac{(1-r^2)}{2\pi} \sum\limits_{k=0}^{\infty} \frac{(2)_k}{k!} r^{k+1} e^{i(k+1)\alpha} \sum\limits_{n=-\infty}^{\infty} a_n \int\limits_0^{2\pi} e^{i(n-k-1)\theta}\, d\theta$$

$$= (1-r^2) \sum\limits_{k=0}^{\infty} \frac{(2)_k}{k!} r^{k+1} e^{i(k+1)\alpha} a_{(k+1)}. \qquad (3.43)$$

Thus we recover (3.3). We see that the above calculations are exact. So the errors in actual implementation will arise from finite truncation of the the Fourier series and approximate evaluation of the one dimensional integrals. This concludes the proof of Theorem 3.1.2 and provides the mathematical foundation to solve the (D1) problem by the first approach. □

The second approach to solve the (D1) problem is based on the decomposition

34

of the problem into two Poisson problems and a corresponding homogeneous (D1) biharmonic problem. (see[24]). The (D1) biharmonic problem can be decomposed in the following way

$$\omega = \omega_1 + \omega_2$$

where ω_1 and ω_2 satisfy

$$\begin{cases} (\partial_z\partial_{\bar{z}})u &= f \quad \text{in} \quad \mathbf{D} \\ u &= 0 \quad \text{on} \quad \partial\mathbf{D} \end{cases} \qquad \begin{cases} (\partial_z\partial_{\bar{z}})\omega_1 &= u \quad \text{in} \quad \mathbf{D} \\ \omega_1 &= h_0 \quad \text{on} \quad \partial\mathbf{D} \end{cases}$$

and

$$\begin{cases} (\partial_z\partial_{\bar{z}})^2\omega_2 &= 0, \quad & \text{in} \quad \mathbf{D} \\ \omega_2 &= 0, \quad & \text{on} \quad \partial\mathbf{D} \\ \partial_{\bar{z}}\omega_2 &= h_1 - \omega_{1\bar{z}}, \quad & \text{on} \quad \partial\mathbf{D}. \end{cases}$$

The Poisson problems are solved as discussed in Section.2 and for the homogeneous biharmonic problem we just need the boundary integral of the (D1) problem in Theorem 3.1.2.

4. THEORETICAL FOUNDATION: DIRICHLET-2 BIHARMONIC PROBLEM

In this section, we focus on the Dirichlet-2 (D2) biharmonic problem and develop the mathematical foundation to obtain the fast algorithm for this problem. The following theorem is taken from [7].

4.1 Mathematical Formulation Of Dirichlet-2 Biharmonic Problem

Theorem 4.1.1. *The Dirichlet-2 problem for the biharmonic equation is given by*

$$
\begin{cases}
(\partial_z \partial_{\bar{z}})^2 \omega & = f, \quad\quad in \quad \mathbf{D}, \\
\omega & = h_0, \quad\quad on \quad \partial\mathbf{D}, \\
\partial_z \partial_{\bar{z}} \omega & = h_2, \quad\quad on \quad \partial\mathbf{D}.
\end{cases}
\tag{D2}
$$

is uniquely solvable for $f \in L_1(\mathbf{D}; \mathbb{C}), h_0 \in C(\partial\mathbf{D}, \mathbb{C}), h_2 \in C(\partial\mathbf{D}, \mathbb{C})$ and the solution is given by

$$
\omega(z) \quad = \quad u_2(z) + v_3(z) + Gf(z).
$$

36

where

$$u_2(z) = \frac{1}{2\pi i} \int_{\partial \mathbf{D}} g_1(z, \zeta) h_0(\zeta) \frac{d\zeta}{\zeta},$$

$$v_3(z) = \frac{1}{2\pi i} \int_{\partial \mathbf{D}} H_2(z, \zeta) h_2(\zeta) \frac{d\zeta}{\zeta},$$

$$Gf(z) = -\frac{1}{\pi} \int_{\mathbf{D}} G_{12}(z, \zeta) f(\zeta) d\xi d\eta,$$

$$H_2(z, \zeta) = (1 - |z|^2) \left[\frac{1}{z\bar{\zeta}} \log(1 - z\bar{\zeta}) + \frac{1}{\bar{z}\zeta} \log(1 - \bar{z}\zeta) + 1 \right],$$

$$G_{12}(z, \zeta) = |\zeta - z|^2 \log \left| \frac{1 - z\bar{\zeta}}{\zeta - z} \right|^2 + (1 - |z|^2)(1 - |\zeta|^2) \left[\frac{\log(1 - z\bar{\zeta})}{z\bar{\zeta}} + \frac{\log(1 - \bar{z}\zeta)}{\bar{z}\zeta} \right].$$

Here $G_{12}(z, \zeta)$ is the Green's function for (D2) biharmonic problem and $g_1(z, \zeta)$ is given in Section. 3.

Substituting the expression of $H_2(z, \zeta)$ and $G_{12}(z, \zeta)$ in the expression of $v_3(z)$ and $Gf(z)$ respectively we obtain the following expression.

$$v_3(z) = \frac{1}{2\pi i}(1 - |z|^2) \int_{\partial \mathbf{D}} \frac{h_2(\zeta) \log(1 - z\bar{\zeta})}{z|\zeta|^2} d\zeta + \frac{1}{2\pi i}(1 - |z|^2) \int_{\partial \mathbf{D}} \frac{h_2(\zeta) \log(1 - \zeta\bar{z})}{\bar{z}\zeta^2} d\zeta$$

$$+ \frac{1}{2\pi i}(1 - |z|^2) \int_{\partial \mathbf{D}} h_1(\zeta) \frac{d\zeta}{\zeta}.$$

$$Gf(z) = -\frac{2}{\pi} \int_{\mathbf{D}} |\zeta - z|^2 \log|1 - z\bar{\zeta}| f(\zeta) d\xi d\eta + \frac{2}{\pi} \int_{\mathbf{D}} |\zeta - z|^2 \log|\zeta - z| f(\zeta) d\xi d\eta$$

$$- \frac{1}{\pi} \frac{(1 - |z|^2)}{z} \int_{\mathbf{D}} (1 - |\zeta|^2) \frac{\log(1 - \bar{\zeta}z)}{\bar{\zeta}} f(\zeta) d\xi d\eta$$

$$- \frac{1}{\pi} \frac{(1 - |z|^2)}{\bar{z}} \int_{\mathbf{D}} (1 - |\zeta|^2) \frac{\log(1 - \bar{z}\zeta)}{\zeta} f(\zeta) d\xi d\eta$$

$$= I_4(z) + I_5(z) + I_6(z) + I_7(z), \tag{4.1}$$

where

$$I_4(z) = -\frac{2}{\pi} \int_{\mathbf{D}} |\zeta - z|^2 \log|1 - z\bar{\zeta}| f(\zeta) d\xi d\eta,$$

$$I_5(z) = \frac{2}{\pi} \int_{\mathbf{D}} |\zeta - z|^2 \log|\zeta - z| f(\zeta) d\xi d\eta,$$

$$I_6(z) = -\frac{1}{\pi} \frac{(1 - |z|^2)}{z} \int_{\mathbf{D}} (1 - |\zeta|^2) \frac{\log(1 - \bar{\zeta}z))}{\bar{\zeta}} f(\zeta) d\xi d\eta,$$

$$I_7(z) = -\frac{1}{\pi} \frac{(1 - |z|^2)}{\bar{z}} \int_{\mathbf{D}} (1 - |\zeta|^2) \frac{\log(1 - \bar{z}\zeta))}{\zeta} f(\zeta) d\xi d\eta.$$

Our goal is to develop fast and accurate algorithms to solve the singular integrals appearing above in the expression of $Gf(z)$. This will lead to the desired fast algorithms for solving (D2) biharmonic problem (see Thm. 4.1.1).

Theorem 4.1.2. *If $\omega(r, \alpha)$ is the solution of the (D2) biharmonic problem, $z = re^{i\alpha}$,*
$$f(re^{i\alpha}) = \sum_{n=-\infty}^{\infty} f_n(r) e^{in\alpha}, \quad h_0(re^{i\alpha}) = \sum_{n=-\infty}^{\infty} a_n e^{in\alpha}, \quad and \quad h_2(e^{i\alpha}) = \sum_{n=-\infty}^{\infty} c_n e^{in\alpha}$$
then the Fourier coefficients $\omega_n(r)$ of $\omega(r, \alpha)$ can be written as

$$\omega_n(r) = I_{4,n}(r) + I_{5,n}(r) + I_{6,n}(r) + I_{7,n}(r) + u_{2,n}(r) + v_{3,n}(r),$$

where $I_{4,n}(r), I_{5,n}(r)$ and $u_{2,n}(r)$ are same as in Theorem (3.1.2) and

$$I_{6,n}(r) = \begin{cases} \frac{2(1-r^2)r^n}{(n+1)} \int_0^1 \rho^{(n+1)}(1 - \rho^2) f_n(\rho) d\rho, & if \quad n \geq 0 \\ 0, & if \ n < 0. \end{cases} \tag{4.2}$$

$$I_{7,n}(r) = \begin{cases} \frac{2(1-r^2)r^{-n}}{(1-n)} \int_0^1 \rho^{(1-n)}(1 - \rho^2) f_n(\rho) d\rho, & if \quad n \leq 0 \\ 0. & if \ n > 0. \end{cases} \tag{4.3}$$

38

$$v_{3,n}(r) = \begin{cases} \dfrac{c_n(r^{|n|+2}-r^{|n|})}{n+1}, & if \, n \neq 0 \\[2mm] c_0(1 - r^2), & if \, n = 0. \end{cases}$$

Proof. We first compute $I_{6,n}(r)$ and $I_{7,n}(r)$. We first evaluate the Fourier coefficients $I_{6,n}(r)$ of $I_6(z)$.

$$I_{6,n}(r) = \frac{1}{2\pi^2} \iint_{\mathbf{D}} f(\zeta) P_n(r,\zeta) d\zeta d\eta, \tag{4.4}$$

where

$$P_n(r,\zeta) = (r^2-1)(1-|\zeta|^2) \int_0^{2\pi} e^{-in\alpha} \frac{\log(1-z\bar{\zeta})}{z\bar{\zeta}} d\alpha. \tag{4.5}$$

$$= (r^2-1)(1-|\zeta|^2) \int_0^{2\pi} e^{-in\alpha} \frac{\log(1-z\bar{\zeta})}{z\bar{\zeta}} d\alpha$$

$$= (r^2-1)(1-|\zeta|^2) \int_0^{2\pi} e^{-in\alpha} \sum_{m=1}^{\infty} -\frac{(z\bar{\zeta})^m}{m(z\bar{\zeta})} d\alpha$$

$$= (1-r^2)(1-|\zeta|^2) \sum_{m=1}^{\infty} \frac{(r\bar{\zeta})^{(m-1)}}{m} \int_0^{2\pi} e^{-i(m-n-1)\alpha} d\alpha$$

$$= \begin{cases} 2\pi \dfrac{(1-r^2)(1-|\zeta|^2)(r\bar{\zeta})^n}{(n+1)}, & \text{if} \quad n \geq 0, \\[2mm] 0, & \text{if} \quad n < 0. \end{cases} \tag{4.6}$$

Substituting (4.6) in (4.4) we recover (4.2).

$$I_{6,n}(r) = \frac{(1-r^2)r^n}{\pi(n+1)} \int_0^1 \rho^{(n+1)}(1-\rho^2) \sum_{m=-\infty}^{\infty} f_m(\rho) \int_0^{2\pi} e^{i(m-n)\theta} d\theta d\rho$$

$$= \begin{cases} \dfrac{2(1-r^2)r^n}{(n+1)} \int_0^1 \rho^{(n+1)}(1-\rho^2) f_n(\rho) d\rho, & \text{if} \quad n \geq 0 \\[2mm] 0, & \text{if} \quad n < 0. \end{cases} \tag{4.7}$$

Similarly let,

$$I_{7,n}(r) = \frac{1}{2\pi^2} \iint\limits_{\mathbf{D}} f(\zeta) S_n(r, \zeta) d\zeta d\eta. \tag{4.8}$$

where

$$S_n(r, \zeta) = (r^2 - 1)(1 - |\zeta|^2) \int_0^{2\pi} e^{-in\alpha} \frac{\log(1 - \zeta\bar{z})}{\zeta\bar{z}} d\alpha$$

$$= (r^2 - 1)(1 - |\zeta|^2) \int_0^{2\pi} e^{-in\alpha} \frac{\log(1 - \zeta\bar{z})}{\zeta\bar{z}} d\alpha$$

$$= (r^2 - 1)(1 - |\zeta|^2) \int_0^{2\pi} e^{-in\alpha} \sum_{m=1}^{\infty} -\frac{(\zeta\bar{z})^m}{m(\zeta\bar{z})} d\alpha$$

$$= (1 - r^2)(1 - |\zeta|^2) \sum_{m=1}^{\infty} \frac{(r\zeta)^{(m-1)}}{m} \int_0^{2\pi} e^{i(1-m-n)\alpha} d\alpha$$

$$= \begin{cases} 2\pi \frac{(1-r^2)(1-|\zeta|^2)(r\zeta)^{-n}}{(1-n)}, & \text{if} \quad n \le 0, \\ 0, & \text{if} \quad n > 0. \end{cases} \tag{4.9}$$

Hence substituting (4.9) in (4.8) we recover (4.3).

$$I_{7,n}(r) = \frac{(1 - r^2)r^{-n}}{\pi(1 - n)} \int_0^1 \rho^{(1-n)}(1 - \rho^2) \sum_{m=-\infty}^{\infty} f_m(\rho) \int_0^{2\pi} e^{i(m-n)\theta} d\theta d\rho$$

$$= \begin{cases} \frac{2(1-r^2)r^{-n}}{(1-n)} \int_0^1 \rho^{(1-n)}(1 - \rho^2) f_n(\rho) d\rho, & \text{if} \quad n \le 0. \\ 0, & \text{if} \quad n > 0. \end{cases} \tag{4.10}$$

The boundary integrals are computed in a similar fashion as earlier but we provide the details for the sake of completeness. Let

$$v_3(z) = v_3^{(1)}(z) + v_3^{(2)}(z) + v_3^{(3)}(z), \tag{4.11}$$

where

$$v_3^{(1)}(z) = \frac{1}{2\pi i}(1 - |z|^2) \int_{\partial \mathbf{D}} \frac{h_2(\zeta) \log(1 - z\bar{\zeta})}{z|\zeta|^2} d\zeta,$$

$$v_3^{(2)}(z) = \frac{1}{2\pi i}(1 - |z|^2) \int_{\partial \mathbf{D}} \frac{h_2(\zeta) \log(1 - \zeta\bar{z})}{\bar{z}\zeta^2} d\zeta,$$

$$v_3^{(3)}(z) = \frac{1}{2\pi i}(1 - |z|^2) \int_{\partial \mathbf{D}} h_2(\zeta) \frac{d\zeta}{\zeta}.$$

We now evaluate the integrals $v_3^{(1)}(z), v_3^{(2)}(z), v_3^{(3)}(z)$ in terms of Fourier coefficients of $h_2(e^{i\alpha}) = \sum_{n=-\infty}^{\infty} c_n e^{in\alpha}$ in the the following way.

$$\begin{aligned}
v_3^{(1)}(z) &= \frac{1}{2\pi z}(1 - r^2) \int_{\partial \mathbf{D}} h_2(e^{i\theta}) \log(1 - re^{i(\alpha-\theta)}) e^{i\theta} d\theta \\
&= \frac{-1}{2\pi z}(1 - r^2) \sum_{n=1}^{\infty} \frac{r^n}{n} \int_0^{2\pi} h_2(e^{i\theta}) e^{in(\alpha-\theta)} e^{i\theta} d\theta \\
&= \frac{-1}{2\pi z}(1 - r^2) \sum_{n=1}^{\infty} \frac{r^n}{n} \int_0^{2\pi} \sum_{m=-\infty}^{\infty} c_m e^{im\theta} e^{in(\alpha-\theta)} e^{i\theta} d\theta \\
&= \frac{-1}{2\pi z}(1 - r^2) \sum_{n=1}^{\infty} \frac{r^n}{n} e^{in\alpha} \sum_{m=-\infty}^{\infty} c_m \int_0^{2\pi} e^{i(m-n+1)\theta} d\theta \\
&= \sum_{n=1}^{\infty} \frac{r^{(n-1)}(r^2 - 1)}{n} e^{i(n-1)\alpha} c_{n-1} \\
&= \sum_{n=0}^{\infty} \frac{r^n(r^2 - 1)}{n+1} e^{in\alpha} c_n \\
&= \sum_{n=0}^{\infty} \frac{c_n}{n+1}(r^{n+2} - r^n) e^{in\alpha}.
\end{aligned}$$

41

$$v_3^{(2)}(z) = \frac{(1-r^2)}{2\pi\bar{z}} \int_0^{2\pi} h_2(e^{i\theta}) \log(1 - re^{i(\theta-\alpha)}) e^{-i\theta} d\theta$$

$$= \frac{(r^2-1)}{2\pi\bar{z}} \int_0^{2\pi} h_2(e^{i\theta}) \sum_{n=1}^{\infty} \frac{r^n e^{in(\alpha-\theta)}}{n} e^{-i\theta} d\theta$$

$$= \frac{(r^2-1)}{2\pi\bar{z}} \sum_{n=1}^{\infty} \frac{r^n}{n} e^{-in\alpha} \int_0^{2\pi} \sum_{m=-\infty}^{\infty} c_m e^{im\theta} e^{i(n-1)\theta} d\theta$$

$$= \frac{(r^2-1)}{2\pi\bar{z}} \sum_{n=1}^{\infty} \frac{r^n}{n} e^{-in\alpha} \sum_{m=-\infty}^{\infty} c_m \int_0^{2\pi} e^{i(m+n-1)\theta} d\theta$$

$$= \frac{(r^2-1)}{\bar{z}} \sum_{n=1}^{\infty} \frac{r^n}{n} e^{-in\alpha} c_{1-n}$$

$$= \sum_{m=-\infty}^{0} \frac{c_m}{1-m} (r^{2-m} - r^{-m}) e^{im\alpha}.$$

$$v_3^{(3)}(z) = \frac{(1-r^2)}{2\pi} \int_0^{2\pi} h_2(e^{i\theta}) d\theta$$

$$= \frac{(1-r^2)}{2\pi} \int_0^{2\pi} \sum_{m=-\infty}^{\infty} c_m e^{im\theta} d\theta$$

$$= \frac{(1-r^2)}{2\pi} \sum_{m=-\infty}^{\infty} c_m \int_0^{2\pi} e^{im\theta} d\theta$$

$$= c_0(1-r^2).$$

Substituting these in (4.11) we find the Fourier coefficients of $v_3(z) = \sum_{n=-\infty}^{\infty} v_n(r) e^{in\alpha}$ as

$$v_{3,n}(r) = \begin{cases} \frac{c_n(r^{|n|+2} - r^{|n|})}{1+|n|}, & \text{if } n \neq 0, \\ c_0(1-r^2), & \text{if } n = 0. \end{cases} \tag{4.12}$$

Thus we obtain the proof for the Thm.4.1.2. □

We note here that the (D2) biharmonic problem can be decomposed into two Poisson problems.

$$
\begin{cases}
(\partial_z \partial_{\bar{z}})u = f & \text{in} \quad \mathbf{D} \\
u = h_2 & \text{on} \quad \partial \mathbf{D}
\end{cases}
\tag{4.13}
$$

$$
\begin{cases}
(\partial_z \partial_{\bar{z}})\omega = u & \text{in} \quad \mathbf{D} \\
\omega = h_0 & \text{on} \quad \partial \mathbf{D}
\end{cases}
\tag{4.14}
$$

Hence it can be solved using the fast Poisson solver discussed in Section. 2. We first solve (4.13) for u and then (4.14) to obtain ω. We implement both the methods namely the direct and the double Poisson and compare our results in Section. 10.

4.1.1 Validation Of The Method

We illustrate the direct method with an explicit example of the Dirichlet-2 (D2) biharmonic problem. The main reason to do this is to give an explicit demonstration of the operations if f is known explicitly and the ability of the algorithm to evaluate the integrals analytically which is an advantage for this method. We consider

$$f(z) = z^p \bar{z}^q$$

where p, q are constants and $k = p - q \in Z$. The Fourier coefficients of f are given by

$$f_n(r) = \begin{cases} r^{p+q} & \text{if } n = k \\ 0 & \text{if } n \neq k \end{cases}$$

We notice the following.

$$
\begin{aligned}
I_{4,n}^{(j)}(r) &= 0, & \text{for} \quad n \neq k, j = 1, 2, 3, 4 \\
I_{5,n}^{(j)}(r) &= 0, & \text{for} \quad n \neq k, j = 1, 2, 3, 4 \\
I_{6,n}(r) &= 0, & \text{for} \quad n \neq k, \\
I_{7,n}(r) &= 0, & \text{for} \quad n \neq k.
\end{aligned}
$$

Now we compute the non zero Fourier coefficients for $n = k$.

For $k > 0$ the Fourier coefficients of $I_{4,k}(r)$ is

$$I_{4,k}^{(1)}(r) = 2r^2 \int_0^1 \frac{(r\rho)^k}{k} \rho^{p+q+1} d\rho$$

$$= \frac{2r^{k+2}}{k(p+q+k+2)} \quad \text{when} \quad (p+q+k+2) \neq 0.$$

For $k > 0$ and $(p+q+k+2) = 0$, $I_{4,k}^{(1)}(r) = \infty$. The integral is unbounded as f is not in L^1 and hence the condition for Thm.4.1.1 is not satisfied.

For $k < 0$,

$$I_{4,k}^{(1)}(r) = -2r^{2-k} \int_0^1 \frac{(\rho)^{p+q+1-k}}{k} d\rho$$

$$= \frac{-2r^{2-k}}{k(p+q-k+2)} \quad \text{when} \quad (p+q-k+2) \neq 0.$$

For $k < 0$ and $(p+q-k+2) = 0$, $I_{4,k}^{(1)}(r) = \infty$. As before f is not in L^1 and Thm.4.1.1 is not satisfied so the integral is unbounded.

For $k = 0$, $I_{4,k}^{(1)}(r) = 0$,

For $k > 0$,

$$I_{4,k}^{(2)}(r) = 2r^k \int_0^1 \frac{(\rho)^k}{k} \rho^{p+q+3} d\rho$$

$$= \frac{2r^k}{k(p+q+k+4)} \quad \text{when} \quad (p+q+k+4) \neq 0.$$

For $k > 0$ and $(p+q+k+4) = 0$, $I_{4,k}^{(2)}(r) = \infty$. The reason for unboundedness is same as above.

For $k < 0$,

$$I_{4,k}^{(2)}(r) = -2r^{-k} \int_0^1 \frac{(\rho)^{p+q+3-k}}{k} d\rho$$

$$= \frac{-2r^{-k}}{k(p+q-k+4)} \quad \text{when} \quad (p+q-k+4) \neq 0.$$

For $k < 0$ and $(p+q-k+4) = 0$, $I_{4,k}^{(2)}(r) = \infty$ as f is not in L^1.

For $k = 0$, $I_{4,k}^{(2)}(r) = 0$.

For $k > -1$,

$$I_{4,k}^{(3)}(r) = -2r^2 \int_0^1 \frac{(r\rho)^{k+2}}{k+1} \rho^{p+q+1} d\rho$$

$$= -\frac{2r^{k+2}}{(k+1)(p+q+k+4)} \quad \text{when} \quad (p+q+k+4) \neq 0.$$

For $k > -1$ and $(p+q+k+4) = 0$, $I_{4,k}^{(3)}(r) = \infty$ as f is not in L^1.

For $k < -1$,

$$I_{4,k}^{(3)}(r) = 2r^{-k} \int_0^1 \frac{(\rho)^{p+q+1-k}}{k+1} d\rho$$

$$= \frac{2r^{-k}}{(k+1)(p+q-k+2)} \quad \text{when} \quad (p+q-k+2) \neq 0.$$

For $k < -1$ and $(p+q-k+2) = 0$, $I_{4,k}^{(3)}(r) = \infty$ as f is not in L^1.

For $k = -1$, $I_{4,k}^{(3)}(r) = 0$.

For $k > 1$,

$$I_{4,k}^{(4)}(r) = -2 \int_0^1 \frac{(r\rho)^k}{k-1} \rho^{p+q+1} d\rho$$

$$= -\frac{2r^k}{(k-1)(p+q+k+2)} \quad \text{when} \quad (p+q+k+2) \neq 0.$$

For $k > 1$ and $(p+q+k+2) = 0$, $I_{4,k}^{(4)}(r) = \infty$ as f is not in L^1.

For $k < 1$,

$$I_{4,k}^{(4)}(r) = 2r^{2-k} \int_0^1 \frac{(\rho)^{p+q+3-k}}{k-1} d\rho$$

$$= \frac{2r^{2-k}}{(k-1)(p+q-k+4)} \quad \text{when} \quad (p+q-k+4) \neq 0.$$

For $k < 1$ and $(p+q-k+4) = 0$, $I_{4,k}^{(4)}(r) = \infty$ as f is not in L^1.

For $k = 1$, $I_{4,k}^{(4)}(r) = 0$.

For $k > 0$ and $(p+q-k+2)(p+q+k+2) \neq 0$

$$I_{5,k}^{(1)}(r) = -2r^2 \int_0^r \left(\frac{\rho}{r}\right)^k \frac{\rho}{k} \rho^{p+q} d\rho - r^2 \int_r^1 \left(\frac{r}{\rho}\right)^k \frac{\rho}{k} \rho^{p+q} d\rho,$$

$$= -\frac{2r^{2-k}}{k} \int_0^r \rho^{p+q+k+1} d\rho - \frac{2r^{2+k}}{k} \int_r^1 \rho^{p+q-k+1} d\rho,$$

$$= \frac{4r^{p+q+4}}{(p+q-k+2)(p+q+k+2)} - \frac{2r^{k+2}}{k(p+q+2-k)}.$$

For $k > 0$ and $(p+q-k+2) = 0$,

$$I_{5,k}^{(1)}(r) = -\frac{r^{k+2}}{k^2} + \frac{2r^{k+2} \log r}{k}.$$

47

For $k > 0$ and $(p + q + k + 2) = 0$, $I_{5,k}^{(1)}(r) = \infty$ as f is not in L^1.

For $k < 0$ and $(p + q - k + 2)(p + q + k + 2) \neq 0$

$$
\begin{aligned}
I_{5,k}^{(1)}(r) &= 2r^2 \int_0^r \left(\frac{r}{\rho}\right)^k \frac{\rho}{k} \rho^{p+q} d\rho + 2r^2 \int_r^1 \left(\frac{\rho}{r}\right)^k \frac{\rho}{k} \rho^{p+q} d\rho, \\
&= \frac{4r^{p+q+4}}{(p+q-k+2)(p+q+k+2)} + \frac{2r^{2-k}}{k(p+q+2+k)}.
\end{aligned}
$$

For $k < 0$ and $(p + q + k + 2) = 0$,

$$
I_{5,k}^{(1)}(r) = \frac{r^{2-k}}{k^2} - \frac{2r^{2-k}\log r}{k}.
$$

For $k < 0$ and $(p + q - k + 2) = 0$, $I_{5,k}^{(1)}(r) = \infty$ as f is not in L^1.

For $k = 0$,

$$
\begin{aligned}
I_{5,k}^{(1)}(r) &= 4r^2 \int_0^r \rho^{p+q+1} \log r \, d\rho + 4r^2 \int_r^1 \rho^{p+q+1} \log \rho \, d\rho \\
&= \frac{-4r^2}{(p+q+2)^2} \left[1 - r^{p+q+2}\right] \quad \text{when} \quad (p+q+2) \neq 0.
\end{aligned}
$$

For $k = 0$ and $p + q + 2 = 0$, $I_{5,k}^{(1)}(r) = \infty$.

For $k > 0$ and $(p + q - k + 4)(p + q + k + 4) \neq 0$,

$$
\begin{aligned}
I_{5,k}^{(2)}(r) &= -2 \int_0^r \left(\frac{\rho}{r}\right)^k \frac{\rho^3}{k} \rho^{p+q} d\rho - 2 \int_r^1 \left(\frac{r}{\rho}\right)^k \frac{\rho^3}{k} \rho^{p+q} d\rho, \\
&= -\frac{2r^{-k}}{k} \int_0^r \rho^{p+q+k+3} d\rho - \frac{2r^k}{k} \int_r^1 \rho^{p+q-k+3} d\rho, \\
&= \frac{4r^{p+q+4}}{(p+q-k+4)(p+q+k+4)} - \frac{2r^k}{k(p+q+4-k)}.
\end{aligned}
$$

48

For $k > 0$ and $(p + q - k + 4) = 0$,

$$I_{5,k}^{(2)}(r) = -\frac{r^k}{k^2} + \frac{2r^k \log r}{k}.$$

For $k > 0$ and $(p + q + k + 4) = 0$, $I_{5,k}^{(2)}(r) = \infty$ as f is not in L^1 and hence Thm.4.1.1 is not satisfied.

For $k < 0$ and $(p + q - k + 4)(p + q + k + 4) \neq 0$,

$$I_{5,k}^{(2)}(r) = 2\int_0^r \left(\frac{r}{\rho}\right)^k \frac{\rho^3}{k}\rho^{p+q}d\rho + 2\int_r^1 \left(\frac{\rho}{r}\right)^k \frac{\rho^3}{k}\rho^{p+q}d\rho,$$

$$= \frac{4r^{p+q+4}}{(p+q-k+4)(p+q+k+4)} + \frac{2r^{-k}}{k(p+q+4+k)}.$$

For $k < 0$ and $(p + q + k + 4) = 0$,

$$I_{5,k}^{(2)}(r) = \frac{r^{-k}}{k^2} - \frac{2r^{-k} \log r}{k}.$$

For $k < 0$ and $(p + q - k + 4) = 0$, $I_{5,k}^{(2)}(r) = \infty$ as f is not in L^1.

For $k = 0$,

$$I_{5,k}^{(2)}(r) = 4\int_0^r \rho^{p+q+3} \log r d\rho + 4\int_r^1 \rho^{p+q+3} \log \rho d\rho$$

$$= \frac{4}{(p+q+4)^2}\left[r^{p+q+4} - 1\right] \quad \text{when} \quad (p+q+4) \neq 0.$$

For $k = 0$ and $p + q + 4 = 0$, $I_{5,k}^{(2)}(r) = \infty$ as f is not in L^1.

For $k < -1$ and $(p + q - k + 2)(p + q + k + 4) \neq 0$,

$$
\begin{aligned}
I_{5,k}^{(3)}(r) &= -\frac{2r}{(k+1)} \int_0^r \left(\frac{r}{\rho}\right)^{(k+1)} \rho^{p+q+2} d\rho - \frac{2r}{(k+1)} \int_r^1 \left(\frac{\rho}{r}\right)^{(k+1)} \rho^{p+q+2} d\rho, \\
&= -\frac{2r^{k+2}}{(k+1)} \int_0^r \rho^{p+q-k+1} d\rho - \frac{2r^{-k}}{(k+1)} \int_r^1 \rho^{p+q+k+3} d\rho, \\
&= -\frac{2r^{p+q+4}}{(k+1)(p+q-k+2)} + \frac{2(r^{p+q+4} - r^{-k})}{(k+1)(p+q+4+k)}.
\end{aligned}
$$

For $k < -1$ and $(p + q + k + 4) = 0$,

$$
I_{5,k}^{(3)}(r) = \frac{r^{-k}}{(k+1)^2} + 2\frac{r^{-k} \log r}{(k+1)}.
$$

For $k < -1$ and $(p + q - k + 2) = 0$, $I_{5,k}^{(3)}(r) = \infty$ as f is not in L^1.

For $k > -1$ and $(p + q - k + 2)(p + q + k + 4) \neq 0$,

$$
\begin{aligned}
I_{5,k}^{(3)}(r) &= -\frac{2r}{(k+1)} \int_0^r \left(\frac{\rho}{r}\right)^{(k+1)} \rho^{p+q+2} d\rho + \frac{2r}{(k+1)} \int_r^1 \left(\frac{r}{\rho}\right)^{(k+1)} \rho^{p+q+2} d\rho, \\
&= -\frac{2r^{-k}}{(k+1)} \int_0^r \rho^{p+q+k+3} d\rho + \frac{2r^{k+2}}{(k+1)} \int_r^1 \rho^{p+q-k+1} d\rho, \\
&= -\frac{4r^{p+q+4}}{(p+q+k+4)(p+q-k+2)} + \frac{2r^{(k+2)}}{(k+1)(p+q+2-k)}.
\end{aligned}
$$

For $k > -1$ and $(p + q - k + 2) = 0$,

$$
I_{5,k}^{(3)}(r) = \frac{r^{k+2}}{(k+1)^2} - \frac{2r^{k+2} \log r}{(k+1)}.
$$

For $k > -1$ and $(p + q + k + 4) = 0$, $I_{5,k}^{(3)}(r) = \infty$ as f is not in L^1.

For $k = -1$,

$$
\begin{aligned}
I_{5,k}^{(3)}(r) &= -4r \int_0^r \rho^{p+q+2} \log r d\rho + 4r \int_r^1 \rho^{p+q+2} \log \rho d\rho \\
&= \frac{4r}{(p+q+3)^2} \left[1 - r^{p+q+3}\right] \quad \text{when} \quad (p+q+3) \neq 0.
\end{aligned}
$$

For $k = -1$ and $p + q + 3 = 0$, $I_{5,k}^{(3)}(r) = \infty$ as f is not in L^1.

For $k < 1$ and $(p + q + k + 2)(p + q - k + 4) \neq 0$,

$$
\begin{aligned}
I_{5,k}^{(4)}(r) &= -\frac{2r}{(k-1)} \int_0^r \left(\frac{r}{\rho}\right)^{(k-1)} \rho^{p+q+2} d\rho - \frac{2r}{(k-1)} \int_r^1 \left(\frac{\rho}{r}\right)^{(k-1)} \rho^{p+q+2} d\rho, \\
&= -\frac{2r^k}{(k-1)} \int_0^r \rho^{p+q-k+3} d\rho - \frac{2r^{2-k}}{(k-1)} \int_r^1 \rho^{p+q+k+1} d\rho, \\
&= -\frac{4r^{p+q+4}}{(p+q+k+2)(p+q-k+4)} - \frac{2r^{2-k}}{(k-1)(p+q+2+k)}.
\end{aligned}
$$

For $k < 1$ and $(p + q + k + 2) = 0$,

$$
I_{5,k}^{(4)}(r) = \frac{r^{2-k}}{(k-1)^2} + 2\frac{2r^{2-k} \log r}{(k-1)}.
$$

For $k < 1$ and $(p+q-k+4) = 0$, $I_{5,k}^{(4)}(r) = \infty$ as f is not in L^1.

For $k > 1$, $(p+q+k+2)(p+q-k+4) \neq 0$,

$$
\begin{aligned}
I_{5,k}^{(4)}(r) &= \frac{2r}{(k-1)} \int_0^r \left(\frac{\rho}{r}\right)^{(k-1)} \rho^{p+q+2} d\rho + \frac{2r}{(k-1)} \int_r^1 \left(\frac{r}{\rho}\right)^{(k-1)} \rho^{p+q+2} d\rho, \\
&= \frac{2r^{2-k}}{(k-1)} \int_0^r \rho^{p+q+k+1} d\rho + \frac{2r^k}{(k-1)} \int_r^1 \rho^{p+q-k+3} d\rho, \\
&= -\frac{4r^{p+q+4}}{(p+q+k+2)(p+q-k+4)} + \frac{2r^k}{(k-1)(p+q+4-k)}.
\end{aligned}
$$

For $k > 1$ and $(p+q-k+4) = 0$,

$$
I_{5,k}^{(4)}(r) = \frac{r^k}{(k-1)^2} - \frac{2r^k \log r}{(k-1)}.
$$

For $k > 1$ and $(p+q+k+2) = 0$, $I_{5,k}^{(4)}(r) = \infty$ as f is not in L^1.

For $k = -1$,

$$
\begin{aligned}
I_{5,k}^{(4)}(r) &= -4r \int_0^r \rho^{p+q+2} \log r d\rho + 4r \int_r^1 \rho^{p+q+2} \log \rho d\rho \\
&= \frac{4r}{(p+q+3)^2} \left[1 - r^{p+q+3}\right] \quad \text{when} \quad (p+q+3) \neq 0.
\end{aligned}
$$

For $k = -1$ and $p+q+3 = 0$, $I_{5,k}^{(4)}(r) = \infty$ as f is not in L^1. So we have for the nonzero Fourier coefficient of $I_6(z)$ and $I_7(z)$,

$$
\begin{aligned}
I_{6,k}(r) &= \frac{2(1-r^2)r^k}{(k+1)} \int_0^1 \rho^{(k+1)}(1-\rho^2) f_k(\rho) d\rho & k \geq 0 \\
&= \frac{2(1-r^2)r^k}{(k+1)} \int_0^1 \rho^{(k+1)}(1-\rho^2)\rho^{p+q} d\rho \\
&= \frac{2(1-r^2)r^k}{(k+1)} \left[\frac{1}{p+q+k+2} - \frac{1}{p+q+k+4}\right] & k \geq 0.
\end{aligned}
$$

Hence,

$$
I_{6,k}(r) = \begin{cases} \frac{2(1-r^2)r^k}{(k+1)} \left[\frac{1}{p+q+k+2} - \frac{1}{p+q+k+4} \right], & \text{if} \quad p+q+k \neq -2, -4, \\ 0, & \text{if} \quad k < 0, \\ \infty, & \text{if} \quad p+q+k = -2, -4. \end{cases}
$$

$$
\begin{aligned}
I_{7,k}(r) &= \frac{2(1-r^2)r^{-k}}{(1-k)} \int_0^1 \rho^{(1-k)}(1-\rho^2) f_k(\rho) d\rho && k \leq 0 \\
&= \frac{2(1-r^2)r^{-k}}{(1-k)} \int_0^1 \rho^{(1-k)}(1-\rho^2)\rho^{p+q} d\rho \\
&= \frac{2(1-r^2)r^{-k}}{(1-k)} \left[\frac{1}{p+q-k+2} - \frac{1}{p+q-k+4} \right] && k \leq 0.
\end{aligned}
$$

Hence,

$$
I_{7,k}(r) = \begin{cases} \frac{2(1-r^2)r^{-k}}{(1-k)} \left[\frac{1}{p+q-k+2} - \frac{1}{p+q-k+4} \right], & \text{if} \quad p+q-k \neq -2, -4 \\ 0, & \text{if} \quad k > 0, \\ \infty, & \text{if} \quad p+q-k = -2, -4. \end{cases}
$$

5. THEORETICAL FOUNDATION: DIRICHLET-NEUMANN BIHARMONIC PROBLEMS

In this section, we explore the Neumann (D3) biharmonic problem given by the following theorems [7],[8].

5.1 Mathematical Formulation Of Dirichlet-Neumann Biharmonic Problem

Theorem 5.1.1. *The Dirichlet-Neumann1 (D3) problem for the biharmonic equation is given by*

$$\begin{cases} (\partial_z \partial_{\bar{z}})^2 \omega \ = f, & in \quad \mathbf{D}, \\ \omega \ = h_0, & on \quad \partial\mathbf{D}, \\ \partial_\nu \omega \ = h_1, & on \quad \partial\mathbf{D}, \end{cases} \tag{D3}$$

is uniquely solvable for $f \in L_1(\mathbf{D}, \mathbb{C})$, $h_0 \in C^2(\partial\mathbf{D}; \mathbb{C})$, $h_1 \in C^1(\partial\mathbf{D}; \mathbb{C})$ and the solution is given by

$$\omega(z) = \frac{(1+|z|^2)}{4\pi i} \int_{\partial\mathbf{D}} g_1(z,\zeta) h_0(\zeta) \frac{d\zeta}{\zeta} + \frac{(1-|z|^2)}{4\pi i} \int_{\partial\mathbf{D}} g_2(z,\zeta) h_0(\zeta) \frac{d\zeta}{\zeta}$$

$$- \frac{(1-|z|^2)}{2\pi i} \int_{\partial\mathbf{D}} g_1(z,\zeta) h_1(\zeta) \frac{d\zeta}{\zeta} - \frac{1}{\pi} \iint_D G_2(z,\zeta) f(\zeta) d\xi d\eta,$$

where

$$g_2(z,\zeta) \ = \ \frac{1}{(1-z\bar{\zeta})^2} + \frac{1}{(1-\bar{z}\zeta)^2} - 1,$$

and $G_2(z, \zeta)$ is the Green's function for the biharmonic problem with (D3) *boundary condition given by*

$$G_2(z, \zeta) = |\zeta - z|^2 \log \left| \frac{1 - z\bar{\zeta}}{\zeta - z} \right|^2 - (1 - |z|^2)(1 - |\zeta|^2).$$

We write $\omega(z)$ as

$$\omega(z) = u_3(z) + h_3(z) + r_3(z) + I_3(z) + I_4(z) + I_5(z) \tag{5.1}$$

where

$$u_3(z) = \frac{(1 + |z|^2)}{4\pi i} \int_{\partial \mathbf{D}} g_1(z, \zeta) h_0(\zeta) \frac{d\zeta}{\zeta}, \tag{5.2}$$

$$h_3(z) = \frac{(1 - |z|^2)}{4\pi i} \int_{\partial \mathbf{D}} g_2(z, \zeta) h_0(\zeta) \frac{d\zeta}{\zeta}, \tag{5.3}$$

$$r_3(z) = -\frac{(1 - |z|^2)}{4\pi i} \int_{\partial \mathbf{D}} g_1(z, \zeta) h_1(\zeta) \frac{d\zeta}{\zeta}. \tag{5.4}$$

Notice that $I_3(z), I_4(z), I_5(z)$ are same as (3.17), (3.18), (3.19) as the Green's function associated is same as in the (D1) biharmonic problem and hence the associated integrals are same. So, we focus on the boundary integrals here.

Theorem 5.1.2. *If $\omega(r, \alpha)$ is the solution of the (D3) biharmonic problem mentioned in Thm. 5.1.1, $z = re^{i\alpha}$, $f(re^{i\alpha}) = \sum_{n=-\infty}^{\infty} f_n(r)e^{in\alpha}$, $h_0(re^{i\alpha}) = \sum_{n=-\infty}^{\infty} a_n(r)e^{in\alpha}$, and $h_1(re^{i\alpha}) = \sum_{n=-\infty}^{\infty} b_n(r)e^{in\alpha}$, then the Fourier coefficients $\omega_n(r)$ of $\omega(r, \alpha)$ can be*

55

written as

$$\omega_n(r) = I_{3,n}(r) + I_{4,n}(r) + I_{5,n}(r) + u_{3,n}(r) + h_{3,n}(r) + r_{3,n}(r),$$

where the boundary integrals are

$$u_{3,n}(r) = \begin{cases} \frac{1+r^2}{2} r^{|n|} a_n, & if\, n \neq 0, \\ \frac{1+r^2}{2} a_0, & if\ n = 0, \end{cases}$$

$$h_{3,n}(r) = \begin{cases} \frac{(1-r^2)}{2} \frac{(2)_n}{(n)} r^n a_n, & if\, n > 0, \\ \frac{(1-r^2)}{2} \frac{(2)_{-n}}{(-n)} r^{-n} a_n, & if\, n < 0, \\ \frac{(1-r^2)}{2} a_0, & if\ n = 0, \end{cases}$$

$$r_{3,n}(r) = \begin{cases} -\frac{(1-r^2)}{2} b_n r^{|n|}, & if\, n \neq 0, \\ -\frac{(1-r^2)}{2} b_0, & if\ n = 0. \end{cases}$$

The Fourier coefficients $I_{3,n}(r), I_{4,n}(r), I_{5,n}(r)$ have already been evaluated in Section.4.

Proof. Let $\omega(z) = u_3(z) + h_3(z) + r_3(z) + I_3(z) + I_4(z) + I_5(z)$, where

$$u_3(z) = \frac{(1+r^2)}{4\pi i} \int_{\partial \mathbf{D}} g_1(z,\zeta) h_0(\zeta) \frac{d\zeta}{\zeta}, \tag{5.5}$$

$$h_3(z) = \frac{(1-|z|^2)}{4\pi i} \int_{\partial \mathbf{D}} g_2(z,\zeta) h_0(\zeta) \frac{d\zeta}{\zeta}, \tag{5.6}$$

$$r_3(z) = -\frac{(1-|z|^2)}{4\pi i} \int_{\partial \mathbf{D}} g_1(z,\zeta) h_1(\zeta) \frac{d\zeta}{\zeta}. \tag{5.7}$$

$I_3(z), I_4(z), I_5(z)$ are same as in (3.17),(3.18),(3.19). Now we compute the above

56

boundary integrals (5.5),(5.6), (5.7). Simple analysis for $u_3(z)$ shows that

$$
\begin{aligned}
u_3^{(1)}(z) &= \frac{(1+r^2)}{4\pi} \int_0^{2\pi} \frac{h_0(e^{i\theta})}{1 - re^{i(\alpha-\theta)}} d\theta \\
&= \sum_{n=0}^{\infty} \frac{(1+r^2)}{4\pi} \int_0^{2\pi} h_0(e^{i\theta}) r^n e^{in(\alpha-\theta)} d\theta \\
&= \sum_{n=0}^{\infty} \frac{(1+r^2)}{4\pi} \int_0^{2\pi} \sum_{m=-\infty}^{\infty} a_m e^{im\theta} r^n e^{in(\alpha-\theta)} d\theta \\
&= \sum_{n=0}^{\infty} \frac{(1+r^2)}{4\pi} r^n e^{in\alpha} \sum_{m=-\infty}^{\infty} a_m \int_0^{2\pi} e^{i(m-n)\theta} d\theta \\
&= \sum_{n=0}^{\infty} a_n \frac{(1+r^2)}{2} r^n e^{in\alpha}.
\end{aligned}
$$

$$u_3^{(2)}(z) = \frac{(1+r^2)}{4\pi} \int\limits_0^{2\pi} \frac{h_0(e^{i\theta})}{1 - re^{i(\theta-\alpha)}} d\theta$$

$$= \sum_{n=0}^{\infty} \frac{(1+r^2)}{4\pi} \int\limits_0^{2\pi} h_0(e^{i\theta}) r^n e^{in(\theta-\alpha)} d\theta$$

$$= \sum_{n=0}^{\infty} \frac{(1+r^2)}{4\pi} \int\limits_0^{2\pi} \sum_{m=-\infty}^{\infty} a_m e^{im\theta} r^n e^{in(\theta-\alpha)} d\theta$$

$$= \sum_{n=0}^{\infty} \frac{(1+r^2)}{4\pi} r^n e^{-in\alpha} \sum_{m=-\infty}^{\infty} a_m \int\limits_0^{2\pi} e^{i(m+n)\theta} d\theta$$

$$= \sum_{n=0}^{\infty} a_{-n} \frac{1+r^2}{2} r^n e^{-in\alpha}.$$

$$u_3^{(3)}(z) = -\frac{(1+r^2)}{4\pi} \int\limits_0^{2\pi} h(e^{i\theta}) d\theta$$

$$= -\frac{(1+r^2)}{4\pi} \int\limits_0^{2\pi} \sum_{m=-\infty}^{\infty} a_m e^{im\theta} d\theta$$

$$= -\frac{(1+r^2)}{4\pi} \sum_{m=-\infty}^{\infty} \frac{1+r^2}{2} a_m \int\limits_0^{2\pi} e^{im\theta} d\theta$$

$$= -\frac{(1+r^2)}{2} a_0.$$

Hence,

$$u_{3,n}(r) = \begin{cases} \frac{(1+r^2)}{2} r^{|n|} a_n, & \text{if } n \neq 0, \\ \frac{(1+r^2)}{2} a_0, & \text{if } n = 0. \end{cases}$$

Similar is the analysis for $r_{3n}(r)$. For $h_3(z)$ we write,

$$h_3(z) = h_3^{(1)}(z) + h_3^{(2)}(z) + h_3^{(3)}(z)$$

where

$$h_3^{(1)}(z) = \frac{(1-|z|^2)}{4\pi i} \int\limits_{\partial \mathbf{D}} \frac{h_0(\zeta)}{(1-z\bar\zeta)^2} \frac{d\zeta}{\zeta}, \tag{5.8}$$

$$h_3^{(2)}(z) = \frac{(1-|z|^2)}{4\pi i} \int\limits_{\partial \mathbf{D}} \frac{h_0(\zeta)}{(1-\bar z\zeta)^2} \frac{d\zeta}{\zeta}, \tag{5.9}$$

$$h_3^{(3)}(z) = -\frac{(1-|z|^2)}{4\pi i} \int\limits_{\partial \mathbf{D}} h_0(\zeta) \frac{d\zeta}{\zeta}. \tag{5.10}$$

We first evaluate $h_3^{(1)}(z), h_3^{(2)}(z)$ and $h_3^{(3)}(z)$ to compute $h_3(z)$. Let $z = re^{i\alpha}, \quad \zeta = \rho e^{i\theta}$ where $r, \quad \rho \neq 0$ and $h_0(e^{i\theta}) = \sum\limits_{m=-\infty}^{\infty} a_m e^{im\theta}$ and $h_3(z) = \sum\limits_{n=-\infty}^{\infty} h_{3n}(r)e^{in\alpha}$. Since $|r| < 1$ and $\rho = 1$ on the boundary, we have

$$\begin{aligned}
h_3^{(1)}(z) &= \frac{(1-|z|^2)}{4\pi} \int\limits_0^{2\pi} \frac{h_0(e^{i\theta})}{(1-re^{i(\alpha-\theta)})^2} d\theta \\
&= \frac{(1-r^2)}{4\pi} \sum\limits_{n=0}^{\infty} \frac{(2)_n}{n} r^n \int\limits_0^{2\pi} h_0(e^{i\theta}) e^{in(\alpha-\theta)} d\theta \\
&= \frac{(1-r^2)}{4\pi} \sum\limits_{n=0}^{\infty} \frac{(2)_n}{n} r^n e^{in\alpha} \sum\limits_{m=-\infty}^{\infty} a_m \int\limits_0^{2\pi} e^{i(m-k)\theta} d\theta \\
&= \frac{(1-r^2)}{2} \sum\limits_{n=0}^{\infty} \frac{(2)_n}{n} r^n e^{in\alpha} a_n,
\end{aligned}$$

where $(x)_n = x(x+1)(x+2)......(x+n-1)$.

$$
\begin{aligned}
h_3^{(2)}(z) &= \frac{(1 - |z|^2)}{4\pi} \int_0^{2\pi} \frac{h_0(e^{i\theta})}{(1 - re^{i(\theta - \alpha)})^2} d\theta \\
&= \frac{(1 - r^2)}{4\pi} \sum_{n=0}^{\infty} \frac{(2)_n}{n} r^n \int_0^{2\pi} h_0(e^{i\theta}) e^{in(\alpha - \theta)} d\theta \\
&= \sum_{n=0}^{\infty} \frac{1}{2\pi} \int_0^{2\pi} \sum_{m=-\infty}^{\infty} a_m e^{im\theta} r^n e^{in(\theta - \alpha)} d\theta \\
&= \frac{(1 - r^2)}{4\pi} \sum_{n=0}^{\infty} \frac{(2)_n}{n} r^n e^{-in\alpha} \sum_{m=-\infty}^{\infty} a_m \int_0^{2\pi} e^{i(m+k)\theta} d\theta \\
&= \frac{(1 - r^2)}{2} \sum_{n=0}^{\infty} \frac{(2)_n}{n} r^n e^{-in\alpha} a_{-n} \\
h_3^{(3)}(z) &= -\frac{(1 - r^2)}{4\pi} \int_0^{2\pi} h_0(e^{i\theta}) d\theta \\
&= -\frac{(1 - r^2)}{4\pi} \int_0^{2\pi} \sum_{m=-\infty}^{\infty} a_m e^{im\theta} d\theta \\
&= -\frac{(1 - r^2)}{2} a_0.
\end{aligned}
$$

So,

$$
h_{3,n}(r) = \begin{cases}
\frac{(1-r^2)}{2} \frac{(2)_n}{(n)} r^n a_n, & \text{if } n > 0, \\
\frac{(1-r^2)}{2} \frac{(2)_{-n}}{(-n)} r^{-n} a_n, & \text{if } n < 0, \\
\frac{(1-r^2)}{2} a_0, & \text{if } n = 0.
\end{cases}
$$

Hence we obtain the proof for Thm.5.1.2 $\qquad\qquad \square$

The second approach for solving the Dirichlet-Neumann1(D3) problem is same as in (D1) and for the sake of completeness we provide here the decomposition.

$$
\omega = \omega_1 + \omega_2
$$

60

where ω_1 and ω_2 satisfy

$$\begin{cases} (\partial_z\partial_{\bar{z}})u & = f, & \text{in} \quad \mathbf{D} \\ u & = 0, & \text{on} \quad \partial\mathbf{D} \end{cases}$$

$$\begin{cases} (\partial_z\partial_{\bar{z}})\omega_1 & = u, & \text{in} \quad \mathbf{D} \\ \omega_1 & = h_0, & \text{on} \quad \partial\mathbf{D} \end{cases}$$

and

$$\begin{cases} (\partial_z\partial_{\bar{z}})^2\omega_2 & = 0, & \text{in} \quad \mathbf{D} \\ \omega_2 & = 0, & \text{on} \quad \partial\mathbf{D} \\ \partial_\nu\omega_2 & = h_1 - \partial_\nu\omega_1, & \text{on} \quad \partial\mathbf{D} \end{cases}$$

As discussed earlier we solve the Poisson problems with our Poisson solver and for the homogeneous biharmonic problem we just need the boundary integrals from the first approach. We now consider Dirichlet-Neumann2((D4)) biharmonic problem and we obtain the following theorem from ([7],[3]).

Theorem 5.1.3. *The Dirichlet-Neumann2* (D4) *problem for the biharmonic equation given by*

$$\begin{cases} (\partial_z\partial_{\bar{z}})^2 w & = f & \text{in} \quad \mathbf{D}, \\ w & = h_0 & \text{on} \quad \partial\mathbf{D}, \\ \partial_\nu w_{z\bar{z}} & = h_2 & \text{on} \quad \partial\mathbf{D}, \end{cases} \tag{D4}$$

is uniquely solvable for $f \in L_1(\mathbf{D}, \mathbb{C}) \quad h_0, h_2 \in (\partial\mathbf{D}; \mathbb{C})$ if and only if $\frac{1}{4i} \int_{\partial\mathbf{D}} h_2(\zeta)\frac{d\zeta}{\zeta} =$

$\int_{\mathbf{D}} f(\zeta) d\xi d\eta$ and the solution obtained directly using the Green's function is given by

$$w(z) = k(|z|^2 - 1) + \frac{1}{2\pi i} \int_{\partial \mathbf{D}} g_1(z, \zeta) g_0(\zeta) \frac{d\zeta}{\zeta} + \frac{1}{4\pi i} \int_{\partial \mathbf{D}} G_{13}(z, \zeta) g_3(\zeta) \frac{d\zeta}{\zeta}$$

$$- \frac{1}{\pi} \iint_{\mathbf{D}} G_{13}(z, \zeta) f(\zeta) d\xi d\eta, \tag{5.11}$$

where

$$G_{13}(z, \zeta) = -|\zeta - z|^2 \log |\zeta - z|^2$$

$$- (1 - |z|^2) \left(4 + \frac{(1 - z\bar{\zeta})}{z\bar{\zeta}} \log(1 - z\bar{\zeta}) + \frac{(1 - \bar{z}\zeta)}{\bar{z}\zeta} \log(1 - \bar{z}\zeta) \right)$$

$$- \frac{(\zeta - z)(1 - z\bar{\zeta})}{z} \log(1 - z\bar{\zeta})$$

$$- \frac{\overline{(\zeta - z)}(1 - \bar{z}\zeta)}{\bar{z}} \log(1 - \bar{z}\zeta). \tag{5.12}$$

In order to construct the algorithm we evaluate the following integrals to obtain the solution of the (D4) problem.

$$u^{(1)}(z) = \frac{1}{2\pi i} \int_{\partial \mathbf{D}} g_1(z, \zeta) h_0(\zeta) \frac{d\zeta}{\zeta}. \tag{5.13}$$

$$V(z) = \frac{1}{4\pi i} \int_{\partial \mathbf{D}} G_{13}(z, \zeta) h_2(\zeta) \frac{d\zeta}{\zeta}. \tag{5.14}$$

$$I(z) = -\frac{1}{\pi} \int_{\mathbf{D}} G_{13}(z, \zeta) f(\zeta) d\xi d\eta. \tag{5.15}$$

We notice here $u^{(1)}(z)$ is similar to (5.2). So we evaluate $V(z)$ and $I(z)$. We write

$$V(z) = V^{(1)}(z) + V^{(2)}(z) + V^{(3)}(z) + V^{(4)}(z)$$

where

$$V^{(1)}(z) = -\frac{1}{4\pi i}\int\limits_{\partial\mathbf{D}} |\zeta - z|^2 \log|\zeta - z|^2 h_2(\zeta)\frac{d\zeta}{\zeta},$$

$$V^{(2)}(z) = -\frac{(1-|z|^2)}{4\pi i}\int\limits_{\partial\mathbf{D}}\left(4 + \frac{(1-z\bar\zeta)}{z\bar\zeta}\log(1-z\bar\zeta) + \frac{(1-\bar z\zeta)}{\bar z\zeta}\log(1-\bar z\zeta)\right)h_2(\zeta)\frac{d\zeta}{\zeta},$$

$$V^{(3)}(z) = -\frac{1}{4\pi i}\int\limits_{\partial\mathbf{D}} \frac{(\zeta - z)(1-z\bar\zeta)}{z}\log(1-z\bar\zeta)h_2(\zeta)\frac{d\zeta}{\zeta},$$

$$V^{(4)}(z) = -\frac{1}{4\pi i}\int\limits_{\partial\mathbf{D}} \frac{\overline{(\zeta - z)}(1-\bar z\zeta)}{\bar z}\log(1-\bar z\zeta)h_2(\zeta)\frac{d\zeta}{\zeta}.$$

Also we write $I(z) = I^{(1)}(z) + I^{(2)}(z) + I^{(3)}(z) + I^{(4)}(z) + I^{(5)}(z) + I^{(6)}(z)$

where,

$$I^{(1)}(z) = \frac{2}{\pi}\int\limits_{\mathbf{D}} |\zeta - z|^2 \log|\zeta - z| f(\zeta)d\xi d\eta,$$

$$I^{(2)}(z) = \frac{4}{\pi}(1-|z|^2)\int\limits_{\mathbf{D}} f(\zeta)d\xi d\eta,$$

$$I^{(3)}(z) = \frac{(1-|z|^2)}{\pi z}\int\limits_{\mathbf{D}} \frac{(1-z\bar\zeta)}{\bar\zeta}\log(1-z\bar\zeta)f(\zeta)d\xi d\eta,$$

$$I^{(4)}(z) = \frac{(1-|z|^2)}{\pi\bar z}\int\limits_{\mathbf{D}} \frac{(1-\bar z\zeta)}{\zeta}\log(1-\bar z\zeta)f(\zeta)d\xi d\eta,$$

$$I^{(5)}(z) = \frac{1}{\pi z}\int\limits_{\mathbf{D}} \frac{(\zeta - z)(1-z\bar\zeta)}{z}\log(1-z\bar\zeta)f(\zeta)d\xi d\eta,$$

$$I^{(6)}(z) = \frac{1}{\pi\bar z}\int\limits_{\mathbf{D}} \frac{\overline{(\zeta - z)}(1-\bar z\zeta)}{\bar z}\log(1-\bar z\zeta)f(\zeta)d\xi d\eta.$$

5.1.1 Evaluation Of The Integrals

Now we evaluate each of the boundary integral $V^{(i)}(z)$ for $i = 1, 2, 3, 4$. We note the following.

$$|1 - z\bar{\zeta}|^2 \log|1 - z\bar{\zeta}| = -(1 - \bar{z}\zeta - z\bar{\zeta} + r^2)\left(\sum_{n \neq 0} \frac{|z\bar{\zeta}|^{|n|}}{2|n|} e^{in\tau}\right).$$

Now,

$$
\begin{aligned}
V^{(1)}(z) &= -\frac{1}{4\pi i}\int_{\partial \mathbf{D}} |\zeta - z|^2 \log|\zeta - z|^2 h_2(\zeta)\frac{d\zeta}{\zeta} \\
&= -\frac{1}{2\pi i}\int_{\partial \mathbf{D}} |1 - z\bar{\zeta}|^2 \log|1 - z\bar{\zeta}| h_2(\zeta)\frac{d\zeta}{\zeta} \\
&= \frac{1}{2\pi i}\int_{\partial \mathbf{D}} (1 - \bar{z}\zeta - z\bar{\zeta} + r^2)\left(\sum_{n \neq 0} \frac{|z\bar{\zeta}|^{|n|}}{2|n|} e^{in\tau}\right) h_2(\zeta)\frac{d\zeta}{\zeta}.
\end{aligned}
$$

Let $V^{(1)}(z) = V_1^{(1)}(z) + V_2^{(1)}(z) + V_3^{(1)}(z)$ and $h_2(e^{i\theta}) = \sum_{n=-\infty}^{\infty} c_n e^{in\theta}$. Now we evaluate the boundary integrals $V_i^{(1)}(z)$ for $i = 1, 2, 3$.

$$
\begin{aligned}
V_1^{(1)}(z) &= \frac{(1 + r^2)}{2\pi i}\int_{\partial \mathbf{D}} \sum_{n \neq 0} \frac{|z\bar{\zeta}|^{|n|}}{2|n|} e^{in\tau} h_2(\zeta)\frac{d\zeta}{\zeta} \\
&= \frac{(1 + r^2)}{2\pi i} \sum_{n \neq 0} \frac{r^{|n|}}{2|n|} \int_0^{2\pi} e^{in(\alpha - \theta)} h_2(e^{i\theta})d\theta \\
&= \frac{(1 + r^2)}{2\pi} \sum_{n \neq 0} \frac{r^{|n|}}{2|n|} e^{in\alpha} \sum_{m=-\infty}^{\infty} c_m \int_0^{2\pi} e^{i(m-n)\theta}d\theta \\
&= (1 + r^2) \sum_{n \neq 0} \frac{r^{|n|}}{2|n|} e^{in\alpha} c_n.
\end{aligned}
$$

64

Hence,

$$
V_{1,n}^{(1)}(r) = \begin{cases} \frac{1+r^2}{2n} r^n c_n, & \text{if } n > 0, \\[2mm] -\frac{1+r^2}{2n} r^{-n} c_n, & \text{if } n < 0, \\[2mm] 0, & \text{if } n = 0. \end{cases}
$$

$$
\begin{aligned}
V_2^{(1)}(z) &= -\frac{\bar{z}}{2\pi i} \int_{\partial \mathbf{D}} \sum_{n \neq 0} \frac{|z\bar{\zeta}|^{|n|}}{2|n|} e^{in\tau} h_2(\zeta) d\zeta \\[2mm]
&= -\frac{\bar{z}}{2\pi} \sum_{n \neq 0} \frac{r^{|n|}}{2|n|} \int_0^{2\pi} e^{in\tau} h_2(e^{i\theta}) e^{i\theta} d\theta \\[2mm]
&= -\frac{\bar{z}}{2\pi} \sum_{n \neq 0} \frac{r^{|n|}}{2|n|} e^{in\alpha} \sum_{m=-\infty}^{\infty} c_m \int_0^{2\pi} e^{i(m+1-n)\theta} d\theta \\[2mm]
&= -\bar{z} \sum_{n \neq 0} \frac{r^{|n|}}{2|n|} e^{in\alpha} c_{n-1}
\end{aligned}
$$

Hence,

$$
V_{2,n}^{(1)}(r) = \begin{cases} -\frac{r^{n+2}}{2(n+1)} c_n, & \text{if } n > -1, \\[2mm] \frac{r^{-n}}{2(n+1)} c_n, & \text{if } n < -1, \\[2mm] 0, & \text{if } n = -1. \end{cases}
$$

$$
\begin{aligned}
V_2^{(1)}(z) &= -\frac{z}{2\pi i} \int_{\partial \mathbf{D}} \sum_{n \neq 0} \frac{|z\bar{\zeta}|^{|n|}}{2|n|} e^{in\tau} \bar{\zeta}^2 h_2(\zeta) d\zeta \\[2mm]
&= -\frac{\bar{z}}{2\pi} \sum_{n \neq 0} \frac{r^{|n|}}{2|n|} \int_0^{2\pi} e^{in\tau} e^{-2i\theta} h_2(e^{i\theta}) e^{i\theta} d\theta \\[2mm]
&= -\frac{\bar{z}}{2\pi} \sum_{n \neq 0} \frac{r^{|n|}}{2|n|} e^{in\alpha} \sum_{m=-\infty}^{\infty} c_m \int_0^{2\pi} e^{i(m-1-n)\theta} d\theta \\[2mm]
&= -\bar{z} \sum_{n \neq 0} \frac{r^{|n|}}{2|n|} e^{in\alpha} c_{n-1}.
\end{aligned}
$$

Hence,

$$
V_{3,n}^{(1)}(r) = \begin{cases} -\frac{r^n}{2(n-1)}c_n, & \text{if } n > 1, \\ \frac{r^{2-n}}{2(n-1)}c_n, & \text{if } n < 1, \\ 0, & \text{if } n = 1. \end{cases}
$$

We now evaluate $V^{(2)}(z)$. We write $V^{(2)}(z) = V_1^{(2)}(z) + V_2^{(2)}(z) + V_3^{(2)}(z)$ and evaluate each of $V_i^{(2)}(z), i = 1, 2, 3$.

$$
V_1^{(2)}(z) = \frac{(|z|^2 - 1)}{\pi i} \int_{\partial \mathbf{D}} h_2(\zeta) \frac{d\zeta}{\zeta}
$$

$$
= \frac{(r^2 - 1)}{\pi} \int_0^{2\pi} h_2(e^{i\theta}) d\theta
$$

$$
= \frac{(r^2 - 1)}{\pi} \sum_{m \neq 0} \int_0^{2\pi} e^{im\theta} d\theta
$$

$$
= 2(r^2 - 1)c_0. \tag{5.16}
$$

$$
V_2^{(2)}(z) = \frac{(|z|^2 - 1)}{4\pi i z} \int_{\partial \mathbf{D}} (1 - z\bar{\zeta}) \log(1 - z\bar{\zeta}) h_2(\zeta) d\zeta
$$

$$
= \frac{(r^2 - 1)}{4\pi i z} \int_{\partial \mathbf{D}} (1 - z\bar{\zeta}) \sum_{n=1}^{\infty} -\frac{(z\bar{\zeta})^n}{n} h_2(\zeta) d\zeta
$$

$$
= \frac{(1 - r^2)}{4\pi z} \sum_{n=1}^{\infty} \frac{z^n}{n} \int_0^{2\pi} e^{-in\theta} h_2(e^{i\theta}) e^{i\theta} d\theta + \frac{(r^2 - 1)}{4\pi} \sum_{n=1}^{\infty} \frac{z^n}{n} \int_0^{2\pi} e^{-in\theta} h_2(e^{i\theta}) d\theta
$$

$$
= \frac{(1 - r^2)}{4\pi z} \sum_{n=1}^{\infty} \frac{z^n}{n} \left(\sum_{m=-\infty}^{\infty} c_m \int_0^{2\pi} e^{i(m+1-n)\theta} d\theta \right)
$$

$$
+ \frac{(r^2 - 1)}{4\pi} \sum_{n=1}^{\infty} \frac{z^n}{n} \left(\sum_{m=-\infty}^{\infty} c_m \int_0^{2\pi} e^{i(m-n)\theta} d\theta \right)
$$

Hence,

$$V_{2,n}^{(2)}(r) = \begin{cases} \frac{(1-r^2)}{2}c_0, & \text{if } n = 0, \\ \frac{(r^2-1)r^n}{2n(1+n)}c_n, & \text{if } n \geq 1, \\ 0, & \text{if } n < 0. \end{cases} \tag{5.17}$$

$$\begin{aligned} V_3^{(2)}(z) = & = \frac{|z|^2-1}{4\pi i \bar{z}} \int_{\partial \mathbf{D}} \frac{(1-\bar{z}\zeta)}{\zeta^2} \log(1-\bar{z}\zeta)h_2(\zeta)d\zeta \\ & = \frac{(|z|^2-1)}{4\pi i \bar{z}} \int_{\partial \mathbf{D}} \frac{(1-\bar{z}\zeta)}{\zeta^2} \left(\sum_{n=1}^{\infty} -\frac{(\bar{z}\zeta)^n}{n} h_2(\zeta)d\zeta \right) \\ & = \frac{(1-r^2)}{4\pi i \bar{z}} \left(\sum_{n=1}^{\infty} \frac{\bar{z}^n}{n} \int_{\partial \mathbf{D}} \zeta^{n-2} h_2(\zeta)d\zeta \right) \\ & \quad + \frac{(r^2-1)}{4\pi i \bar{z}} \left(\sum_{n=1}^{\infty} \frac{\bar{z}^n}{n} \int_{\partial \mathbf{D}} \zeta^{n-1} h_2(\zeta)d\zeta \right) \\ & = \frac{(1-r^2)}{4\pi} \sum_{n=1}^{\infty} \frac{(\bar{z})^{n-1}}{n} \left(\sum_{m=-\infty}^{\infty} c_m \int_0^{2\pi} e^{i(m+n-1)\theta} d\theta \right) \\ & \quad + \frac{(r^2-1)}{4\pi} \frac{\bar{z}^n}{n} \left(\sum_{m=-\infty}^{\infty} c_m \int_0^{2\pi} e^{i(m+n)\theta} d\theta \right) \end{aligned}$$

Hence,

$$V_{3,n}^{(2)}(r) = \begin{cases} \frac{(1-r^2)}{2}c_0, & \text{if } n = 0, \\ \frac{(1-r^2)r^{-n}}{2n(1-n)}c_n, & \text{if } n \leq -1, \\ 0, & \text{if } n > 0. \end{cases} \tag{5.18}$$

67

Combining (5.16), (5.17), (5.18) we have,

$$V_n^{(2)}(r) = \begin{cases} (r^2 - 1)c_0, & \text{if } n = 0, \\ \frac{(1-r^2)r^{-n}}{2n(1-n)}c_n, & \text{if } n \leq -1, \\ \frac{(r^2-1)r^n}{2n(1+n)}c_n, & \text{if } n \geq 1. \end{cases} \tag{5.19}$$

We now evaluate $V^{(3)}(z) = -\frac{1}{4\pi i}\int_{\partial \mathbf{D}} \frac{(\zeta-z))1-z\bar{\zeta})}{z}\log(1-\bar{z}\zeta)h_2(\zeta)\frac{d\zeta}{\zeta}$. We write $V^{(3)}(z) = V_1^{(3)}(z) + V_2^{(3)}(z) + V_3^{(3)}(z)$ and evaluate each of the integral $V_i^{(3)}(z), i = 1, 2, 3$.

$$\begin{aligned} V_1^{(3)}(z) &= -\frac{1}{4\pi i z}\int_{\partial \mathbf{D}} \log(1 - \bar{\zeta}z)h_2(\zeta)d\zeta \\ &= \frac{1}{4\pi i z}\sum_{n=1}^{\infty}\frac{z^n}{n}\int_{\partial \mathbf{D}} \bar{\zeta}^n h_2(\zeta)d\zeta \\ &= \frac{1}{4\pi}\sum_{n=1}^{\infty}\frac{z^{n-1}}{n}\sum_{m=-\infty}^{\infty}c_m\int_0^{2\pi} e^{i(m-n+1)\theta}d\theta \\ &= \frac{1}{2}\sum_{n=1}^{\infty}\frac{z^{n-1}}{n}c_{n-1}. \end{aligned} \tag{5.20}$$

$$\begin{aligned} V_2^{(3)}(z) &= \frac{1}{2\pi i}\int_{\partial \mathbf{D}} \bar{\zeta}\log(1 - \bar{\zeta}z)h_2(\zeta)d\zeta \\ &= -\frac{1}{2\pi i}\sum_{n=1}^{\infty}\frac{z^n}{n}\int_{\partial \mathbf{D}} \bar{\zeta}^{(n+1)}h_2(\zeta)d\zeta \\ &= -\frac{1}{2\pi}\sum_{n=1}^{\infty}\frac{z^n}{n}\sum_{m=-\infty}^{\infty}c_m\int_0^{2\pi} e^{i(m-n)\theta}d\theta \\ &= -\frac{1}{2}\sum_{n=1}^{\infty}\frac{z^n}{n}c_n. \end{aligned} \tag{5.21}$$

68

$$V_3^{(3)}(z) = \frac{z}{4\pi i} \int_{\partial \mathbf{D}} \bar{\zeta}^2 \log(1 - \bar{\zeta}z) h_2(\zeta) d\zeta$$

$$= \frac{z}{4\pi i} \sum_{n=1}^{\infty} \frac{z^n}{n} \int_{\partial \mathbf{D}} \bar{\zeta}^{(n+2)} h_2(\zeta) d\zeta$$

$$= \frac{1}{4\pi} \sum_{n=1}^{\infty} \frac{z^{n+1}}{n} \sum_{m=-\infty}^{\infty} c_m \int_0^{2\pi} e^{i(m-n-1)\theta} d\theta$$

$$= \frac{1}{2} \sum_{n=1}^{\infty} \frac{z^{n+1}}{n} c_{n+1}. \tag{5.22}$$

Combining (5.20), (5.21), (5.22) we obtain,

$$V_n^{(3)}(r) = \begin{cases} \frac{1}{2}c_0, & \text{if } n = 0, \\[2mm] -\frac{3}{4}rc_1, & \text{if } n = 1, \\[2mm] \frac{r^n}{2(n+1)}c_n - \frac{r^n}{n}c_n + \frac{r^n}{2(n-1)}c_n, & \text{if } n \geq 2. \\[2mm] 0, & \text{if } n < 0. \end{cases} \tag{5.23}$$

We now evaluate, $V^{(4)}(z) = -\frac{1}{4\pi i} \int_{\partial \mathbf{D}} \frac{\overline{(\zeta-z)(1-z\bar{\zeta})}}{z} \log(1-\bar{z}\zeta) h_2(\zeta) \frac{d\zeta}{\zeta}$. We write $V^{(4)}(z) = V_1^{(4)}(z) + V_2^{(4)}(z) + V_3^{(4)}(z)$ and evaluate each of $V_i^{(4)}(z), i = 1, 2, 3$.

$$V_1^{(4)}(z) = -\frac{1}{4\pi i\bar{z}} \int_{\partial \mathbf{D}} \bar{\zeta}^2 \log(1 - \bar{z}\zeta) h_2(\zeta) d\zeta$$

$$= \frac{1}{4\pi i\bar{z}} \sum_{n=1}^{\infty} \frac{\bar{z}^n}{n} \int_{\partial \mathbf{D}} \zeta^{n-2} h_2(\zeta) d\zeta$$

$$= \frac{1}{4\pi} \sum_{n=1}^{\infty} \frac{\bar{z}^{n-1}}{n} \sum_{m=-\infty}^{\infty} c_m \int_0^{2\pi} e^{i(m+n-1)\theta} d\theta$$

$$= \frac{1}{2} \sum_{n=1}^{\infty} \frac{\bar{z}^{n-1}}{n} c_{1-n}. \tag{5.24}$$

69

$$V_2^{(4)}(z) = \frac{1}{2\pi i} \int_{\partial \mathbf{D}} \bar{\zeta} \log(1 - \bar{z}\zeta) h_2(\zeta) d\zeta$$

$$= -\frac{1}{2\pi i} \sum_{n=1}^{\infty} \frac{\bar{z}^n}{n} \int_{\partial \mathbf{D}} \zeta^{(n-1)} h_2(\zeta) d\zeta$$

$$= -\frac{1}{2\pi} \sum_{n=1}^{\infty} \frac{\bar{z}^n}{n} \sum_{m=-\infty}^{\infty} c_m \int_0^{2\pi} e^{i(m+n)\theta} d\theta$$

$$= -\frac{1}{2} \sum_{n=1}^{\infty} \frac{\bar{z}^n}{n} c_{-n}. \tag{5.25}$$

$$V_3^{(4)}(z) = -\frac{\bar{z}}{4\pi i} \int_{\partial \mathbf{D}} \log(1 - \bar{z}\zeta) h_2(\zeta) d\zeta$$

$$= \frac{\bar{z}}{4\pi i} \sum_{n=1}^{\infty} \frac{\bar{z}^n}{n} \int_{\partial \mathbf{D}} \zeta^n h_2(\zeta) d\zeta$$

$$= \frac{1}{4\pi} \sum_{n=1}^{\infty} \frac{\bar{z}^{(n+1)}}{n} \sum_{m=-\infty}^{\infty} c_m \int_0^{2\pi} e^{i(m+n+1)\theta} d\theta$$

$$= \frac{1}{2} \sum_{n=1}^{\infty} \frac{\bar{z}^{(n+1)}}{n} c_{-n-1}. \tag{5.26}$$

Combining (5.24), (5.25), (5.26) we obtain,

$$V_n^{(4)}(r) = \begin{cases} \frac{1}{2} c_n, & \text{if } n = 0, \\ \frac{3}{4} r c_n, & \text{if } n = -1, \\ \frac{r^{-n}}{2(1-n)} c_n - \frac{r^{-n}}{n} c_n - \frac{r^n}{2(n+1)} c_n, & \text{if } n \le -2, \\ 0, & \text{if } n > 0. \end{cases} \tag{5.27}$$

Now we develop the integral $I(z)$ here. The idea is same as the Dirichlet problem, but we prove it here for the sake of clarity and completeness. Here the singular integral $I_1(z)$ is the same as in (3.19) and we skip the details.

So we start with the formulation of $I^{(2)}(z)$. Now,

$$I^{(2)}(z) = \frac{(1 - |z|^2)}{\pi} \tilde{I}^{(2)}(z) \tag{5.28}$$

where

$$\tilde{I}^{(2)}(z) = \int\limits_{\mathbf{D}} 4f(\zeta)d\xi d\eta.$$

The Fourier coeficients of $\tilde{I}^{(2)}(z)$ are given by

$$\begin{aligned}
\tilde{I}_n^{(2)}(r) &= \frac{1}{2\pi} \int\limits_{\mathbf{D}} f(\zeta) \int\limits_0^{2\pi} 4e^{-in\alpha} d\alpha d\xi d\eta \\
&= \frac{1}{2\pi} \int\limits_0^1 \int\limits_0^{2\pi} f(\rho, \theta)e^{-in\theta} \int\limits_{-\theta}^{2\pi-\theta} 4e^{-in\tau} d\tau \rho d\theta d\rho \\
&= 2\pi \int\limits_0^1 f_n(\rho)\tilde{G}_n^{(2)}(r, \rho)\rho d\rho. \tag{5.29}
\end{aligned}$$

where

$$\begin{aligned}
\tilde{G}_n^{(2)}(r, \rho) &= \frac{1}{2\pi} \int\limits_{-\theta}^{2\pi-\theta} 4e^{-in\tau} d\tau \\
&= \begin{cases} 4, & \text{if } n = 0, \\ 0, & \text{if } n \neq 0. \end{cases} \tag{5.30}
\end{aligned}$$

Substituting (5.30) in (5.29) and using (5.28) we obtain,

$$I_n^{(2)}(r) = \begin{cases} 8(1 - r^2) \int_0^1 f_n(\rho)\rho d\rho, & \text{if } n = 0, \\ 0, & \text{if } n \neq 0. \end{cases} \tag{5.31}$$

71

Let

$$I^{(3)}(z) = \frac{1 - |z|^2}{\pi} \tilde{I}^{(3)}(z) \tag{5.32}$$

where

$$\tilde{I}^{(3)}(z) = \int_{\mathbf{D}} \frac{(1 - z\bar{\zeta})}{z\bar{\zeta}} \log(1 - z\bar{\zeta}) f(\zeta) d\xi d\eta.$$

The Fourier coefficients of $\tilde{I}^{(3)}(z)$ are given by

$$\tilde{I}_n^{(3)}(r) = \frac{1}{2\pi} \int_{\mathbf{D}} f(\zeta) \int_0^{2\pi} \frac{(1 - z\bar{\zeta})}{z\bar{\zeta}} \log(1 - z\bar{\zeta}) e^{-in\alpha} d\alpha d\xi d\eta$$

$$= \frac{1}{2\pi} \int_0^1 \int_0^{2\pi} f(\rho, \theta) e^{-in\theta} \int_{-\theta}^{2\pi-\theta} \frac{(1 - z\bar{\zeta})}{z\bar{\zeta}} \log(1 - z\bar{\zeta}) e^{-in\tau} d\tau \rho d\theta d\rho$$

$$= 2\pi \int_0^1 f_n(\rho) \tilde{G}_{3,n}(r, \rho) \rho d\rho. \tag{5.33}$$

where

$$\tilde{G}_n^{(3)}(r, \rho) = \frac{1}{2\pi} \int_{-\theta}^{2\pi-\theta} \frac{(1 - z\bar{\zeta})}{z\bar{\zeta}} \log(1 - z\bar{\zeta}) e^{-in\tau} d\tau$$

$$= -\frac{1}{2\pi} \int_{-\theta}^{2\pi-\theta} \frac{(1 - z\bar{\zeta})}{z\bar{\zeta}} \sum_{m=1}^{\infty} \frac{(z\bar{\zeta})^m}{m} e^{-in\tau} d\tau$$

$$= -\frac{1}{2\pi} \sum_{m=1}^{\infty} \int_{-\theta}^{2\pi-\theta} \frac{(z\bar{\zeta})^{m-1}}{m} e^{-in\tau} d\tau + \frac{1}{2\pi} \sum_{m=1}^{\infty} \int_{-\theta}^{2\pi-\theta} \frac{(z\bar{\zeta})^m}{m} e^{-in\tau} d\tau$$

$$= -\frac{1}{2\pi}\sum_{m=1}^{\infty}\frac{(r\rho)^{m-1}}{m}\int_{-\theta}^{2\pi-\theta}e^{i(m-n-1)\tau}d\tau + \frac{1}{2\pi}displaystyle\sum_{m=1}^{\infty}\frac{(r\rho)^{m}}{m}\int_{-\theta}^{2\pi-\theta}e^{i(m-n)\tau}d\tau$$

$$= \begin{cases} -\frac{(r\rho)^n}{(1+n)}, & \text{if } n = 0, \\[2mm] \frac{(r\rho)^n}{n}, & \text{if } n \geq 1, \\[2mm] 0, & \text{if } n < 0. \end{cases} \tag{5.34}$$

Substituting (5.34) in (5.33) and using (5.32) we obtain,

$$I_n^{(3)}(r) = \begin{cases} 2(r^2 - 1)\int_0^1 f_n(\rho)\rho d\rho, & \text{if } n = 0, \\[2mm] \frac{2(1-r^2)}{n}r^n\int_0^1 \rho^{n+1}f_n(\rho)d\rho, & \text{if } n \geq 1, \\[2mm] 0, & \text{if } n < 0. \end{cases} \tag{5.35}$$

Let

$$I^{(4)}(z) = \frac{1-|z|^2}{\pi}\tilde{I}^{(4)}(z) \tag{5.36}$$

where

$$\tilde{I}^{(4)}(z) = \int_{\mathbf{D}}\frac{(1-\zeta\bar{z})}{\zeta\bar{z}}\log(1-\zeta\bar{z})f(\zeta)d\xi d\eta.$$

The Fourier coefficients of $\tilde{I}^{(4)}(z)$ are given by

$$\tilde{I}_n^{(4)}(r) = \frac{1}{2\pi}\int_{\mathbf{D}}f(\zeta)\int_0^{2\pi}\frac{(1-\bar{z}\zeta)}{\bar{z}\zeta}\log(1-\bar{z}\zeta)e^{-in\alpha}d\alpha d\xi d\eta$$

$$= \frac{1}{2\pi}\int_0^1\int_0^{2\pi}f(\rho,\theta)e^{-in\theta}\int_{-\theta}^{2\pi-\theta}\frac{(1-\bar{z}\zeta)}{\bar{z}\zeta}\log(1-\bar{z}\zeta)e^{-in\alpha}d\alpha d\xi d\eta.$$

$$= 2\pi\int_0^1 f_n(\rho)\tilde{G}_{4,n}(r,\rho,\theta)\rho d\rho \tag{5.37}$$

73

where

$$\tilde{G}_n^{(4)}(r,\rho,\theta) = \frac{1}{2\pi}\int\limits_{-\theta}^{2\pi-\theta}\frac{(1-\bar{z}\zeta)}{\bar{z}\zeta}\log(1-\bar{z}\zeta)e^{-in\tau}d\tau$$

$$= -\frac{1}{2\pi}\int\limits_{-\theta}^{2\pi-\theta}\frac{(1-\bar{z}\zeta)}{\bar{z}\zeta}\sum_{m=1}^{\infty}\frac{(\bar{z})\zeta^m}{m}e^{-in\tau}d\tau$$

$$= -\frac{1}{2\pi}\sum_{m=1}^{\infty}\int\limits_{-\theta}^{2\pi-\theta}\frac{(\bar{z}\zeta)^{(m-1)}}{m}e^{-in\tau}d\tau + \frac{1}{2\pi}\sum_{m=1}^{\infty}\int\limits_{-\theta}^{2\pi-\theta}\frac{(\bar{z}\zeta)^m}{m}e^{-in\tau}d\tau$$

$$= -\frac{1}{2\pi}\sum_{m=1}^{\infty}\frac{(r\rho)^{m-1}}{m}\int\limits_{-\theta}^{2\pi-\theta}e^{i(-m-n+1)\tau}d\tau + \frac{1}{2\pi}\sum_{m=1}^{\infty}\frac{(r\rho)^m}{m}\int\limits_{-\theta}^{2\pi-\theta}e^{i(-m-n)\tau}d\tau$$

$$= \begin{cases} -\frac{(r\rho)^{-n}}{(1-n)}, & \text{if } n \le 0, \\ \frac{(r\rho)^{-n}}{-n}, & \text{if } n \le -1, \\ 0, & \text{if } n > 0. \end{cases} \tag{5.38}$$

Substituting (5.38) in (5.37) and using (5.36) we obtain,

$$I_n^{(4)}(r) = \begin{cases} 2(r^2-1)\int_0^1 f_n(\rho)\rho d\rho, & \text{if } n = 0, \\ \frac{2(1-r^2)}{n(n-1)}r^{-n}\int_0^1 \rho^{1-n}f_n(\rho)d\rho, & \text{if } n \le -1, \\ 0, & \text{if } n > 0. \end{cases} \tag{5.39}$$

We write $I^{(5)}(z) = I_1^{(5)}(z) + I_2^{(5)}(z)$ where,

$$I_1^{(5)}(z) = \frac{1}{\pi z}\int\limits_{D}\zeta(1-z\bar{\zeta})\log(1-z\bar{\zeta})f(\zeta)d\xi d\eta.$$

$$I_2^{(5)}(z) = -\frac{1}{\pi}\int\limits_{D}(1-z\bar{\zeta})\log(1-z\bar{\zeta})f(\zeta)d\xi d\eta.$$

Now we evaluate $I_{5,n}^{(1)}(r)$.

$$I_{1,n}^{(5)}(r) = \frac{1}{2\pi^2 z} \int\limits_0^1 \int\limits_0^{2\pi} f(\rho,\theta)e^{-in\theta} \int\limits_{-\theta}^{2\pi-\theta} \zeta(1-z\bar\zeta)\log(1-z\bar\zeta)e^{-in\tau}d\tau\rho d\theta d\rho$$

$$= 2\int\limits_0^1 f_n(\rho)G_{1,n}^{(5)}(r,\rho)\rho d\rho, \tag{5.40}$$

where

$$G_{1,n}^{(5)}(r,\rho) = \frac{1}{2\pi} \int\limits_{-\theta}^{2\pi-\theta} \frac{\zeta(1-z\bar\zeta)\log(1-z\bar\zeta)}{z}e^{-in\tau}d\tau$$

$$= -\frac{1}{2\pi}\sum_{m=1}^{\infty} \int\limits_{-\theta}^{2\pi-\theta} \frac{\zeta(1-z\bar\zeta)}{z}\frac{(z\bar\zeta)^m}{m}e^{-in\tau}d\tau$$

$$= -\frac{1}{2\pi}\sum_{m=1}^{\infty} \frac{\rho^{m+1}r^{m-1}}{m} \int\limits_{-\theta}^{2\pi-\theta} e^{i(m-n-1)\tau}d\tau + \frac{1}{2\pi}\sum_{m=1}^{\infty} \frac{\rho^{m+2}r^m}{m} \int\limits_{-\theta}^{2\pi-\theta} e^{i(m-n)\tau}d\tau$$

$$= \begin{cases} -\rho^2, & \text{if } n = 0, \\ \frac{r^n\rho^{n+2}}{n(n+1)}, & \text{if } n \geq 1, \\ 0, & \text{if } n < 0. \end{cases} \tag{5.41}$$

Substituting (5.41) in (5.40) we obtain,

$$I_{1,n}^{(5)}(r) = \begin{cases} -2\int_0^1 f_0(\rho)\rho^3 d\rho, & \text{if } n = 0, \\ \frac{2r^n}{n(n+1)}\int_0^1 \rho^{n+3}f_n(\rho)d\rho, & \text{if } n \geq 1, \\ 0, & \text{if } n < 0. \end{cases} \tag{5.42}$$

75

$$I_{2,n}^{(5)}(r) = -\frac{1}{2\pi^2} \int\limits_0^1 \int\limits_0^{2\pi} f(\rho,\theta)e^{-in\theta} \int\limits_{-\theta}^{2\pi-\theta} (1-z\bar{\zeta})\log(1-z\bar{\zeta})e^{-in\tau}d\tau\rho d\theta d\rho$$

$$= -2\int\limits_0^1 f_n(\rho)G_{5,n}^{(2)}(r,\rho)\rho d\rho, \tag{5.43}$$

where

$$G_{2,n}^{(5)}(r,\rho) = \frac{1}{2\pi} \int\limits_{-\theta}^{2\pi-\theta} (1-z\bar{\zeta})\log(1-z\bar{\zeta})e^{-in\tau}d\tau$$

$$= -\frac{1}{2\pi}\sum_{m=1}^{\infty} \int\limits_{-\theta}^{2\pi-\theta} (1-z\bar{\zeta})\frac{(z\bar{\zeta})^m}{m}e^{-in\tau}d\tau$$

$$= -\frac{1}{2\pi}\sum_{m=1}^{\infty}\frac{(r\rho)^m}{m} \int\limits_{-\theta}^{2\pi-\theta} e^{i(m-n)\tau}d\tau + \frac{1}{2\pi}\sum_{m=1}^{\infty}\frac{(r\rho)^{m+1}}{m} \int\limits_{-\theta}^{2\pi-\theta} e^{i(m+1-n)\tau}d\tau$$

$$= \begin{cases} -\rho r, & \text{if } n = 1, \\ \frac{(r\rho)^n}{n(n-1)}, & \text{if } n \geq 2, \\ 0, & \text{if } n < 1. \end{cases} \tag{5.44}$$

Substituting (5.44) in (5.43) we obtain,

$$I_{2,n}^{(5)}(r) = \begin{cases} 2r\int_0^1 f_n(\rho)\rho^2 d\rho, & \text{if } n = 1, \\ -\frac{2(r^n)}{n(n-1)}\int_0^1 \rho^{n+1}f_n(\rho)d\rho, & \text{if } n \geq 2, \\ 0, & \text{if } n < 1. \end{cases} \tag{5.45}$$

We now write $I^6(z) = I_1^{(6)} + I_2^{(6)}$ where,

$$I_1^{(6)}(z) = \frac{1}{\pi \bar{z}} \int_{\mathbf{D}} \bar{\zeta}(1 - \zeta\bar{z}) \log(1 - \zeta\bar{z}) f(\zeta) d\xi d\eta.$$

$$I_2^{(6)}(z) = -\frac{1}{\pi} \int_{\mathbf{D}} (1 - \zeta\bar{z}) \log(1 - \zeta\bar{z}) f(\zeta) d\xi d\eta.$$

Now we focus onto the Fourier coefficients.

$$I_{1,n}^{(6)}(r) = \frac{1}{2\pi^2} \int_0^1 \int_0^{2\pi} f(\rho, \theta) e^{-in\theta} \int_{-\theta}^{2\pi-\theta} \frac{\bar{\zeta}}{\bar{z}}(1 - \zeta\bar{z}) \log(1 - \zeta\bar{z}) e^{-in\tau} d\tau \rho d\theta d\rho$$

$$= 2 \int_0^1 f_n(\rho) G_{1,n}^{(6)}(r, \rho) \rho d\rho, \tag{5.46}$$

where

$$G_{1,n}^{(6)}(r, \rho) = \frac{1}{2\pi} \int_{-\theta}^{2\pi-\theta} \frac{\bar{\zeta}}{\bar{z}}(1 - \zeta\bar{z}) \log(1 - \zeta\bar{z}) e^{-in\tau} d\tau$$

$$= -\frac{1}{2\pi} \sum_{m=1}^{\infty} \int_{-\theta}^{2\pi-\theta} \frac{\bar{\zeta}}{\bar{z}}(1 - \zeta\bar{z}) \frac{(\bar{z}\zeta)^m}{m} e^{-in\tau} d\tau$$

$$= -\frac{1}{2\pi} \sum_{m=1}^{\infty} \frac{\rho^{m+1} r^{m-1}}{m} \int_{-\theta}^{2\pi-\theta} e^{-i(m+n-1)\tau} d\tau + \frac{1}{2\pi} \sum_{m=1}^{\infty} \frac{\rho^{m+2} r^m}{m} \int_{-\theta}^{2\pi-\theta} e^{-i(m+n)\tau} d\tau$$

$$= \begin{cases} -\rho^2, & \text{if } n = 0, \\ \frac{r^{-n}\rho^{2-n}}{n(n-1)}, & \text{if } n \leq -1, \\ 0, & \text{if } n > 0. \end{cases} \tag{5.47}$$

77

Substituting (5.47) in (5.46) we obtain,

$$
I_{1,n}^{(6)}(r) = \begin{cases} -2 \int_0^1 f_0(\rho)\rho^3 d\rho, & \text{if } n = 0, \\ 2\frac{r^{-n}}{n(n-1)} \int_0^1 \rho^{3-n} f_n(\rho) d\rho, & \text{if } n \leq -1, \\ 0, & \text{if } n > 0. \end{cases} \tag{5.48}
$$

$$
I_{2,n}^{(6)}(r) = \frac{1}{\pi^2} \int_0^1 \int_0^{2\pi} f(\rho,\theta)e^{-in\theta} \int_{-\theta}^{2\pi-\theta} \bar{\zeta}(1-\zeta\bar{z})\log(1-\zeta\bar{z}e^{-in\tau} d\tau \rho d\theta d\rho
$$

$$
= -2 \int_0^1 f_n(\rho) G_{2,n}^{(6)}(r,\rho)\rho d\rho, \tag{5.49}
$$

where

$$
G_{2,n}^{(6)}(r,\rho) = \frac{1}{2\pi} \int_{-\theta}^{2\pi-\theta} (1-\bar{z}\zeta)\log(1-\bar{z}\zeta)e^{-in\tau} d\tau
$$

$$
= -\frac{1}{2\pi} \sum_{m=1}^{\infty} \int_{-\theta}^{2\pi-\theta} \frac{(\bar{z}\zeta)^m}{m}e^{-in\tau} d\tau + \frac{1}{2\pi} \sum_{m=1}^{\infty} \int_{-\theta}^{2\pi-\theta} \frac{(\bar{z}\zeta)^{m+1}}{m}e^{-in\tau} d\tau
$$

$$
= -\frac{1}{2\pi} \sum_{m=1}^{\infty} \int_{-\theta}^{2\pi-\theta} \frac{(r\rho)^m}{m}e^{-i(m+n)\tau} d\tau + \frac{1}{2\pi} \sum_{m=1}^{\infty} \int_{-\theta}^{2\pi-\theta} \frac{(r\rho)^{m+1}}{m}e^{-i(m+n+1)\tau} d\tau
$$

$$
= \begin{cases} -r\rho, & \text{if } n = -1, \\ \frac{(r\rho)^{-n}}{n(n+1)}, & \text{if } n \leq -2, \\ 0, & \text{if } n > -1. \end{cases} \tag{5.50}
$$

Substituting (5.50) in (5.49) we obtain,

$$
I_{2,n}^{(6)}(r) = \begin{cases} 2r \int_0^1 f_{-1}(\rho)\rho^2 d\rho, & \text{if } n = 0, \\[2mm] -2\frac{r^{-n}}{n(n+1)} \int_0^1 \rho^{1-n} f_n(\rho)d\rho, & \text{if } n \le -2, \\[2mm] 0, & \text{if } n > -1. \end{cases} \tag{5.51}
$$

The second approach to solve this system is the method of decomposition into two Poisson problems as follows

$$
\begin{cases} (\partial_z \partial_{\bar{z}})u = f, & \text{in } \mathbf{D}, \\[2mm] \partial_\nu u = h_2, & \text{on } \partial\mathbf{D}, \end{cases} \tag{5.52}
$$

$$
\begin{cases} (\partial_z \partial_{\bar{z}})w = u, & \text{in } \mathbf{D}, \\[2mm] \omega = h_0, & \text{on } \partial\mathbf{D}. \end{cases} \tag{5.53}
$$

The solution is obtained by solving the Poisson problem with Dirichlet boundary condition and then with Neumann boundary condition. The evaluation of the integrals lead us to the Fourier coefficients $w_n(r)$ of the solution $w(z)$.

6. RECURSIVE RELATIONS

In this section, we present the recursive relations necessary to build the fast algorithm see ([12],[15], [16]). First we obtain the recursive relations for the singular integral (2.3). From Section.2 we recall the epression for $v_n(r)$.

$$v_n(r) = \begin{cases} 4 \int_0^r \rho \log r f_0(\rho)d\rho + 4 \int_r^1 \rho \log \rho f_0(\rho)d\rho, & \text{if } n = 0, \\ -2 \int_0^r \left(\frac{\rho}{r}\right)^n \frac{\rho}{n} f_n(\rho)d\rho - 2 \int_r^1 \left(\frac{r}{\rho}\right)^n \frac{\rho}{n} f_n(\rho)d\rho, & \text{if } n > 0, \\ 2 \int_0^r \left(\frac{r}{\rho}\right)^n \frac{\rho}{n} f_n(\rho)d\rho + 2 \int_r^1 \left(\frac{\rho}{r}\right)^n \frac{\rho}{n} f_n(\rho)d\rho, & \text{if } n < 0. \end{cases}$$

Now we define the following.

$$p_{1,n}^{(1)}(r) = -2 \int_0^r \left(\frac{\rho}{r}\right)^n \frac{\rho}{n} f_n(\rho)d\rho,$$

$$p_{2,n}^{(1)}(r) = -2 \int_r^1 \left(\frac{r}{\rho}\right)^n \frac{\rho}{n} f_n(\rho)d\rho,$$

$$s_{1,n}^{(1)}(r) = 2 \int_0^r \left(\frac{r}{\rho}\right)^n \frac{\rho}{n} f_n(\rho)d\rho,$$

$$s_{2,n}^{(1)}(r) = 2 \int_r^1 \left(\frac{\rho}{r}\right)^n \frac{\rho}{n} f_n(\rho)d\rho,$$

$$t_{1,0}^{(1)}(r) = 4 \int_0^r \rho \log r f_0(\rho)d\rho,$$

$$t_{2,0}^{(1)}(r) = 4 \int_r^1 \rho \log \rho f_0(\rho)d\rho.$$

Note that $p_{1,n}^{(1)}(0) = 0, \quad p_{2,n}^{(1)}(1) = 0, \quad s_{1,n}^{(1)}(0) = 0, \quad s_{1,n}^{(1)}(1) = 0$. We see that $v_n(r)$ can be written as

$$
v_n(r) = \begin{cases} (\log r\, t_{1,n}^{(1)}(r) + t_{2,n}^{(1)}(r)), & \text{if } n = 0, \\ (p_{1,n}^{(1)}(r) + p_{2,n}^{(1)}(r)), & \text{if } n > 0, \\ (s_{1,n}^{(1)}(r) + s_{2,n}^{(1)}(r)), & \text{if } n < 0. \end{cases}
$$

Now for $r_j > r_i, \quad n = 0$, we define

$$
A_{0,1}^{i,j} = 4 \int_{r_i}^{r_j} \rho f_0(\rho) d\rho, \tag{6.1}
$$

$$
B_{0,1}^{i,j} = 4 \int_{r_i}^{r_j} \rho \log \rho f_0(\rho) d\rho. \tag{6.2}
$$

For $r_j > r_i, \quad n \neq 0$, we define

$$
A_{n,1}^{i,j} = 2 \int_{r_i}^{r_j} \left(\frac{R}{\rho}\right)^n \frac{\rho}{n} f_n(\rho) d\rho, \tag{6.3}
$$

where,

$$
R = \begin{cases} r_i & \text{if } n > 0, \\ r_j & \text{if } n < 0, \end{cases}
$$

$$
B_{n,1}^{i,j} = 2 \int_{r_i}^{r_j} \left(\frac{\rho}{R}\right)^n \frac{\rho}{n} f_n(\rho) d\rho, \tag{6.4}
$$

where

$$
R = \begin{cases} r_j & \text{if } n > 0, \\ r_i & \text{if } n < 0. \end{cases}
$$

Algebraic computation with $r_l < r_i < r_j$ shows that,

$$p_{1,n}^{(1)}(r_i) = \left(\frac{r_l}{r_i}\right)^n p_{1,n}^{(1)}(r_l) - B_n^{l,i}, \qquad n > 0, \tag{6.5}$$

$$p_{2,n}^{(1)}(r_i) = \left(\frac{r_i}{r_j}\right)^n p_{2,n}^{(1)}(r_j) - A_n^{i,j}, \qquad n > 0, \tag{6.6}$$

$$s_{1,n}^{(1)}(r_i) = \left(\frac{r_i}{r_l}\right)^n s_{1,n}^{(1)}(r_l) + A_n^{l,i}, \qquad n < 0, \tag{6.7}$$

$$s_{2,n}^{(1)}(r_i) = \left(\frac{r_j}{r_i}\right)^n s_{2,n}^{(1)}(r_j) + B_n^{i,j}, \qquad n < 0, \tag{6.8}$$

$$t_{1,0}^{(1)}(r_i) = t_{1,0}^{(1)}(r_l) + A_0^{l,i}, \qquad n = 0, \tag{6.9}$$

$$t_{2,0}^{(1)}(r_i) = t_{2,0}^{(1)}(r_j) + B_0^{i,j}, \qquad n = 0. \tag{6.10}$$

6.1 Recursive Relations For Biharmonic Problem

Now we build the recursive relation for the Fourier coefficients of the singular integral $I_5(z)$ in Section.3. We recall that $I_{5,n}(r) = I_{5,n}^{(1)}(r) + I_{5,n}^{(2)}(r) + I_{5,n}^{(3)}(r) + I_{5,n}^{(4)}(r)$. We see that $I_{5,n}^{(1)}(r)$ is same as $v_n(r)$. So we first compute $I_{5,n}^{(2)}(r)$. Now

$$I_{5,n}^{(2)}(r) = \begin{cases} 4\int_0^r \rho^3 \log r f_0(\rho)d\rho + 4\int_r^1 \rho^3 \log \rho f_0(\rho)d\rho, & \text{if } n = 0, \\ -2\int_0^r \left(\frac{\rho}{r}\right)^n \frac{\rho}{n} f_n(\rho)d\rho - 2\int_r^1 \left(\frac{r}{\rho}\right)^n \frac{\rho}{n} f_n(\rho)d\rho, & \text{if } n > 0, \\ 2\int_0^r \left(\frac{r}{\rho}\right)^n \frac{\rho}{n} f_n(\rho)d\rho + 2\int_r^1 \left(\frac{\rho}{r}\right)^n \frac{\rho}{n} f_n(\rho)d\rho, & \text{if } n < 0. \end{cases}$$

We define the following.

$$p_{1,n}^{(2)}(r) \;=\; -2 \int_0^r \left(\frac{\rho}{r}\right)^n \frac{\rho^3}{n} f_n(\rho) d\rho,$$

$$p_{2,n}^{(2)}(r) \;=\; -2 \int_r^1 \left(\frac{r}{\rho}\right)^n \frac{\rho^3}{n} f_n(\rho) d\rho,$$

$$s_{1,n}^{(2)}(r) \;=\; 2 \int_0^r \left(\frac{r}{\rho}\right)^n \frac{\rho^3}{n} f_n(\rho) d\rho,$$

$$s_{2,n}^{(2)}(r) \;=\; 2 \int_r^1 \left(\frac{\rho}{r}\right)^n \frac{\rho^3}{n} f_n(\rho) d\rho,$$

$$t_{1,0}^{(2)}(r) \;=\; 4 \int_0^r \rho^3 \log r \, f_0(\rho) d\rho,$$

$$t_{2,0}^{(2)}(r) \;=\; 4 \int_r^1 \rho^3 \log \rho \, f_0(\rho) d\rho.$$

Note that $p_{1,n}^{(2)}(0) = 0$, $p_{2,n}^{(2)}(1) = 0$, $s_{1,n}^{(2)}(0) = 0$, $s_{1,n}^{(2)}(1) = 0$. So we have,

$$I_{5,n}^{(2)}(r) = \begin{cases} (\log r t_{1,n}^{(2)}(r) + t_{2,n}^{(2)}(r)), & \text{if } n = 0 \\ (p_{1,n}^{(2)}(r) + p_{2,n}^{(2)}(r)) & \text{if } n > 0, \\ (s_{1,n}^{(2)}(r) + s_{2,n}^{(2)}(r)), & \text{if } n < 0, \end{cases}$$

Now for $r_j > r_i$, $\quad n = 0$ we define

$$A_{0,2}^{i,j} \;=\; 4 \int_{r_i}^{r_j} \rho f_0(\rho) d\rho, \tag{6.11}$$

$$B_{0,2}^{i,j} \;=\; 4 \int_{r_i}^{r_j} \rho \log \rho \, f_0(\rho) d\rho. \tag{6.12}$$

For $r_j > r_i$, $\quad n \neq 0$ we define

$$A_{n,2}^{i,j} \;=\; 2\int\limits_{r_i}^{r_j} \left(\frac{R}{\rho}\right)^n \frac{\rho^3}{n} f_n(\rho)d\rho, \qquad (6.13)$$

where,

$$R = \begin{cases} r_i & \text{if } n > 0, \\[2mm] r_j & \text{if } n < 0. \end{cases}$$

For $r_j > r_i$, $\quad n \neq 0$ we define

$$B_{n,2}^{i,j} = 2\int\limits_{r_i}^{r_j} \left(\frac{\rho}{R}\right)^n \frac{\rho^3}{n} f_n(\rho)d\rho, \qquad (6.14)$$

where

$$R = \begin{cases} r_j & \text{if } n > 0, \\[2mm] r_i & \text{if } n < 0. \end{cases}$$

Algebraic computation with $r_l < r_i < r_j$ shows that

$$p_{1,n}^{(2)}(r_i) = \left(\frac{r_l}{r_i}\right)^n p_{1,n}^{(2)}(r_l) - B_{n,2}^{l,i} \qquad n > 0, \tag{6.15}$$

$$p_{2,n}^{(2)}(r_i) = \left(\frac{r_i}{r_j}\right)^n p_{2,n}^{(2)}(r_j) - A_{n,2}^{i,j} \qquad n > 0, \tag{6.16}$$

$$s_{1,n}^{(2)}(r_i) = \left(\frac{r_i}{r_l}\right)^n s_{1,n}^{(2)}(r_l) + A_{n,2}^{l,i} \qquad n < 0, \tag{6.17}$$

$$s_{2,n}^{(2)}(r_i) = \left(\frac{r_j}{r_i}\right)^n s_{2,n}^{(2)} r_j) + B_{n,2}^{i,j} \qquad n < 0, \tag{6.18}$$

$$t_{1,0}^{(2)}(r_i) = t_{1,0}^{(2)}(r_l) + A_{0,2}^{l,i} \qquad n = 0, \tag{6.19}$$

$$t_{2,0}^{(2)}(r_i) = t_{2,0}^{(2)}(r_j) + B_{0,2}^{i,j} \qquad n = 0. \tag{6.20}$$

We similarly build the recursive relation for $I_{5,n}^{(3)}(r)$ and $I_{5,n}^{(4)}(r)$. Now $I_{5,n}^{(3)}(r)$ is given by

$$I_{5,n}^{(3)}(r) = \begin{cases} \frac{2r}{(n+1)} \left[\int_0^r f_n(\rho)(\frac{\rho}{r})^{(n+1)} \rho^2 d\rho + \int_r^1 f_n(\rho)(\frac{r}{\rho})^{(n+1)} \rho^2 d\rho, \right] & \text{if } n > -1, \\[2mm] -\frac{2r}{(n+1)} \left[\int_0^r f_n(\rho)(\frac{r}{\rho})^{(n+1)} \rho^2 d\rho + \int_r^1 f_n(\rho)(\frac{\rho}{r})^{(n+1)} \rho^2 d\rho, \right] & \text{if } n < -1, \\[2mm] -2r \left[\int_0^r f_{-1}(\rho)\rho^2 \log r d\rho + \int_1^r f_{-1}(\rho)\rho^2 \log \rho d\rho, \right] & \text{if } n = -1. \end{cases}$$

Now we define the following.

$$p_{1,n}^{(3)}(r) = 2\int_0^r \left(\frac{\rho}{r}\right)^{(n+1)} \frac{\rho^2}{(n+1)} f_n(\rho)d\rho,$$

$$p_{2,n}^{(3)}(r) = 2\int_r^1 \left(\frac{r}{\rho}\right)^{(n+1)} \frac{\rho^2}{(n+1)} f_n(\rho)d\rho,$$

$$s_{1,n}^{(3)}(r) = -2\int_0^r \left(\frac{r}{\rho}\right)^{(n+1)} \frac{\rho^2}{(n+1)} f_n(\rho),$$

$$s_{2,n}^{(3)}(r) = -2\int_r^1 \left(\frac{\rho}{r}\right)^{(n+1)} \frac{\rho^2}{(n+1)} f_n(\rho),$$

$$t_{1,-1}^{(3)}(r) = -4\int_0^r \rho^2 \log r f_{-1}(\rho)d\rho,$$

$$t_{2,-1}^{(3)}(r) = -4\int_r^1 \rho^2 \log \rho f_{-1}(\rho)d\rho.$$

Note that $p_{1,n}^{(3)}(0) = 0,\quad p_{2,n}^{(3)}(1) = 0,\quad s_{1,n}^{(3)}(0) = 0,\quad s_{1,n}^{(3)}(1) = 0$. So we have for

$$I_{5,n}^{(3)}(r) = \begin{cases} r(\log r t_{1,n}^{(3)}(r) + t_{1,n}^{(3)}(r)), & \text{if } n = -1, \\ r(p_{1,n}^{(3)}(r) + p_{2,n}^{(3)}(r)), & \text{if } n > -1, \\ r(s_{1,n}^{(3)}(r) + s_{2,n}^{(3)}(r)), & \text{if } n < -1. \end{cases}$$

Now for $r_j > r_i, n = -1$ we define

$$A_{-1,3}^{i,j} = 4\int_{r_i}^{r_j} \rho^2 f_{-1}(\rho)d\rho, \tag{6.21}$$

$$B_{-1,3}^{i,j} = 4\int_{r_i}^{r_j} \rho^2 \log \rho f_{-1}(\rho)d\rho. \tag{6.22}$$

86

For $r_j > r_i$, $\quad n \neq -1$ we define

$$A_{n,3}^{i,j} \;=\; 2 \int\limits_{r_i}^{r_j} \left(\frac{R}{\rho}\right)^{(n+1)} \frac{\rho^2}{(n+1)} f_n(\rho) d\rho, \tag{6.23}$$

where

$$R = \begin{cases} r_i & \text{if } n > -1, \\[2mm] r_j & \text{if } n < -1, \end{cases}$$

$$B_{n,3}^{i,j} = 2 \int\limits_{r_i}^{r_j} \left(\frac{\rho}{R}\right)^{(n+1)} \frac{\rho^3}{(n+1)} f_n(\rho) d\rho, \tag{6.24}$$

where

$$R = \begin{cases} r_j & \text{if } n > -1, \\[2mm] r_i & \text{if } n < -1. \end{cases}$$

Algebraic computation with $r_l < r_i < r_j$ shows that,

$$p_{1,n}^{(3)}(r_i) = \left(\frac{r_l}{r_i}\right)^{(n+1)} p_{1,n}^{(3)}(r_l) + B_{n,3}^{l,i}, \qquad n > -1, \tag{6.25}$$

$$p_{2,n}^{(3)}(r_i) = \left(\frac{r_i}{r_j}\right)^{(n+1)} p_{2,n}^{(3)}(r_j) + A_{n,3}^{i,j}, \qquad n > -1, \tag{6.26}$$

$$s_{1,n}^{(3)}(r_i) = \left(\frac{r_i}{r_l}\right)^{(n+1)} s_{1,n}^{(3)}(r_l) - A_{n,3}^{l,i}, \qquad n < -1, \tag{6.27}$$

$$s_{2,n}^{(3)}(r_i) = \left(\frac{r_j}{r_i}\right)^{(n+1)} s_{2,n}^{(3)} r_j) - B_{n,3}^{i,j}, \qquad n < -1, \tag{6.28}$$

$$t_{1,-1}^{(3)}(r_i) = t_{1,-1}^{(3)}(r_l) + A_{-1,3}^{l,i}, \qquad n = -1, \tag{6.29}$$

$$t_{2,-1}^{(3)}(r_i) = t_{2,-1}^{(3)}(r_j) + B_{-1,3}^{i,j}. \qquad n = -1. \tag{6.30}$$

$I_{5,n}^{(4)}(r)$ is given by

$$
I_{5,n}^{(4)}(r) = \begin{cases} \frac{2r}{(n-1)}\left[\int_0^r f_n(\rho)(\frac{\rho}{r})^{(n-1)}\rho^2 d\rho + \int_r^1 f_n(\rho)(\frac{r}{\rho})^{(n-1)}\rho^2 d\rho\right], & \text{if } n > 1, \\[2mm] \frac{-2r}{(n-1)}\left[\int_0^r f_n(\rho)(\frac{r}{\rho})^{(n-1)}\rho^2 d\rho + \int_r^1 f_n(\rho)(\frac{\rho}{r})^{(n-1)}\rho^2 d\rho\right], & \text{if } n < 1, \\[2mm] -4r\left[\int_0^r f_1(\rho)\rho^2 \log r d\rho + \int_r^1 f_1(\rho)\rho^2 \log \rho d\rho\right], & \text{if } n = 1. \end{cases}
$$

We define the following.

$$
p_{1,n}^{(4)}(r) = 2\int_0^r \left(\frac{\rho}{r}\right)^{(n-1)} \frac{\rho^2}{(n-1)} f_n(\rho)d\rho,
$$

$$
p_{2,n}^{(4)}(r) = 2\int_r^1 \left(\frac{r}{\rho}\right)^{(n-1)} \frac{\rho^2}{(n-1)} f_n(\rho)d\rho,
$$

$$
s_{1,n}^{(4)}(r) = -2\int_0^r \left(\frac{r}{\rho}\right)^{(n-1)} \frac{\rho^2}{(n-1)} f_n(\rho)d\rho,
$$

$$
s_{2,n}^{(4)}(r) = -2\int_r^1 \left(\frac{\rho}{r}\right)^{(n-1)} \frac{\rho^2}{(n-1)} f_n(\rho)d\rho,
$$

$$
t_{1,1}^{(4)}(r) = -4\int_0^r \rho^2 \log r f_1(\rho)d\rho,
$$

$$
t_{2,1}^{(4)}(r) = -4\int_r^1 \rho^2 \log \rho f_1(\rho)d\rho.
$$

Note that $p_{1,n}^{(4)}(0) = 0, \quad p_{2,n}^{(4)}(1) = 0, \quad s_{1,n}^{(4)}(0) = 0, \quad s_{1,n}^{(4)}(1) = 0.$ So we have for

$$
I_{5,n}^{(4)}(r) = \begin{cases} r(\log r t_{1,n}^{(4)}(r) + t_{2,n}^{(4)}(r)), & \text{if } n = 1, \\[2mm] r(p_{1,n}^{(4)}(r) + p_{2,n}^{(4)}(r)), & \text{if } n > 1, \\[2mm] r(s_{1,n}^{(4)}(r) + s_{2,n}^{(4)}(r)), & \text{if } n < 1. \end{cases}
$$

Now for $r_j > r_i$, $n = 1$ we define

$$A_{1,4}^{i,j} = 4 \int_{r_i}^{r_j} \rho^2 f_1(\rho) d\rho, \tag{6.31}$$

$$B_{1,4}^{i,j} = 4 \int_{r_i}^{r_j} \rho^2 \log \rho f_1(\rho) d\rho. \tag{6.32}$$

For $r_j > r_i$, $n \neq 1$ we define

$$A_{n,4}^{i,j} = 2 \int_{r_i}^{r_j} \left(\frac{R}{\rho}\right)^{(n-1)} \frac{\rho^2}{(n-1)} f_n(\rho) d\rho, \tag{6.33}$$

where,

$$R = \begin{cases} r_i & \text{if } n > 1, \\ r_j & \text{if } n < 1, \end{cases}$$

Also define,

$$B_{n,4}^{i,j} = 2 \int_{r_i}^{r_j} \left(\frac{\rho}{R}\right)^{(n-1)} \frac{\rho^2}{(n-1)} f_n(\rho) d\rho, \tag{6.34}$$

where,

$$R = \begin{cases} r_j & \text{if } n > 1, \\ r_i & \text{if } n < 1, \end{cases}$$

89

Algebraic computation with $r_l < r_i < r_j$ shows that

$$p_{1,n}^{(4)}(r_i) = \left(\frac{r_l}{r_i}\right)^{(n-1)} p_{1,n}^{(4)}(r_l) + B_{n,4}^{l,i}, \qquad n > 1, \tag{6.35}$$

$$p_{2,n}^{(4)}(r_i) = \left(\frac{r_i}{r_j}\right)^{(n-1)} p_{2,n}^{(4)}(r_j) + A_{n,4}^{i,j}, \qquad n > 1, \tag{6.36}$$

$$s_{1,n}^{(4)}(r_i) = \left(\frac{r_i}{r_l}\right)^{(n-1)} s_{1,n}^{(4)}(r_l) - A_{n,4}^{l,i}, \qquad n < 1, \tag{6.37}$$

$$s_{2,n}^{(4)}(r_i) = \left(\frac{r_j}{r_i}\right)^{(n-1)} s_{2,n}^{(4)}(r_j) - B_{n,4}^{i,j}, \qquad n < 1, \tag{6.38}$$

$$t_{1,1}^{(4)}(r_i) = t_{1,1}^{(4)}(r_l) + A_{1,4}^{l,i}, \qquad n = 1, \tag{6.39}$$

$$t_{2,1}^{(4)}(r_i) = t_{2,1}^{(4)}(r_j) + B_{1,4}^{i,j}, \qquad n = 1. \tag{6.40}$$

7. FAST ALGORITHM AND QUADRATURE METHODS

In this section we discuss about the quadrature methods used to compute $A_{n,k}^{i,j}$ and $B_{n,k}^{i,j}$. We use Trapezoidal, Simpson, and Euler-Maclaurin formula to compute the integrals. Here we provide some important theorems from [39],[27],[37] for the Euler-Maclaurin expansion.

7.1 Quadrature Methods

Let $x_l = a + lh$, $l = 0, 1, ..M$, $h = \frac{b-a}{M}$ and M a positive integer. We state the following theorems from [39].

Theorem 7.1.1. *If a function $f(x)$ is 2n times differentiable on $[a, b]$ then*

$$\int_a^b f(x)dx = h \sum_{i=0}^{\acute{K}} f(x_i) + \sum_{\nu=1}^{n-1} \frac{B_{2\nu}}{2\nu}[f^{(2\nu-1)}(a) - f^{(2\nu-1)}(b)]h^{2\nu} + R_{2n}[f;(a,b)],$$

where

$$R_{2n}[f;(a,b)] = h^{2n} \int_a^b \frac{\bar{B}_{2n}[(x-a)/h] - B_{2n}}{2n} f^{(2n)}(x)dx.$$

B_ν *are the Bernoulli numbers and $\bar{B}_\nu(x)$ are periodic Bernoullian function of order ν and $\sum_{i=0}^{\acute{K}} f(x_i)$ is the summation with the first and the last terms multiplied with $\frac{1}{2}$.*
If $f(x)$ is infinitely differentiable on $[a, b]$ then

$$\int_a^b f(x)dx = h \sum_{i=0}^{\acute{K}} f(x_i) + \sum_{\nu=1}^{\infty} \frac{B_{2\nu}}{2\nu!}[f^{(2\nu-1)}(a) - f^{(2\nu-1)}(b)]h^{2\nu} \quad as \quad h \to 0$$

Theorem 7.1.2. *If a function $f(x)$ is $2n$ times differentiable on $[a,b]$ and $F(x) = (x-a)^s f(x), s > -1$, then*

$$\int_a^b F(x)dx = h\sum_{i=1}^{\dot{K}} F(x_i) - \sum_{\nu=1}^{n-1} \frac{B_{2\nu}}{(2\nu)!} F^{(2\nu-1)}(b)h^{2\nu} - \sum_{\nu=0}^{2n-1} \frac{\zeta(-s-\nu)}{\nu!} f^{(\nu)(a)} h^{\nu+s+1} + \rho_{2n}$$

where $\zeta(t)$ is the Riemann zeta function for $Re(t) > 1$ and $\rho_{2n} = \mathcal{O}(h^{2n})$ as $h \to 0$. If $f(x)$ is infinitely differentiable on $[a,b]$ then, as $h \to 0$

$$\int_a^b F(x)dx = h\sum_{i=0}^{\dot{K}} F(x_i) - \sum_{\nu=1}^{\infty} \frac{B_{2\nu}}{(2\nu)!} F^{(2\nu-1)}(b)h^{2\nu} - \sum_{\nu=0}^{\infty} \frac{\zeta(-s-\nu)}{\nu!} f^{(\nu)(a)} h^{\nu+s+1}.$$

Theorem 7.1.3. *If a function $f(x)$ is $2n$ times differentiable on $[a,b]$ and $F(x) = (x-a)^s \log(x-a) f(x), s > -1$ then*

$$\int_a^b F(x)dx = h\sum_{i=1}^{\dot{K}} F(x_i) - \sum_{\nu=1}^{n-1} \frac{B_{2\nu}}{(2\nu)!} F^{(2\nu-1)}(b)h^{2\nu}$$
$$- \sum_{\nu=0}^{2n-1} [\zeta'(-s-\nu) + \zeta(-s-\nu)\log h]\frac{f^{(\nu)(a)}}{\nu!} h^{\nu+s+1} + \rho_{2n}$$

where $\zeta'(t) = \frac{d\zeta(t)}{dt}$ and $\rho_{2n} = \mathcal{O}(h^{2n})$ as $h \to 0$.

   If $f(x)$ is infinitely differentiable on $[a,b]$ then

$$\int_a^b F(x)dx = h\sum_{i=0}^{\dot{K}} F(x_i) - \sum_{\nu=1}^{\infty} \frac{B_{2\nu}}{(2\nu)!} F^{(2\nu-1)}(b)h^{2\nu}$$
$$- \sum_{\nu=0}^{\infty} [-\zeta'(-s-\nu) + \zeta(-s-\nu)\log h]\frac{f^{(\nu)(a)}}{\nu!} h^{\nu+s+1}$$

In our implementation to compute $A_{n,k}^{i,j}$ and $B_{n,k}^{i,j}$, we used two point quadrature ie, $K = 1$ for each $i = 1, 2...M$ and the first order derivative of the integrands of $A_{n,k}^{i,j}$ and $B_{n,k}^{i,j}$ are computed for $\nu = 1$, to incorporate the correction term as given in the theorems. These theorems provide a very high order accuracy for computing $A_{n,k}^{i,j}$ and $B_{n,k}^{i,j}$.

7.2   Fast Algorithm

Now with the tools ready, we can build the fast, high order accurate algorithm for solving the Poisson and biharmonic problems. We discretize the unit disk using $M \times N$ equidistant points, M in the radial direction and N in the angular direction as in Fig. 7.1. To obtain a numerical method for evaluating the domain integral, the interior of the disk is divided into a collection of annular regions. Let $0 = r_1 < r_2 < .....r_M = 1$.

Figure 7.1: The unit disk with equidistant radial points
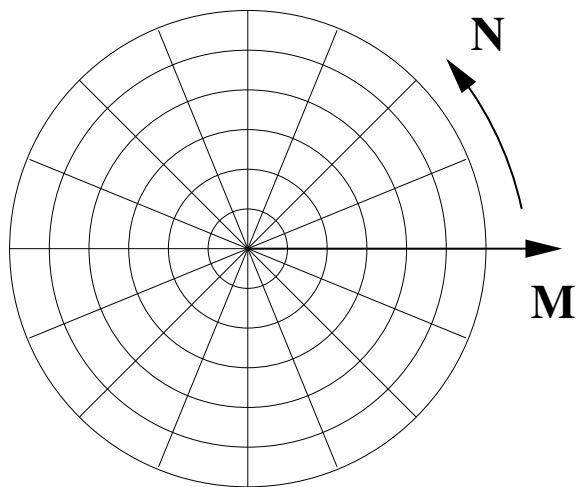
We consider the Poisson problem (P1) defined in Section. 2.

Initialization: Choose M and N. Define $K = \frac{N}{2}$.

Inputs: M, N, $\gamma(e^{\frac{2\pi i k}{N}})$, $f(r_l e^{\frac{2\pi i k}{N}})$, $l \in [1, M]$, $k = 1.....N$ and $n \in [-K+1, K]$

Step 1. Compute the Fourier coefficients $\gamma_n(r_l)$, $f_n(r_l)$ using FFT for all $n \in [-K+1, K]$, $l \in [1, M]$.

Step 2. Compute $u_n(r_l)$ to obtain $u(z)$ for $n \in [-K+1, K]$, $l \in [1, M]$

Step 3. Compute $A_{n,1}^{i,i+1}, A_{0,1}^{i,i+1}, B_{n,1}^{i,i+1}, B_{0,1}^{i,i+1}$ for $i \in [1, M-1]$, $n \in [-K+1, K]$ using (6.3), (6.4),(6.1), (6.2)

Step 4. Compute $p_{1,n}^{(1)}(r_l)$, $p_{2,n}^{(1)}(r_l)$ for $n \in [1, K]$, and $s_{1,n}^{(1)}(r_l)$, $s_{2,n}^{(1)}(r_l)$ for $n \in [-K+1, -1]$, $t_{1,0}^{(1)}(r_l), t_{2,0}^{(1)}(r_l)$ and $l \in [1, M]$ using (6.5), (6.6), (6.7), (6.8), (6.9), (6.10).

Set $p_{1,n}^{(1)}(0) = 0$

for $n = 1........K$

　for $l = 2....M$

$$p_{1,n}^{(1)}(r_l) = \left(\frac{r_{l-1}}{r_l}\right)^n p_{1,n}^{(1)}(r_{l-1}) - B_{n,1}^{l-1,l}$$

　end

end

Set $p_{2,n}^{(1)}(1) = 0$

for $n = 1........K$

　for $l = M-1....1$

$$p_{2,n}^{(1)}(r_l) = \left(\frac{r_l}{r_{l+1}}\right)^n p_{2,n}^{(1)}(r_{l+1}) - A_{n,1}^{l,l+1}$$

　end

end

Set $s_{1,n}^{(1)}(0) = 0$

for $n = -K........-1$

for $l = 2....M$

$$s_{1,n}^{(1)}(r_l) = \left(\frac{r_l}{r_{l-1}}\right)^n s_{1,n}^{(1)}(r_{l-1}) - A_{n,1}^{l-1,l}$$

end

end

Set $s_{2,n}^{(1)}(1) = 0$

for $n = -K........1$

for $l = M - 1....1$

$$s_{2,n}^{(1)}(r_l) = \left(\frac{r_{l+1}}{r_l}\right)^n s_{2,n}^{(1)}(r_{l+1}) + B_{n,1}^{l,l+1}$$

end

end

for $l = 2....M$

$$t_{1,0}^{(1)}(r_l) = \left(\frac{\log r_l}{\log r_{l-1}}\right) t_{1,0}^{(1)}(r_{l-1}) - A_{0,1}^{l-1,l}$$

end

for $l = M - 1....1$

$$t_{2,0}^{(1)}(r_l) = t_{2,0}^{(1)}(r_{l+1}) + B_{0,1}^{l,l+1}$$

end

Step 5. Finally compute $\omega(r_l e^{\frac{2\pi ik}{N}}) = \sum_{n=-K+1}^{K} (v(r_l) + +u_n(r_l)) e^{\frac{2\pi ink}{N}}$.

Similar is the sequential algorithm for the Poisson equation with the Neumann

boundary condition.

7.2.2 Fast Algorithms For Biharmonic Problems

We present here the fast algorithm to solve the (D1) biharmonic problem in the direct method (fast direct method). Let $0 = r_1 < r_2 < .....r_M = 1$.

Initialization: Choose M and N. Define $K = \frac{N}{2}$.

Inputs: $M, N, h_0(e^{\frac{2\pi i k}{N}}), \ h_1(e^{\frac{2\pi i k}{N}}), \ f(r_l e^{\frac{2\pi i k}{N}}), \ l \in [1, M], \ k = 1.....N$ and $n \in [-K + 1, K]$.

Step 1. Compute the Fourier coefficients $a_n, \ b_n, \ f_n$ using FFT for all $n \in [-K + 1, K]$.

Step 2. Compute $u_{2,n}(r_l), \ v_{2,n}(r_l), \ r_{2,n}(r_l), \ I_{3,n}(r_l), \ I_{4,n}^{(k)}(r_l)$ to obtain $I_3(z), \ I_4(z), \ u_2(z), \ v_2(z), \ r_2(z)$ using (3.2), (3.3), (3.4), (3.5), (3.6), (3.7), (3.8), (3.9) respectively for $n \in [-K + 1, K], l \in [1, M], k = 1, 2, 3, 4$

Step 3. Compute $A_{n,k}^{i,i+1}, B_{n,k}^{i,i+1}$ for $i \in [1, M - 1], n \in [-K + 1, K], k = 1, 2, 3, 4$ using (6.3), (6.4), (6.1), (6.2), (6.13), (6.14), (6.11), (6.12), (6.23), (6.24), (6.21), (6.22) (6.33), (6.34), (6.31), (6.32)

Step 4. Compute $p_{1,n}^{(j)}(r_l), p_{2,n}^{(j)}(r_l), t_{1,n}^{(j)}(r_l), t_{2,n}^{(j)}(r_l)$ for $n \in [0, K]$ and $s_{1,n}^{(j)}(r_l), s_{2,n}^{(j)}(r_l)$ for $n \in [-K + 1, -1], \ j = 1, 2, 3, 4$ and $l \in [1, M]$ using (6.5), (6.6), (6.7), (6.8), (6.9), (6.10), (6.15), (6.16),(6.17),(6.18), (6.19), (6.20), (6.25), (6.26), (6.27), (6.28), (6.29), (6.30),
(6.35), (6.36), (6.37), (6.38), (6.39), (6.40) with the following recursive relation.

Now for $j = 1, 2$ we have,

Set $p_{1,n}^{(j)}(0) = 0$

for $n = 1........K$

for $l = 2....M$

$$p_{1,n}^{(j)}(r_l) = \left(\frac{r_{l-1}}{r_l}\right)^n p_{1,n}^{(j)}(r_{l-1}) - B_{n,j}^{l-1,l}$$

end

end

Set $p_{2,n}^{(j)}(1) = 0$

for $n = 1........K$

for $l = M - 1....1$

$$p_{2,n}^{(j)}(r_l) = \left(\frac{r_l}{r_{l+1}}\right)^n p_{2,n}^{(j)}(r_{l+1}) - A_{n,j}^{l,l+1}$$

end

end

Set $s_{1,n}^{(j)}(0) = 0$

for $n = -K........-1$

for $l = 2....M$

$$s_{1,n}^{(j)}(r_l) = \left(\frac{r_l}{r_{l-1}}\right)^n s_{1,n}^{(j)}(r_{l-1}) - A_{n,j}^{l-1,l}$$

end

end

Set $s_{2,n}^{(j)}(1) = 0$

for $n = -K........1$

for $l = M - 1....1$

$$s_{2,n}^{(j)}(r_l) = \left(\frac{r_{l+1}}{r_l}\right)^n s_{2,n}^{(j)}(r_{l+1}) + B_{n,j}^{l,l+1}$$

end

end

for $l = 2....M$

$$t_{1,0}^{(j)}(r_l) = \frac{\log r_l}{\log r_{l-1}} t_{1,0}^{(j)}(r_{l-1}) - A_{0,j}^{l-1,l}$$

end

for $l = M - 1....1$

$$t_{2,0}^{(j)}(r_l) = t_{2,0}^{(j)}(r_{l+1}) + B_{0,j}^{l,l+1}$$

end

For $j = 3, 4$ we have,

Set $p_{1,n}^{(3)}(0) = 0$

for $n = 0........K$

for $l = 2....M$

$$p_{1,n}^{(3)}(r_l) = \left(\frac{r_{l-1}}{r_l}\right)^{(n+1)} p_{1,n}^{(3)}(r_{l-1}) + B_{n,3}^{l-1,l}$$

end

end

Set $p_{2,n}^{(3)}(1) = 0$

for $n = 0........K$

for $l = M - 1....1$

$$p_{2,n}^{(3)}(r_l) = \left(\frac{r_l}{r_{l+1}}\right)^{(n+1)} p_{2,n}^{(3)}(r_{l+1}) + A_{n,3}^{l,l+1}$$

end

end

Set $s_{1,n}^{(3)}(0) = 0$

for $n = -K........-2$

    for $l = 2....M$

$$s_{1,n}^{(3)}(r_l) = \left(\frac{r_l}{r_{l-1}}\right)^{(n+1)} s_{1,n}^{(3)}(r_{l-1}) - A_{n,3}^{l-1,l}$$

    end

end

Set $s_{2,n}^{(3)}(1) = 0$

for $n = -K........-2$

    for $l = M-1....1$

$$s_{2,n}^{(3)}(r_l) = \left(\frac{r_{l+1}}{r_l}\right)^{(n+1)} s_{2,n}^{(3)}(r_{l+1}) - B_{n,3}^{l,l+1}$$

    end

end

for $l = 2....M$

$$t_{1,-1}^{(3)}(r_l) = \frac{\log r_l}{\log r_{l-1}} t_{1,-1}^{(3)}(r_{l-1}) - A_{-1,3}^{l-1,l}$$

end

for $l = M-1....1$

$$t_{2,-1}^{(3)}(r_l) = t_{2,-1}^{(3)}(r_{l+1}) - B_{-1,3}^{l,l+1}$$

    end

Set $p_{1,n}^{(4)}(0) = 0$

for $n = 2........K$

for $l = 2....M$

$$p_{1,n}^{(4)}(r_l) = \left(\frac{r_{l-1}}{r_l}\right)^{(n-1)} p_{1,n}^{(4)}(r_{l-1}) + B_{n,4}^{l-1,l}$$

end

end

Set $p_{2,n}^{(4)}(1) = 0$

for $n = 2........K$

for $l = M - 1....1$

$$p_{2,n}^{(4)}(r_l) = \left(\frac{r_l}{r_{l+1}}\right)^{(n-1)} p_{2,n}^{(4)}(r_{l+1}) + A_{n,4}^{l,l+1}$$

end

end

Set $s_{1,n}^{(4)}(0) = 0$

for $n = -K........0$

for $l = 2....M$

$$s_{1,n}^{(4)}(r_l) = \left(\frac{r_l}{r_{l-1}}\right)^{(n-1)} s_{1,n}^{(4)}(r_{l-1}) - A_{n,4}^{l-1,l}$$

end

end

Set $s_{2,n}^{(4)}(1) = 0$

for $n = -K........0$

for $l = M - 1....1$

$$s_{2,n}^{(4)}(r_l) = \left(\frac{r_{l+1}}{r_l}\right)^{(n-1)} s_{2,n}^{(4)}(r_{l+1}) - B_{n,4}^{l,l+1}$$

end

end

for $l = 2....M$

$$t_{1,1}^{(4)}(r_l) = \frac{\log r_l}{\log r_{l-1}} t_{1,-1}^{(4)}(r_{l-1}) - A_{1,4}^{l-1,l}$$

end

$$\text{for } l = M - 1....1$$

$$t_{2,1}^{(4)}(r_l) = t_{2,1}^{(4)}(r_{l+1}) - B_{1,4}^{l,l+1}$$

end

Step 5. Finally compute

$$\omega(r_l e^{\frac{2\pi ik}{N}}) = \sum_{n=-K+1}^{K} (u_2(r_l) + v_2(r_l) + r_2(r_l) + I_3(r_l) + I_4(r_l) + I_5(r_l)) \, e^{\frac{2\pi nik}{N}} \quad \text{using in-}$$

verse FFT for $k \in [1, N], l \in [1, M]$.

Similar is the algorithm for the direct method of (D3) biharmonic problem. Now we consider the algorithm for the (D2) biharmonic problem.

Let $0 = r_1 < r_2 < .....r_M = 1$.

Initialization: Choose M and N. Define $K = \frac{N}{2}$.

Inputs: M, N, $h_0(e^{\frac{2\pi ik}{N}})$, $h_1(e^{\frac{2\pi ik}{N}})$, $f(r_l e^{\frac{2\pi ik}{N}})$, $l \in [1, M]$, $k = 1.....N$ and $n \in [-K + 1, K]$, $i = 1, 2, 3, 4$.

Step 1. Compute the Fourier coefficient a_n, b_n, f_n using FFT for all $n \in [-K+1, K]$.

Step 2. Compute $u_{2,n}(r_l)$, $v_{3,n}(r_l)$, $I_{4,n}^{(k)}(r_l)$, $I_{6,n}(r_l)$, $I_{7,n}(r_l)$, to obtain $I_4(z)$, $I_6(z)$, $I_7(z)$, $u_2(z)$, $v_3(z)$ using (3.2), (4.12), (3.6), (3.7), (3.8), (3.9), (4.2), (4.3) respectively for $n \in [-K + 1, K]$, $l \in [1, M]$, $k = 1, 2, 3, 4$

Step 3. Compute $A_{n,k}^{i,i+1}$, $B_{n,k}^{i,i+1}$ for $i \in [1, M - 1]$, $n \in [-K + 1, K]$, $k = 1, 2, 3, 4$ using (6.3), (6.4), (6.1), (6.2), (6.13), (6.14), (6.11), (6.12), (6.23), (6.24), (6.21), (6.22) (6.33), (6.34), (6.31), (6.32)

Table 7.1: The complexity at each step for the Poisson equation.

Step	Operation Count
1	The M discrete Fourier transforms of N data sets contribute $\mathcal{O}(\mathcal{M}\mathcal{N}\log\mathcal{N})$.
2	Computation of $A_{n,1}^{i,i+1}$ and $B_{n,1}^{i,i+1}$, $i \in [1, M-1]$ contribute $\mathcal{O}(\mathcal{M}\mathcal{N})$.
3	Computation of $p_{1,n}^{(1)}$, $p_{2,n}^{(1)}$, $s_{1,n}^{(1)}$, $s_{2,n}^{(1)}$, $t_{1,0}^{(1)}$, $t_{2,0}^{(1)}$ contribute $\mathcal{O}(\mathcal{M}\mathcal{N})$.
4	Computation of $\omega(r_l e^{\frac{2\pi i k}{N}})$, $k \in [1, N]$ by FFT contribute $\mathcal{O}(\mathcal{M}\mathcal{N}\log\mathcal{N})$ for $M \times N$ grid points.

Step 4. Compute $p_{1,n}^{(j)}(r_l)$, $p_{2,n}^{(j)}(r_l)$ for $n \in [1, K]$ and $s_{1,n}^{(j)}(r_l)$, $s_{2,n}^{(j)}(r_l)$ for $n \in [-K+1, -1]$, $t_{1,0}^{j}(r_l)$, $t_{2,0}^{j}(r_l), j = 1, 2, 3, 4$ and $l \in [1, M]$ as in (6.5), (6.6), (6.7), (6.8), (6.9), (6.10), (6.15), (6.16), (6.17), (6.18), (6.19), (6.20), (6.25), (6.26), (6.27), (6.28),

(6.29), (6.30), (6.35), (6.36), (6.37) (6.38), (6.39), (6.40) with the recursive relation as in the algorithm with (D1) biharmonic problem.

Step 5. Finally compute $\omega(r_l e^{\frac{2\pi i k}{N}})$ using inverse FFT.

The algorithm is similar for (D4) biharmonic problem. Note here for double Poisson method we apply the algorithm for Poisson solver twice.

7.2.3   Algorithmic Complexity

The computational complexity of the fast algorithm for the Poisson equation and the biharmonic problems in a unit disc in the complex plane has been presented here. The asymptotic operation count and the asymptotic storage has been discussed here and are shown in Tables. 7.1, 7.2.   We consider first the algorithm for (D1)

Table 7.2: The complexity at each step for the (D1) biharmonic problem .

Step	Operation Count
1	The M discrete Fourier transforms of N data sets contribute $\mathcal{O}(\mathcal{M}\mathcal{N}\log\mathcal{N})$.
2	Computation of $I_{3,n}$, $I_{4,n}$, $u_{2,n}$, $v_{2,n}$, $r_{2,n}$ contribute $\mathcal{O}(\mathcal{M}\mathcal{N})$.
3	Computation of $A_{n,j}^{i,i+1}$ and $B_{n,j}^{i,i+1}$, $i \in [1, M-1]$ contribute $\mathcal{O}(\mathcal{M}\mathcal{N})$.
4	Computation of each $p_{1,n}^{(j)}$, $p_{2,n}^{(j)}$, $s_{1,n}^{(j)}$, $s_{2,n}^{(j)}$, $t_{1,0}^{(j)}$, $t_{2,0}^{(j)}$ contribute $\mathcal{O}(\mathcal{M}\mathcal{N})$.
5	Computation of $\omega(r_l e^{\frac{2\pi i k}{N}})$, $k \in [1, N]$ by FFT contributes $\mathcal{O}(\mathcal{M}\mathcal{N}\log\mathcal{N})$ for $M \times N$ grid points.

biharmonic problem to analyse the complexity. The asymptotic operation count for the (D2) biharmonic problem is similar and has same operation count as (D3) and (D4) biharmonic problems discussed in Section. 3, Section. 4.

Remark 1. N must be a power of 2 for use of FFT. This algorithm is highly parallelizable and the estimates can be improved effectively if it is implemented on a parallel machine.

8. BIHARMONIC PROBLEMS IN ANNULAR DOMAIN

In this section, we consider (D2) and (D4) biharmonic problem in an annular disk $\mathbf{\Omega} = \{z \in \mathbb{R}^2 : R_1 < |z| < R_2\}$ and $\partial\mathbf{\Omega} = \{z \in \mathbb{R}^2 : R_1 = |z| \quad \text{or} \quad |z| = R_2\}$. We employ the double Poisson method here.

8.1 Biharmonic Problem In The Concentric Annular Domain

In an annular domain, we decompose the biharmonic problem

$$
\begin{cases}
(\partial_z \partial_{\bar{z}})^2 \omega & = f, \qquad \text{in} \quad \mathbf{\Omega}, \\
\omega & = \gamma_0, \qquad \text{on} \quad \partial\mathbf{\Omega}, \\
(\partial_z \partial_{\bar{z}})\omega & = \gamma_2, \qquad \text{on} \quad \partial\mathbf{\Omega}.
\end{cases}
\tag{8.1}
$$

into two Poisson problems.

$$
\begin{cases}
\partial_z \partial_{\bar{z}} w^P & = f, \qquad \text{in} \quad \mathbf{\Omega}, \\
w^P & = \gamma_2, \qquad \text{on} \quad \partial\mathbf{\Omega}.
\end{cases}
\tag{8.2}
$$

$$
\begin{cases}
\partial_z \partial_{\bar{z}} \omega & = w^P, \qquad \text{in} \quad \mathbf{\Omega}, \\
\omega & = \gamma_0, \qquad \text{on} \quad \partial\mathbf{\Omega}.
\end{cases}
\tag{8.3}
$$

We use the free space Green's function for the Laplace equation to solve the decomposed system here.

104

Let $w^P(r, \theta) = u^P(r, \theta) + v^P(r, \theta)$ where $v^P(r, \theta)$ and $u^P(r, \theta)$ satisfy

$$\partial_z \partial_{\bar{z}} u^P = f \quad \text{in} \quad \mathbf{\Omega} \tag{8.4}$$

and

$$\begin{cases} \partial_z \partial_{\bar{z}} v^P &= 0, & \text{in} \quad \mathbf{\Omega}. \\ v^P &= \gamma_2 - u^P(\theta), & \text{on} \quad \partial\mathbf{\Omega}. \end{cases}$$

Also let

$$\begin{aligned} h_1(\theta) &= \gamma_2(\theta) - u^P(\theta) \quad \text{on} \quad \{z \in \mathbb{R}^2 : |z| = R_1\}, \\ h_2(\theta) &= \gamma_2(\theta) - u^P(\theta) \quad \text{on} \quad \{z \in \mathbb{R}^2 : |z| = R_2\}, \end{aligned}$$

and a_n and b_n be the Fourier coefficients of $h_1(\theta)$ and $h_2(\theta)$ respectively. A particular solution of (8.4) for $z \in \mathbf{\Omega}$ and $\zeta = \xi + i\eta$ can be expressed as

$$u^P(z) = \iint_D f(\zeta)G(z, \zeta)d\xi d\eta, \tag{8.5}$$

where

$$G(z, \zeta) = \frac{1}{2\pi} \log|z - \zeta|,$$

is the free space Green's function for the Laplacian. We first solve for w^P and then employing the same technique we solve for ω. The particular solution for $u^P(z)$ is given by

$$u^P(z) = \frac{2}{\pi} \iint_{\mathbf{\Omega}} \log|\zeta - z| f(\zeta)d\xi d\eta. \tag{8.6}$$

This singular integral is same as the one (2.3) and is given by

$$
u_n^P(r) = \begin{cases}
-2\left[\int_{R_1}^{r} f_n(\rho)\left(\frac{\rho}{r}\right)^n \frac{\rho}{n} d\rho + \int_{r}^{R_2} f_n(\rho)\left(\frac{r}{\rho}\right)^n \frac{\rho}{n} d\rho\right], & \text{if } n > 0, \\[2mm]
2\left[\int_{R_1}^{r} f_n(\rho)\left(\frac{r}{\rho}\right)^n \frac{\rho}{n} d\rho + \int_{r}^{R_2} f_n(\rho)\left(\frac{\rho}{r}\right)^n \frac{\rho}{n} d\rho\right], & \text{if } n < 0, \\[2mm]
4\left[\int_{R_1}^{r} f_0(\rho)\rho \log r\, d\rho + \int_{r}^{R_2} f_0(\rho)\rho \log \rho\, d\rho\right], & \text{if } n = 0.
\end{cases}
$$

The solution of $v^P(z)$ can be found in any standard text book of applied math (see([23],[19])) but we mention here for the sake of completeness.

Theorem 8.1.1. *If $h_{1,n}$ and $h_{2,n}$ are the Fourier coefficient of $h_1(\theta)$ and $h_2(\theta)$ at the boundary then the Fourier coefficient $v_n^P(r)$ of $v^P(r,\theta)$ is given by*

$$
v_n^P(r) = \begin{cases}
\alpha_0 \log(r) + \beta_0, & \text{if } n = 0, \\[2mm]
\alpha_n r^{-n} + \beta_n r^n, & \text{if } n \neq 0.
\end{cases} \tag{8.7}
$$

where,

$$
\alpha_0 = \frac{h_{1,0} - h_{2,0}}{\log\left(\frac{R_1}{R_2}\right)}, \qquad \beta_0 = \frac{h_{2,0}\log R_1 - h_{1,0}\log R_2}{\log\left(\frac{R_1}{R_2}\right)}
$$

and

$$
\alpha_n = \frac{(R_1 R_2)^n (h_{2,n}(R_1)^n - h_{1,n}(R_2)^n)}{(R_1)^{2n} - (R_2)^{2n}}, \qquad \beta_n = \frac{(h_{1,n}(R_1)^n - h_{2,n}(R_2)^n)}{(R_1)^{2n} - (R_2)^{2n}}
$$

Proof. The Fourier series representation of $v^P(z)$ is given by $v^P(r,\theta) = \sum_{n=-\infty}^{\infty} v^P(n,r)e^{in\theta}$ and the Fourier coefficient satisfies the differential equation

$$
\frac{d^2 v_n^P}{dr^2} + \frac{1}{r}\frac{dv_n^P}{dr} - \frac{n^2}{r^2}v_n^P = 0
$$

106

with boundary conditions given by

$v_n^P(r = R_1) = h_{1,n}$ and $v_n^P(r = R_2) = h_{2,n}$

The solution of the Euler differential equation is given by

$$v_n^P(r) = \begin{cases} \alpha_0 \log(r) + \beta_0, & \text{if } n = 0, \\ \alpha_n r^{-n} + \beta_n r^n, & \text{if } n \neq 0. \end{cases}$$

and using the boundary conditions the above system is solved to obtain,

$$\alpha_0 = \frac{h_{1,0} - h_{2,0}}{\log(\frac{R_1}{R_2})}, \tag{8.8}$$

$$\beta_0 = \frac{h_{2,0} \log R_1 - h_{1,0} \log R_2}{\log(\frac{R_1}{R_2})}, \tag{8.9}$$

$$\alpha_n = \frac{(R_1)^n (R_2)^n (h_{2,n}(R_1)^n - h_{1,n}(R_2)^n)}{(R_1)^{2n} - (R_2)^{2n}}, \tag{8.10}$$

$$\beta_n = \frac{(h_{1,n}(R_1)^n - h_{2,n}(R_2)^n)}{(R_1)^{2n} - (R_2)^{2n}}. \tag{8.11}$$

$\square$

Hence we obtain w^P. Similarly using the technique above we obtain ω with this decomposition

$\omega(r, \theta) = u^H(r, \theta) + v^H(r, \theta)$ where $v^H(r, \theta)$ and $u^H(r, \theta)$ satisfy

$$\partial_z \partial_{\bar{z}} u^H = f, \quad \text{in} \quad \mathbf{\Omega}. \tag{8.12}$$

and

$$\begin{cases} \partial_z \partial_{\bar{z}} v^H = 0, & \text{in} \quad \mathbf{\Omega}, \\ v^H = \gamma_2 - u^H(\theta), & \text{on} \quad \partial\mathbf{\Omega}. \end{cases} \tag{8.13}$$

107

Next we consider the (D4) biharmonic problem on an annular disk Ω given by $\Omega = \{z \in \mathbb{R}^2 : R_1 < |z| < R_2\}$ and $\partial\Omega = \{z \in \mathbb{R}^2 : |z| = R_1 \quad \text{or} \quad |z| = R_2\}$. The (D4) problem given by

$$\begin{cases} (\partial_z \partial_{\bar{z}})^2 w & = f, & \text{in} \quad \Omega, \\ w & = h_0, & \text{on} \quad \partial\Omega, \\ \partial_\nu w_{z\bar{z}} & = g, & \text{on} \quad \partial\Omega. \end{cases} \tag{8.14}$$

with $\quad k = \frac{1}{4\pi i} \int_{\partial\Omega} w_{z\bar{z}} \frac{dz}{z}$ and satisfying the condition

$$\frac{1}{4i} \int_{\partial\Omega} g(\zeta) \frac{d\zeta}{\zeta} = \int_{\Omega} f(\zeta) d\xi d\eta,$$

can be decomposed into two Poisson problems

$$\begin{cases} \partial_z \partial_{\bar{z}} w^N & = f, & \text{in} \quad \Omega, \\ \partial_\nu w^N & = g, & \text{on} \quad \partial\Omega. \end{cases} \tag{8.15}$$

$$\begin{cases} \partial_z \partial_{\bar{z}} \omega & = w^N, & \text{in} \quad \Omega, \\ \omega & = h_0, & \text{on} \quad \partial\Omega. \end{cases} \tag{8.16}$$

Let $w^N(r,\theta) = u^N(r,\theta) + v^N(r,\theta)$ where $v^N(r,\theta) \quad \text{and} \quad u^N(r,\theta)$ satisfy

$$\partial_z \partial_{\bar{z}} u^N = f \quad \text{in} \quad \Omega \tag{8.17}$$

and

$$\begin{cases} \partial_z \partial_{\bar{z}} v^N & = 0, & \text{in} \quad \boldsymbol{\Omega}, \\ v^N & = g - \partial_\nu u^N(\theta), & \text{on} \quad \partial\boldsymbol{\Omega}. \end{cases}$$

We note that

$$\begin{aligned} \frac{\partial}{\partial r} w^N(R_1) & = -g_n(R_1) = -g_n^{(1)}, \\ \frac{\partial}{\partial r} w^N(R_2) & = g_n(R_1) = g_n^{(2)}. \end{aligned}$$

Now u^N is same as u^P and solved similarly using the free space Green's function. The solution of v^N is easily obtained from any standard text book of applied math and is given by the following theorem.

Theorem 8.1.2. *If $v_n^N(r)$ and $g_n^1(r), g_n^2(r)$ are the Fourier coefficient of $v^N(z)$ and $g(\theta)$ in the annular disc and at the boundary respectively then the Fourier coefficients $v_n^N(r)$ of $v^N(r,\theta)$ for $n = 0$ and $n \neq 0$ are respectively given by*

$$v_n^N(r) = \begin{cases} -R_1 \log r \left(g_0^1 + d_r u_0^N(R_1) \right) + k, \\ \left(\dfrac{\left(\frac{R_2}{r}\right)^{|n|} + \left(\frac{r}{R_2}\right)^{|n|}}{\left(\frac{R_2}{R_1}\right)^{|n|} - \left(\frac{R_1}{R_2}\right)^{|n|}} \right) \dfrac{R_1\left(d_r u_n^N(R_1) + g_n^1\right)}{|n|} + \left(\dfrac{\left(\frac{R_1}{r}\right)^{|n|} + \left(\frac{r}{R_1}\right)^{|n|}}{\left(\frac{R_1}{R_2}\right)^{|n|} - \left(\frac{R_2}{R_1}\right)^{|n|}} \right) \dfrac{R_2\left(d_r u_n^N(R_2) - g_n^2\right)}{|n|}. \end{cases}$$

$$(8.18)$$

Proof. The Fourier series representation of $v_n^N(z)$ is given by

$$v^N(r,\theta) = \sum_{n=-\infty}^{\infty} v^N(n,r) e^{in\theta}$$

109

and the Fourier coefficients satisfy the differential equation

$$\frac{d^2 v_n^N}{dr^2} + \frac{1}{r}\frac{dv_n^N}{dr} - \frac{n^2}{r^2}v_n^N = 0$$

with boundary conditions given by

$\partial_n v_n^N(r = R_1) = g_n^{(1)} - \partial_n u_n^N(R_1)$ and $\partial_n v_n^N(r = R_2) = g_n^{(2)} - \partial_n u_n^N(R_2)$

The solution of the Euler differential equation is given by

$$v_n^N(r) = \begin{cases} C_0 \log(r) + D_0, & \text{if } n = 0, \\ C_n r^{-n} + D_n r^n, & \text{if } n \neq 0. \end{cases}$$

Applying the boundary condition we get the above formulation of $v_n^N(r)$. $\qquad\square$

Similarly taking $\omega = u^{NH} + v^{NH}$ we solve for u^{NH} and v^{NH} to obtain ω.

8.1.1 Fast Algorithm

For a grid with $M \times N$ equidistant points, M in the radial and N in the circular direction and $r_l = R_1 + \frac{(l-1)(R_2-R_1)}{M-1}, \theta_n = \frac{2\pi n}{N}, l = 1...M$ we find w^P for the (D2) biharmonic problem first.

Initialization: Choose M and N. Define $K = \frac{N}{2}$.

Inputs: $\quad f(r_l e^{\frac{2\pi i k}{N}}), \quad \gamma_2(e^{\frac{2\pi i k}{N}}), \quad l \in [1, M], \quad k = 1.....N$ and $n \in [-K+1, K]$

Step 1. Compute $A_{n,1}^{i,i+1}, \quad A_{0,1}^{i,i+1}, \quad B_{n,1}^{i,i+1}, \quad B_{0,1}^{i,i+1}$ for $i \in [1, M-1], \quad n \in [-K+1, K]$ using (6.3), (6.4),(6.1), (6.2).

Step 2. Compute $p_{1,n}^{(1)}(r_l), \ p_{2,n}^{(1)}(r_l)$ for $n \in [1, K]$ and $s_{1,n}^{(1)}(r_l), \ s_{2,n}^{(1)}(r_l)$ for $n \in [-K+1, -1], \ t_{1,0}^{(1)}(r_l), \ t_{2,0}^{(1)}(r_l)$ and $l \in [1, M]$ using (6.5), (6.6), (6.7), (6.8), (6.9), (6.10) by setting in the following way:

Set $p_{1,n}^{(1)}(0) = 0$

for $n = 1........K$

for $l = 2....M$

$$p_{1,n}^{(1)}(r_l) = \left(\frac{r_{l-1}}{r_l}\right)^n p_{1,n}^{(1)}(r_{l-1}) - B_{n,1}^{l-1,l}$$

end

end

Set $p_{2,n}^{(1)}(1) = 0$

for $n = 1........K$

for $l = M - 1....1$

$$p_{2,n}^{(1)}(r_l) = \left(\frac{r_l}{r_{l+1}}\right)^n p_{2,n}^{(1)}(r_{l+1}) - A_{n,1}^{l,l+1}$$

end

end

Set $s_{1,n}^{(1)}(0) = 0$

for $n = -K........ - 1$

for $l = 2....M$

$$s_{1,n}^{(1)}(r_l) = \left(\frac{r_l}{r_{l-1}}\right)^n s_{1,n}^{(1)}(r_{l-1}) - A_{n,1}^{l-1,l}$$

end

end

Set $s_{2,n}^{(1)}(1) = 0$

for $n = -K........1$

for $l = M - 1....1$

$$s_{2,n}^{(1)}(r_l) = \left(\frac{r_{l+1}}{r_l}\right)^n s_{2,n}^{(1)}(r_{l+1}) + B_{n,1}^{l,l+1}$$

end

end

for $l = 2....M$
$$t_{1,0}^{(1)}(r_l) = \left(\frac{\log r_l}{\log r_{l-1}} \right) t_{1,0}^{(1)}(r_{l-1}) - A_{0,1}^{l-1,l}$$
end

for $l = M - 1....1$
$$t_{2,0}^{(1)}(r_l) = t_{2,0}^{(1)}(r_{l+1}) + B_{0,1}^{l,l+1}$$
end

Step 3. Compute,

$$u_n^P(r_l) = \begin{cases} p_{1,n}^{(1)}(r_l) + p_{2,n}^{(1)}(r_l) & \text{if } n > 0, \\ s_{1,n}^{(1)}(r_l) + s_{2,n}^{(1)}(r_l) & \text{if } n < 0, \\ t_{1,0}^{(1)}(r_l) + t_{2,0}^{(1)}(r_l) & \text{if } n = 0. \end{cases}$$

Step 4. Compute the Fourier coefficient $h_{1,n}(r_l)$, $h_{2,n}(r_l)$ using FFT.

Step 5. Compute α_0, β_0, α_n, β_n using (8.8), (8.9), (8.10), (8.11)

Step 6. Compute the Fourier coefficient $v_n^P(r_l)$, $l = 1..M$.

Step 7. Compute $w^P(r_l e^{r_l \frac{2\pi i k}{N}}) = \sum_{n=-K}^{K} \left(v_n^P(r_l) + u_n^P(r_l) \right) e^{\frac{2\pi i n k}{N}}$.

We repeat the same algorithm to obtain ω from u^H and v^H. The algorithm is similar for (D4) biharmonic problem with changes in step 6 to compute $v_n^N(r)$.

8.1.2 Algebraic Complexity

Each FFT of length N contributes $N \log N$ operations. There are $3M$ FFT's of length N. The computation of $A_{n,1}^{i,i+1}$ and $B_{n,1}^{i,i+1}$, $i \in [1, M - 1]$ in step $1, 2$ and step $3, 4, 5, 6$ require computation of $\mathcal{O}(\mathcal{MN})$. Hence the asymptotic operation count is

$\mathcal{O}(\mathcal{MN}\log\mathcal{N})$ for $M \times N$ grid points. Numerical results will be added in Section.10.

8.2 Biharmonic Equation In An Eccentric Annular Domain

We now give an outline to solve (D2) and (D4) biharmonic problems in an eccentric annular domain. We here take advantage of the algorithm for the concentric annular domain. This is obtained with the help of a conformal mapping which maps the eccentric annular domain Ω_1 into the concentric annular domain Ω. The conformal mapping $\zeta = T(z) = \frac{z - R_1}{z - \frac{1}{R_1}}$ maps the circles $\partial\Omega_1^1 : |z| = 1$ and $\partial\Omega_1^2 : |z - \alpha| = r$ to $\partial\Omega^1 : |\zeta| = R_1$ and $\partial\Omega^2 : |\zeta| = R_2$ respectively. R_1 is given by the smallest root of the equation $\alpha q^2 + (r^2 - \alpha^2 - 1)q + \alpha = 0$ and $R_2 = \sqrt{\frac{R_1(R_1 - \alpha)}{1 - R_1\alpha}}$. It can be verified that $0 < \alpha < R_1 < \alpha + r < 1$ if $\alpha + r < 1$. The biharmonic problem

$$
\begin{aligned}
(\partial_z\partial_{\bar{z}})^2\omega &= f, &\text{in}\quad &\Omega_1, \\
\omega &= \gamma_0, &\text{on}\quad &\partial\Omega_1, \\
\omega_{z\bar{z}} &= \gamma_2, &\text{on}\quad &\partial\Omega_1.
\end{aligned}
$$

decomposed into two Poisson problems

$$
\begin{cases}
\partial_z\partial_{\bar{z}}w^P &= f, &\text{in}\quad \Omega_1, \\
w^P &= \gamma_2, &\text{on}\quad \partial\Omega_1.
\end{cases}
\qquad
\begin{cases}
\partial_z\partial_{\bar{z}}\omega &= w^P, &\text{in}\quad \Omega_1, \\
\omega &= T(\gamma_0), &\text{on}\quad \partial\Omega_1.
\end{cases}
\tag{8.19}
$$

is

$$
\begin{cases}
\partial_z\partial_{\bar{z}}w^P &= T(r,\theta)f, &\text{in}\quad \Omega, \\
w^P &= \gamma_2, &\text{on}\quad \partial\Omega.
\end{cases}
\qquad
\begin{cases}
\partial_z\partial_{\bar{z}}\omega &= T(r,\theta)w^P, &\text{in}\quad \Omega, \\
\omega &= T(\gamma_0), &\text{on}\quad \partial\Omega,
\end{cases}
\tag{8.20}
$$

under the conformal map T. Here $T(r, \theta)$ is given by $T(r, \theta) = \left| \frac{R_1^2 - 1}{4R_1(\zeta - 1)^2} \right|$. Similarly we treat the case of the (D3) biharmonic problem in an eccentric annular disk Ω_1.

9. STEADY, INCOMPRESSIBLE NAVIER-STOKES EQUATIONS IN TWO-DIMENSIONS

In this section, we discuss the application of the fast biharmonic algorithms developed in this thesis. We consider here flows within a circular cylinder (see ([33],[26],[29],[24])). We study the steady state two-dimensional viscous motion within a circular cylinder. Here we use our existing fast algorithm for the biharmonic problems and provide an algorithm to solve the steady, viscous, incompressible flow within a circular cylinder. The practical application of these type of problems arise in recirculation of fluids in cavities and in confined ventilation. The governing equation associated with the steady, viscous, incompressible flow is given by

$$(\mathbf{u} \cdot \nabla)\mathbf{u} \;=\; -\nabla p + \nabla \cdot (R^{-1}\nabla\mathbf{u}) \tag{9.1}$$

$$\nabla \cdot \mathbf{u} \;=\; 0 \tag{9.2}$$

where p is the pressure, R is the Reynolds number, and $\mathbf{u}$ is the velocity vector of the fluid motion. We consider flow in two dimensions with polar coordinates (r, θ). The velocity vector is given by $u_r = \frac{1}{r}\frac{\partial \psi}{\partial \theta}, \quad u_\theta = -\frac{\partial \psi}{\partial r}$ which satisfy the equation of continuity and ψ is the stream function. The vorticity for the planar flow is defined as $\boldsymbol{\varphi} = \nabla \times \mathbf{u} = \varphi\hat{k}$ where φ is given by

$$\varphi \;=\; \frac{1}{r}\partial_r(ru_\theta) - \frac{1}{r}\partial_\theta(u_r) \tag{9.3}$$

Substituting the values of u_r and u_θ in (9.3) we get,

$$\varphi \;=\; -\Delta\psi \tag{9.4}$$

115

Taking curl of both sides and simplifying we get the following vorticity equation (9.1) we obtain,

$$\mathbf{u} \cdot \nabla \varphi \;=\; \frac{1}{R} \Delta \varphi \tag{9.5}$$

Substituting (9.4) in (9.5) we obtain,

$$\Delta^2 \psi \;=\; -RJ[\psi, \Delta \psi], \tag{9.6}$$

where J is the Jacobian given by $J[\psi, \Delta\psi] = \frac{1}{r}(\partial_r\psi\partial_\theta\Delta\psi - \partial_r\Delta\psi\partial_\theta\psi)$. If $R \to 0$, then (9.6) becomes the homogeneous biharmonic equation. Steady, incompressible,viscous flow in a unit disc of the complex plane can be modeled using the following boundary value biharmonic problem (see([33],[26],[29])).

$$\begin{cases} (\partial_z\partial_{\bar{z}})^2\psi = & -\frac{R}{16}J[\psi, \psi_{z\bar{z}}] & \text{in} \quad r < 1 \\ \psi = f_1(\theta) & \text{on} \quad r = 1 \\ \frac{\partial\psi}{\partial r} = -f_2(\theta) & \text{on} \quad r = 1. \end{cases} \tag{9.7}$$

This is precisely the (D3) biharmonic boundary value problem. We use the fast algorithm to solve the above problem (9.7).

9.1 Numerical Formulation

In this section, we develop an iteration scheme to solve (9.7). We use here the solution of the (D3) biharmonic problem on a unit disc (see ([33], [24])).

9.1.1 Stokes Flow

We first consider the slow creeping flow in a disk when $R \to 0$. So, the above boundary value problem reduces to the homogeneous biharmonic problem associated

with (D3) problem in Section. 5. It's solution is given by

$$\psi(z) = \frac{(1 + |z|^2)}{4\pi i} \int_{\partial D} g_1(z, \zeta) f_1(\zeta) \frac{d\zeta}{\zeta} + \frac{(1 - |z|^2)}{4\pi i} \int_{\partial D} g_2(z, \zeta) f_1(\zeta) \frac{d\zeta}{\zeta}$$
$$- \frac{(1 - |z|^2)}{2\pi i} \int_{\partial D} g_1(z, \zeta) f_2(\zeta) \frac{d\zeta}{\zeta}.$$

The solution is obtained by computing the boundary integrals $u_3(z), h_3(z), r_3(z)$ as in (5.2), (5.3), (5.4). This solution later will serve as the initial guess for solving the problem in the iterative method.

9.1.2   Flow At Steady State With Low Reynolds Number

Now we seek the solution for flows with nonzero Reynolds number. We concentrate here on flows with low Reynolds number. We follow an iteration method here. We start with an initial guess $\psi^{(0)}$ obtained from the solution of Stokes flow satisfying

$$\psi^{(0)}_{z\bar{z}z\bar{z}} = 0,$$

and then at each $(k+1)$th stage we solve

$$\begin{aligned}
\psi^{(k+1)}_{z\bar{z}z\bar{z}} &= -\tfrac{R}{16} J[\psi^{(k)}, \psi^{(k)}_{z\bar{z}}] &&\text{in}\quad r < 1, \\
\psi^{k+1} &= f_1(\theta), &&\text{on}\quad r = 1, \\
\tfrac{\partial \psi^{(k+1)}}{\partial r} &= -f_2(\theta), &&\text{on}\quad r = 1.
\end{aligned}$$

The solution is obtained, using the fast algorithm for the (D3) biharmonic problem. The vorticity φ is obtained through $\varphi = -\Delta\psi$. We continue the iteration until the convergence criterion $\frac{||\psi^{k+1}|| - ||\psi^k||}{||\psi^{k+1}||} < tol$ is met. The Jacobian is obtained using the central difference formula on mesh points inside the disk and backward difference, forward difference for points on the boundary.

9.2 Fast Algorithm

We present here a fast algorithm to obtain the stream function for a steady, slow,viscous, incompressible flow. Let $0 = r_1 < r_2 < .....r_M = 1$.

Initialization: Choose M and N. Define $K = \frac{N}{2}$.

Inputs: $M, N, f_1(e^{\frac{2\pi ik}{N}}), f_2(e^{\frac{2\pi ik}{N}}), k = 1.....N$ and $n \in [-K + 1, K]$.

Step 1. Compute the Fourier coefficients $f_{1,n}, f_{2,n}$ using FFT for all $n \in [-K+1, K]$.

Step 2. Compute $u_{3,n}(r_l), h_{3,n}(r_l), r_{3,n}(r_l)$ to obtain $\psi^{(0)}(z)$.

Step 3. Compute $\frac{R}{16} J[\psi^{(k)}, \psi^{(k)}_{z\bar{z}}]$ and obtain it's FFT. Here the superscript 'k' refers to the level of iteration after the suitable initial choice $\psi^{(0)}(z)$ is obtained.

Step 4. Compute the stream function $\psi^{(k)}(z)$ using the algorithm in section (7.2.2) till $\frac{||\psi^{k+1}||-||\psi^k||}{||\psi^{k+1}||} < tol$ is met.

9.3 Algorithmic Complexity

We consider the computational complexity of the above algorithm. In step 1 there are $2M$ FFT's and in step 4 of the algorithm for each new fixed iterate ψ^{k+1} the asymptotic operation count is $\mathcal{O}(\mathcal{MN} \log \mathcal{N})$ for $M \times N$ points, with M being the grid point in radial direction and N in the circumferential direction. All other computations in steps $2, 3$ and 4 are of lower order. So the overall computational complexity for the algorithm is $\mathcal{O}(\mathcal{MN} \log \mathcal{N})$. Also the above algorithms are parallelizable on multi processor machines (see ([12],[11])) But with this iteration procedure, there arises a serious convergence problem for higher Reynolds number. This method converges only for problem with Reynolds number less than 4.

9.4   Flow At Steady State With Moderate Reynolds Number

The previous iteration method fails for Reynolds number > 4. Therefore we modify our iteration method for Reynolds number > 4. We precisely use a relaxation factor as in the Gauss-Siedel SOR method (see [33]). We start with our initial guess as before to obtain $\boldsymbol{\psi}^{(0)}(z)$ and use the fast algorithm to compute the iterate $\psi^{(k+1)}(z)$. For convergence we use two relaxation factors α and β for fields φ and ψ. To update the values of φ and ψ we use

$$
\begin{aligned}
\varphi_{n,l}^{(k+1)} &= \alpha\varphi_{n,l}^{\star(k+1)} + (1-\alpha)\varphi_{n,l}^{(k)} \\
\psi_{n,l}^{(k+1)} &= \beta\psi_{n,l}^{\star(k+1)} + (1-\beta)\psi_{n,l}^{(k)}
\end{aligned}
$$

The starred quantity denotes the value obtained at each iterative step. The relaxation factor helps in convergence and suitable choices for α and β are taken to be $0.3, 0.5$. The convergence is continued until convergence criterion is met. We have applied the algorithm on several numerical problems given in Section. 10.

9.5   Elasticity

We consider here elastic displacements that occur in planes parallel to the (x, y) plane and the displacement components are independent of z. If u_x and u_y are the components of displacement and σ_x, σ_y and $\tau_{x,y}$ are respectively the components of stress, the governing equations of elasticity with equilibrium condition and stress

119

strain relations (see([25]))are given by

$$\frac{\partial \sigma_x}{\partial x} + \frac{\partial \tau_{xy}}{\partial y} = 0, \tag{9.8}$$

$$\frac{\partial \tau_{xy}}{\partial x} + \frac{\partial \sigma_y}{\partial y} = 0, \tag{9.9}$$

$$\sigma_x = (\lambda + 2\mu)\frac{\partial u}{\partial x} + \lambda\frac{\partial v}{\partial y}, \tag{9.10}$$

$$\sigma_y = (\lambda + 2\mu)\frac{\partial v}{\partial y} + \lambda\frac{\partial u}{\partial x}, \tag{9.11}$$

$$\tau_{xy} = \mu\left(\frac{\partial u}{\partial y} + \frac{\partial v}{\partial x}\right). \tag{9.12}$$

Here λ and μ are the Lamé coefficients. In our case, we consider the elastic region to be the unit disc $\mathbf{D}$. We first find the state of elastic equilibrium when the displacements on the boundary $\partial \mathbf{D}$ are given:

$$u_x = f_1(t), u_y = f_2(t) \quad \text{for} \quad t \in \partial \mathbf{D}.$$

Also, if external forces are applied to the boundary $\partial \mathbf{D}$ and their components denoted by X and Y, it is seen that

$$\left(-\frac{\partial x}{\partial s}, \frac{\partial y}{\partial s}\right) \cdot (-\tau_{x,y}, \sigma_x) = X$$

$$\left(-\frac{\partial x}{\partial s}, \frac{\partial y}{\partial s}\right) \cdot (\sigma_y, \tau_{x,y}) = Y$$

where s is the arc length and $\frac{\partial}{\partial s}$ denotes the tangential derivative. We set the following

$$\sigma_x = \frac{\partial^2 W}{\partial y^2} \tag{9.13}$$

$$\sigma_y = \frac{\partial^2 W}{\partial x^2} \tag{9.14}$$

$$\tau_{xy} = -\frac{\partial^2 W}{\partial x \partial y}. \tag{9.15}$$

The function $W(x, y)$ is called the Airy function. Substituting (9.13)-(9.15) in (9.10)-(9.12) yields the biharmonic equation:

$$\Delta^2 W = 0.$$

We also obtain here the following boundary condition:

$$\frac{\partial}{\partial s}\left(\frac{\partial W}{\partial y}\right) = X, \quad \frac{\partial}{\partial s}\left(\frac{\partial W}{\partial x}\right) = -Y$$

where

$$\frac{\partial W}{\partial y} = \int X ds, \quad \frac{\partial W}{\partial x} = -\int Y ds.$$

We consider here the complex plane and these equations together can be written in the unit disc $\mathbf{D}$ in the complex plane as

$$(\partial_z \partial_{\bar{z}})^2 W = 0, \quad \text{in} \quad \mathbf{D},$$

$$\frac{\partial W}{\partial \bar{z}} = \gamma_0, \quad \text{on} \quad \partial \mathbf{D},$$

$$W = 0, \quad \text{on} \quad \partial \mathbf{D}.$$

121

10.   NUMERICAL IMPLEMENTATION OF THE ALGORITHMS

In this section, the numerical results are presented and discussed. The error in the numerical computation arises from the evaluation of the one dimensional integrals in the algorithm and the truncation of the Fourier series. The numerical implementations were done in MATLAB and computation were performed using double precision arithmetics. We provide here the numerical results for both the methods, namely the double Poisson and the direct methods for the different biharmonic boundary value problems. CPU time is also presented for the computations.

10.1   Numerical Results

Example 1. We consider the (D2) biharmonic problem

$$
\begin{aligned}
f(z) &= 12\bar{z} + i12z \\
h_0 &= \bar{z} + iz \\
h_2 &= 6\bar{z} + i6z.
\end{aligned}
$$

The Trapezoidal and Euler-Maclaurin formulas are used for numerical integration in the radial direction and 64 Fourier coefficients are used to represent the functions. Tables 10.1 and 10.2 show the relative error for this problem for different values of M and fixed $N = 64$. In the double Poisson method, a second order convergence using Trapezoidal rule and a fourth order convergence using Euler-Maclaurin rule are observed in the Tables. 10.1 and 10.2. CPU time is also shown in the tables. The Trapezoidal rule for the direct and double Poisson method gives quadratic convergence. The error plot of $f(z) = 12\bar{z} + 12iz$ using Euler-Maclaurin rule for $M = 256$ in double Poisson method is shown in Fig. 10.1 and the plot showing the order of

122
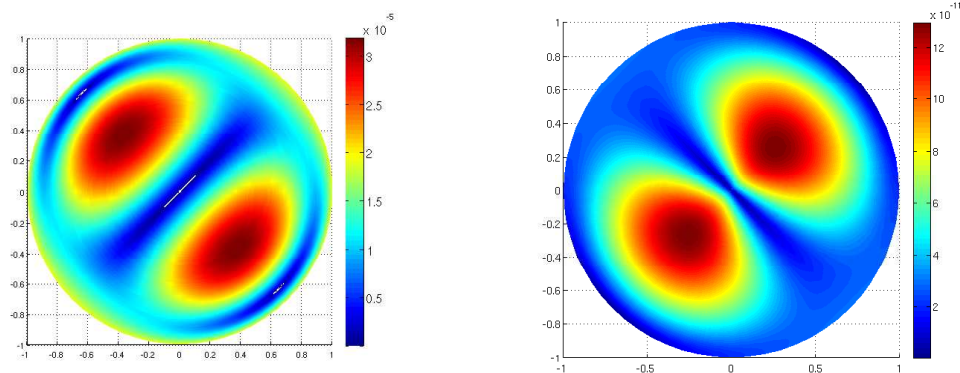
Figure 10.1: The graph depicts the absolute error for (D2) problem with $f = 12\bar{z} + i12z$, $N = 64, M = 513$ for the direct and the double Poisson methods respectively using the Euler-Maclaurin formula. As the table suggests, the plots reflect the bounds for error in **D** at $N = 64, M = 513$. This is a color plot on screen.

accuracy in the $|| \cdot ||_\infty$ norm is shown in Fig. 10.2. We observe that the double Poisson method scores better in terms of accuracy and time here. The numerical and analytical plots of the real and imaginary parts of the solution are depicted for $M = 256, N = 32$ in Fig. 10.3, Fig. 10.4.

Example 2. We consider the homogeneous (D2) biharmonic problem given by

$$
\begin{aligned}
f(z) &= 0 \\
h_0 &= 1 \\
h_2 &= 1.
\end{aligned}
$$

We employ the two algorithms for the (D2) problem using Euler-Maclaurin rule and Trapezoidal rule and we observe the relative errors for different values of M

Table 10.1: Relative error for $f(z) = 12\bar{z} + 12iz$ using Euler-Maclaurin formula.

M	Direct Method			Double Poisson Method		
	$\|\|\cdot\|\|_\infty$	order	T_{dir}	$\|\|\cdot\|\|_\infty$	order	T_{doub}
16	2.8×10^{-2}	0	0.5	3.7×10^{-4}	0	0.25
32	1.1×10^{-2}	1.4	0.56	1.7×10^{-5}	4.39	0.30
64	3.2×10^{-3}	1.7	0.64	1.1×10^{-6}	3.95	0.39
128	8.7×10^{-4}	1.8	0.83	6.6×10^{-8}	4.05	0.57
256	2.3×10^{-4}	1.9	1.25	4.2×10^{-9}	3.97	0.92
512	5.8×10^{-5}	1.7	2.07	2.6×10^{-10}	4.01	1.60

Table 10.2: Relative error for $f(z) = 12\bar{z} + 12iz$ using Trapezoidal rule.

M	Direct Method			Double Poisson Method		
	$\|\|\cdot\|\|_\infty$	order	T_{dir}	$\|\|\cdot\|\|_\infty$	order	T_{doub}
17	1.2×10^{-1}	0	0.25	2.7×10^{-2}	0	0.16
33	3.2×10^{-2}	1.9	0.32	7.1×10^{-3}	1.9	0.20
65	8.2×10^{-3}	1.9	0.55	1.8×10^{-3}	1.9	0.26
129	2.1×10^{-3}	1.9	1.40	4.5×10^{-4}	2.0	0.41
256	5.2×10^{-4}	2.0	4.08	1.14×10^{-4}	1.9	0.71
513	1.3×10^{-4}	2.0	16.57	2.8×10^{-5}	2.1	1.4
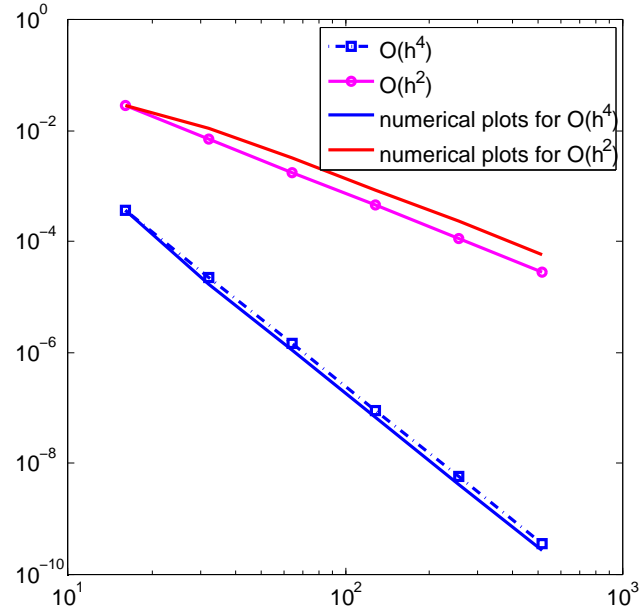
Figure 10.2: The order of accuracy using Euler-Maclaurin formula is plotted here for the direct and the double Poisson method for $f = 12\bar{z} + i12z$. $\mathcal{O}(h^2)$ for direct method and $\mathcal{O}(h^4)$ convergence for double Poisson method in $||\cdot||_\infty$ norm are noted as the mesh is refined. This is a color plot in screen.

and fixed $N = 64$ in Tables. 10.3 and 10.4. The direct method gives us a highly accurate and faster solution than the double Poisson method. The low accuracy in double Poisson method is due to the logarithmic singularity involved and we obtain a quadratic convergence using Euler-Maclaurin formula. First order convergence using Trapezoidal rule in double Poisson method is observed. We notice, even with M as small as 16 a highly accurate solution is obtained in the case of direct method. The order of accuracy in the $||\cdot||_\infty$ norm is shown in Fig. 10.5 and the error plot using Euler-Maclaurin rule is shown in Fig. 10.6.
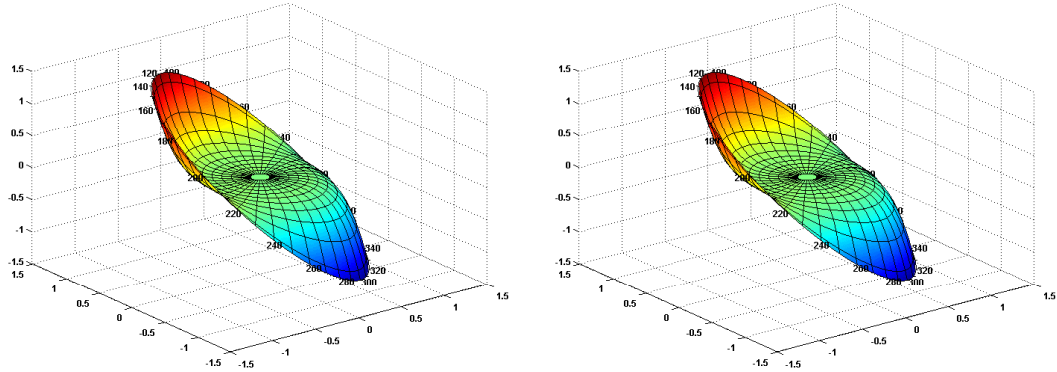
(a) imaginary part of the analytical solution   (b) imaginary part of the numerical solution

Figure 10.3: The graph depicts the analytical and numerical plot of the imaginary part of the solution for $f = 12\bar{z} + i12z, N = 64, M = 256$ in the double Poisson method. This is a color plot on screen.

Table 10.3: Relative error for $f(z) = 0$ using Euler-Maclaurin formula.

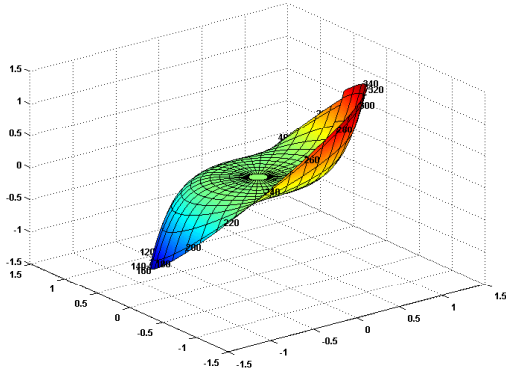|	Direct Method		Double Poisson Method		
M	$\lVert \cdot \rVert_\infty$	T_{dir}	$\lVert \cdot \rVert_\infty$	order	T_{doub}
16	7.22×10^{-15}	0.37	7.2×10^{-3}	0	0.18
32	7.22×10^{-15}	0.39	1.4×10^{-3}	2.4	0.21
64	7.22×10^{-15}	0.43	3.2×10^{-4}	2.1	0.35
128	7.22×10^{-15}	0.51	7.2×10^{-5}	2.4	0.55
256	7.22×10^{-15}	0.66	1.7×10^{-5}	2.1	0.88
512	7.22×10^{-15}	0.90	5.7×10^{-6}	1.6	1.42

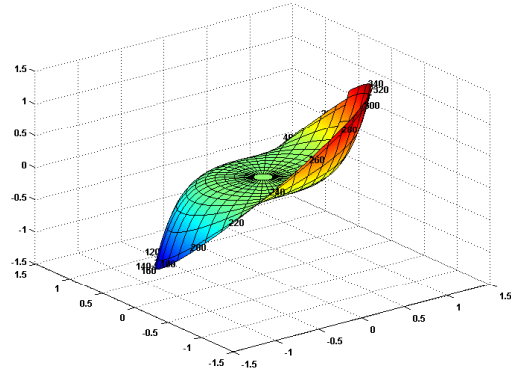(a) real part of the analytical solution   (b) real part of the numerical solution

Figure 10.4: The graph depicts the analytical and numerical plot of the real part of the solution for $f = 12\bar{z} + i12z, N = 64, M = 256$ in the double Poisson method. This is a color plot on screen.

Table 10.4: Relative error for $f(z) = 0$ using Trapezoidal rule.

	Direct Method		Double Poisson Method		
M	$\|\|\cdot\|\|_\infty$	T_{dir}	$\|\|\cdot\|\|_\infty$	order	T_{doub}
17	1.98×10^{-15}	0.15	1.9×10^{-1}	0	0.14
33	1.92×10^{-15}	0.20	9.5×10^{-2}	1.0	0.17
65	1.96×10^{-15}	0.30	4.7×10^{-2}	1.0	0.23
129	1.94×10^{-15}	0.67	2.3×10^{-2}	1.0	0.37
256	1.92×10^{-15}	2.24	1.1×10^{-2}	1.1	0.66
513	1.92×10^{-15}	7.15	4.9×10^{-3}	1.2	1.09
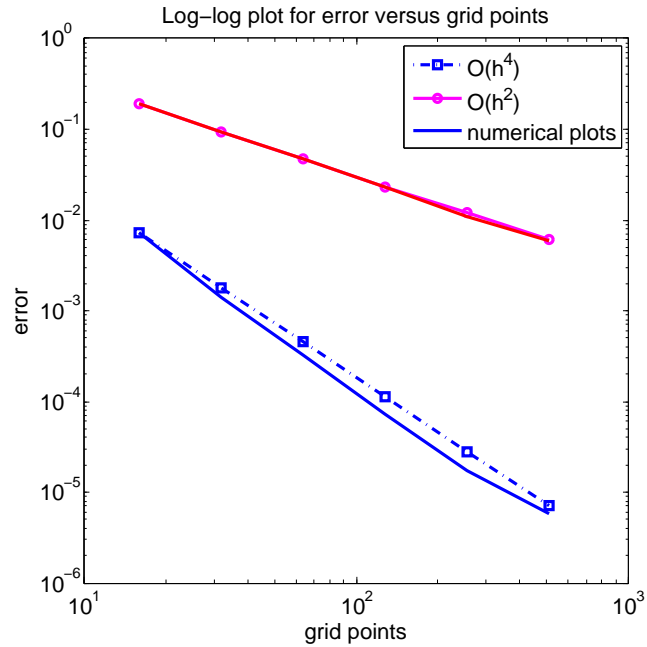
Figure 10.5: The order of accuracy is plotted here using Trapezoidal and Euler-Maclaurin rule in the double Poisson method with $f = 0$. $\mathcal{O}(h)$ with Trapezoidal rule and $\mathcal{O}(h^2)$ convergence with Euler-Maclaurin rule in $|| \cdot ||_\infty$ norm are noted as the mesh is refined. This is a color plot in screen.

Example 3. We consider the (D2) problem given by

$$f(z) = z^2 \bar{z}$$

$$h_0 = 0$$

$$h_2 = 0.$$

This example is of the form $z^p \bar{z}^q$ whose exact solution has been worked out in Section.

4. Trapezoidal rule and Euler-Maclaurin rule were used for numerical integration in
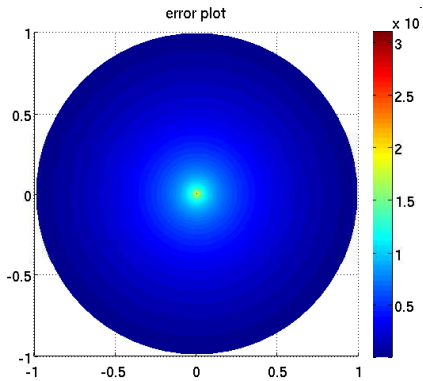
Figure 10.6: The graph depicts the absolute error for (D2) problem with $f = 0$ in the double Poisson method using the Euler Maclaurin expansion for $M = 64, N = 64$. As the table suggests, the plots reflect the bounds for error in $\mathbf{D}$ at $N = 64, M = 64$. This is a color plot on screen.

the radial direction and 64 Fourier coefficients has been used to represent the relative errors in Tables. 10.5, 10.6 for different values of M. The variation in the tables are noted with increase in M and the accuracy too improves thereon. The Trapezoidal rule for direct and double Poisson method gives quadratic convergence. The double Poisson method gives fourth order convergence and direct method shows a quadratic convergence with Euler-Maclaurin formula as is reflected in the Tables. 10.5, 10.6. Although the direct method gives quadratic convergence in both the cases but higher accuracy is obtained with the application of Euler-Maclaurin formula. The relative error plot of $f(z) = z^2\bar{z}$ using Euler-Maclaurin rule for $M = 256$ using double Poisson and direct method is shown in Fig. 10.7 and the order of accuracy in the $||\cdot||_\infty$ norm is shown in Fig. 10.8. The CPU timings are also included in the table. We observe better accuracy in case of double Poisson method.

Table 10.5: Relative error for $f(z) = z^2\bar{z}$ using Euler-Maclaurin formula.

M	Direct Method			Double Poisson method		
	$\|\cdot\|_\infty$	order	T_{dir}	$\|\cdot\|_\infty$	order	T_{doub}
16	4.07×10^{-2}	0	0.48	2.7×10^{-4}	0	0.25
32	1.09×10^{-2}	1.9	0.53	1.99×10^{-5}	3.8	0.3
64	3.7×10^{-3}	1.5	0.61	1.56×10^{-6}	3.7	0.38
128	1.1×10^{-3}	1.8	0.83	1.08×10^{-7}	3.9	0.57
256	3.02×10^{-4}	1.9	1.23	7.58×10^{-9}	3.8	0.93
512	7.85×10^{-5}	1.9	1.98	5.24×10^{-10}	3.9	1.71

Table 10.6: Relative error for $f(z) = z^2\bar{z}$ using Trapezoidal rule.

M	Direct Method			Double Poisson method		
	$\|\cdot\|_\infty$	order	T_{dir}	$\|\cdot\|_\infty$	order	T_{doub}
16	1.8×10^{-1}	0	0.24	1.4×10^{-2}	0	0.15
32	4×10^{-2}	2.2	0.30	3.7×10^{-3}	1.9	0.18
64	1.1×10^{-2}	1.9	0.53	9.1×10^{-4}	2.0	0.26
128	2.8×10^{-3}	1.9	1.37	2.3×10^{-4}	1.9	0.39
256	6.7×10^{-4}	2.1	4.73	5.6×10^{-5}	2.0	0.68
512	1.7×10^{-4}	2.0	16.58	1.4×10^{-5}	1.9	1.21
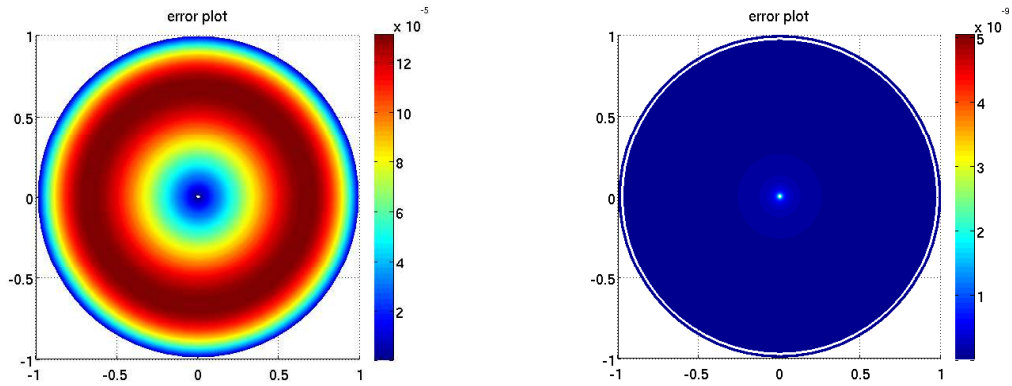
Figure 10.7: The graph depicts the absolute error for (D2) problem with $f = z^2\bar{z}$, $N = 64, M = 256$ for the direct and the Double Poisson method respectively using the Euler Maclaurin formula. As the table suggests, the plots reflect the bounds for error in $\mathbf{D}$ at $N = 64, M = 256$. This is a color plot in screen.

Figure 10.8: The order of accuracy using Euler-Maclaurin formula is plotted here for the direct and the double Poisson method for $f = z^2\bar{z}$. $\mathcal{O}(h^2)$ for direct method and $\mathcal{O}(h^4)$ convergence for double Poisson method in $||\cdot||_\infty$ norm are noted as the mesh is refined. This is a color plot in screen.

Example 4. We now consider the (D4) biharmonic problem

$$
\begin{aligned}
f(z) &= 72z^2\bar{z} + 72z\bar{z}^2 \\
h_0 &= \bar{z} + z \\
h_2 &= 60\bar{z} + 60z.
\end{aligned}
$$

This is a similar kind of example as the previous one and Euler-Maclaurin formula is used for numerical integration. Tables. 10.7 and 10.8 reflect the relative error with

Table 10.7: Relative error for $f(z) = 72z\bar{z}^2 + 72z^2\bar{z}$ using Euler-Maclaurin.

M	Direct Method			Double Poisson Method		
	$\|\cdot\|_\infty$	order	T_{dir}	$\|\cdot\|_\infty$	order	T_{doub}
16	7.5×10^{-1}	0	0.49	6.4×10^{-5}	0	0.25
32	1.2×10^{-1}	2.7	0.54	7.6×10^{-6}	3.1	0.30
64	3.1×10^{-2}	1.9	0.63	4.6×10^{-7}	4.0	0.38
128	8.8×10^{-3}	1.9	0.84	2.7×10^{-8}	4.1	0.56
256	2.2×10^{-3}	2.0	1.27	1.6×10^{-9}	4.1	0.94
512	5.8×10^{-4}	1.9	1.98	1.02×10^{-10}	4.0	1.61

Table 10.8: Relative error for $f(z) = 72z\bar{z}^2 + 72z^2\bar{z}$ using Trapezoidal rule.

M	Direct Method			Double Poisson method		
	$\|\cdot\|_\infty$	order	T_{dir}	$\|\cdot\|_\infty$	order	T_{doub}
16	1.2	0	0.24	9.1×10^{-2}	0	0.16
32	3.5×10^{-1}	1.8	032	2.4×10^{-2}	1.9	0.20
64	9.2×10^{-2}	1.9	0.55	6.2×10^{-3}	2.0	0.27
128	2.3×10^{-2}	2.0	1.37	1.6×10^{-3}	2.0	0.41
256	5.6×10^{-3}	2.0	4.7	3.9×10^{-4}	2.0	0.72
512	1.5×10^{-3}	1.9	16.54	9.9×10^{-5}	2.0	1.21

$f(z) = 72z^2\bar{z} + 72z\bar{z}^2$, different values of M and fixed $N = 64$. CPU time is also given in the tables. The double Poisson method gives an almost fourth order convergence and the direct method shows a quadratic convergence. The Trapezoidal rule gives a quadratic convergence for both the methods as shown in the Tables. 10.7 and 10.8 but higher accuracy for the direct method is obtained using the Euler-Maclaurin formula. The error plot for $f(z) = z^2\bar{z}$ using Euler-Maclaurin formula for $M = 512$ using double Poisson and direct method is shown Fig. 10.9. Like the above example the double Poisson method gives better accuracy than the direct one. The order of accuracy in the $\|\cdot\|_\infty$ norm is shown in the Fig. 10.10.

Figure 10.9: The graph depicts the absolute error for the (D4) biharmonic problem with $f = 72z\bar{z}^2 + 72z^2$, $N = 64, M = 512$ in the direct and the double Poisson method respectively using the Euler-Maclaurin formula. As the table suggests, the plots reflect the bounds for error in $\mathbf{D}$ at $N = 64, M = 512$. This is a color plot in the screen.
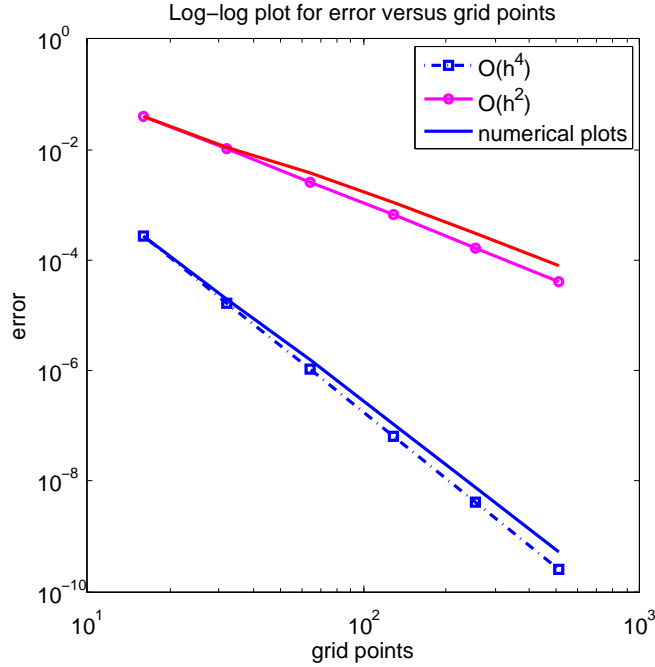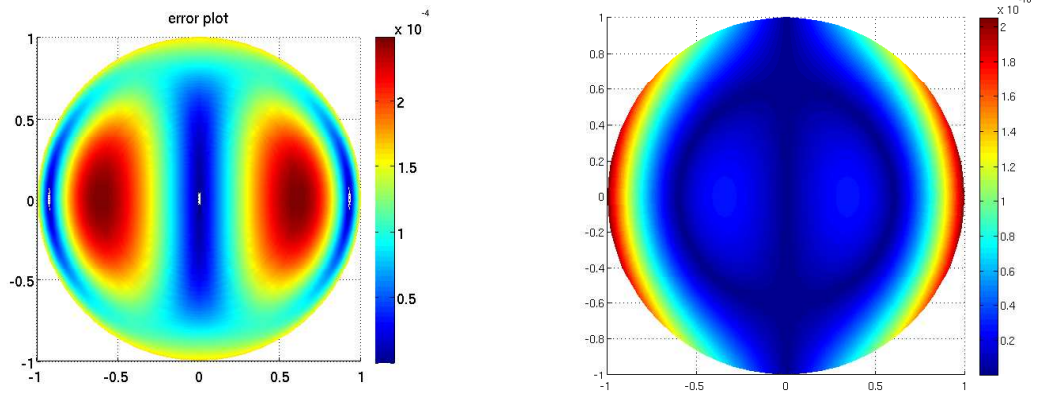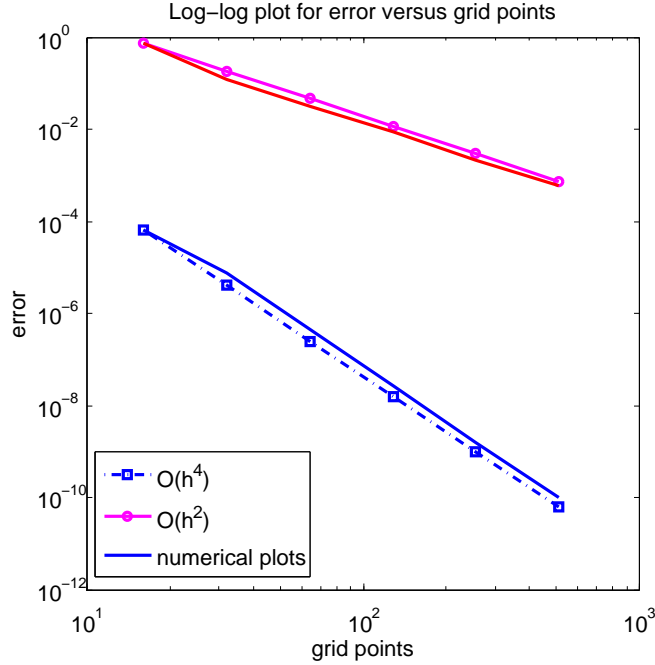
Figure 10.10: The order of accuracy using Euler-Maclaurin formula is plotted here for the direct and the double Poisson method for $f(z) = 72z\bar{z}^2 + 72z^2\bar{z}$. $\mathcal{O}(h^2)$ for direct method and $\mathcal{O}(h^4)$ convergence for double Poisson method in $||\cdot||_\infty$ norm are noted as the mesh is refined. This is a color plot in the screen.

Example 5. Next we consider the following (D4) problem

$$
\begin{aligned}
f(z) &= \frac{45}{16}z^{\frac{-1}{2}}\bar{z}^{\frac{1}{2}} + \frac{45\cdot 16}{21}z^{\frac{1}{2}}\bar{z}^{\frac{5}{2}} \\
h_0 &= \bar{z}^2 + \bar{z} \\
h_2 &= \frac{15}{2}\bar{z} + \frac{225}{4}\bar{z}^2.
\end{aligned}
$$

We test the performance of the function $f(z) = \frac{45}{16}z^{\frac{-1}{2}}\bar{z}^{\frac{1}{2}} + \frac{45\cdot 16}{21}z^{\frac{1}{2}}\bar{z}^{\frac{5}{2}}$ using direct and double Poisson method for different values of M and constant Fourier coefficient

Table 10.9: Relative error for $f(z) = \frac{45}{16}z^{-\frac{1}{2}}\bar{z}^{\frac{1}{2}} + \frac{45 \cdot 16}{21}z^{\frac{1}{2}}\bar{z}^{\frac{5}{2}}$ using Euler-Maclaurin expansion.

	Direct Method			Double Poisson Method		
M	$\|\cdot\|_\infty$	order	T_{dir}	$\|\cdot\|_\infty$	order	T_{doub}
16	6.2×10^{-2}	0	0.43	1.8×10^{-4}	0	0.22
32	1.6×10^{-2}	1.9	0.47	2.3×10^{-5}	3.0	0.25
64	4.1×10^{-3}	1.9	0.52	1.4×10^{-6}	4.0	0.28
128	1.01×10^{-3}	2.0	0.59	1.7×10^{-7}	3.0	0.33
256	2.6×10^{-4}	1.9	0.78	2.1×10^{-8}	3.0	0.49
512	6.4×10^{-5}	2.02	1.1	2.6×10^{-9}	3.0	0.71

Table 10.10: Relative error for $f(z) = \frac{45}{16}z^{-\frac{1}{2}}\bar{z}^{\frac{1}{2}} + \frac{45 \cdot 16}{21}z^{\frac{1}{2}}\bar{z}^{\frac{5}{2}}$ with Trap rule.

	Direct Method			Double Poisson Method		
M	$\|\cdot\|_\infty$	order	T_{dir}	$\|\cdot\|_\infty$	order	T_{doub}
17	2.4×10^{-1}	0	0.23	2.01×10^{-2}	0	0.12
33	1.2×10^{-1}	1.0	0.27	5.01×10^{-3}	2.0	0.14
65	5.7×10^{-2}	1.1	0.37	1.3×10^{-3}	1.9	0.17
129	2.8×10^{-2}	1.0	0.79	3.12×10^{-4}	2.1	0.23
256	1.4×10^{-2}	1.0	2.46	7.8×10^{-5}	2.0	0.32
513	7.1×10^{-3}	2.0	8.05	1.9×10^{-5}	2.0	0.48

$N = 32$. The accuracy of the computations are noted in the error Tables. 10.9, 10.10 and Fig. 10.11 respectively. Using Euler-Maclaurin formula the direct method gives a quadratic error convergence and the double Poisson method shows a third order convergence in error owing to the logarithmic singularity involved at the '0' th coefficient. In case of Trapezoidal rule, first order convergence of error in direct method is observed and second order convergence for double Poisson method is observed. The absolute error plot using Euler-Maclaurin formula is shown in Fig. 10.12. The tables also depict the CPU time taken for the computation.
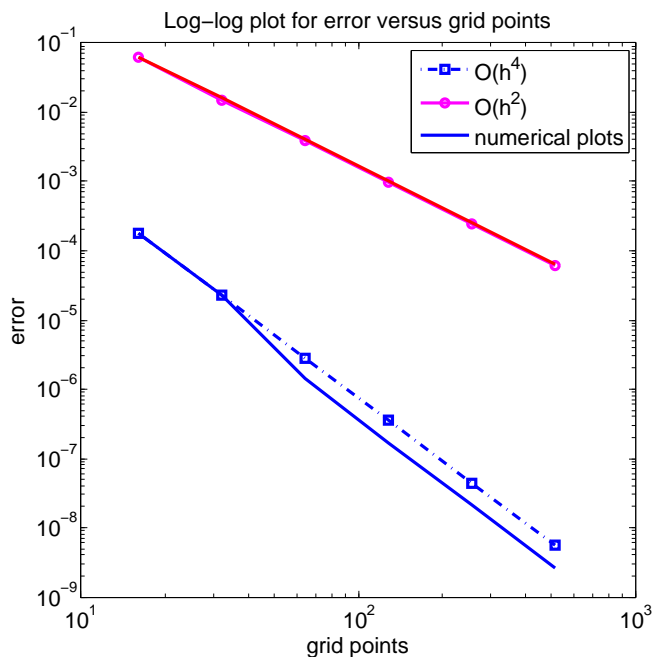
Figure 10.11: The order of accuracy is plotted here for the direct and the double Poisson method using Euler-Maclaurin formula for $f(z) = f(z) = \frac{45}{16} z^{\frac{-1}{2}} \bar{z}^{\frac{1}{2}} + \frac{45 \cdot 16}{21} z^{\frac{1}{2}} \bar{z}^{\frac{5}{2}}$. $\mathcal{O}(h^2)$ for direct method and $\mathcal{O}(h^3)$ convergence for double Poisson method in $|| \cdot ||_\infty$ norm are noted as the mesh is refined. This is a color plot in screen.

Example 6. Now we consider a (D2) problem whose solution is given by

$$
\begin{aligned}
\omega(z) &= z^3 \bar{z} \cos^2 \theta + z^{7/2} z^{5/2} \sin \theta \\
h_0 &= \left(\frac{1}{4} - i \frac{1}{2} \right) + \frac{1}{4} e^{-4i\theta} + \left(\frac{1}{2} + \frac{i}{2} \right) e^{-2i\theta} \\
h_2 &= \left(1 - \frac{9i}{2} \right) + \left(\frac{3}{2} + 4i \right) e^{-2i\theta}
\end{aligned}
$$

Relative error for different values of M and fixed $N = 64$ are shown in Table. 10.11.

The error plots for direct and double Poisson method using Euler-Maclaurin formula
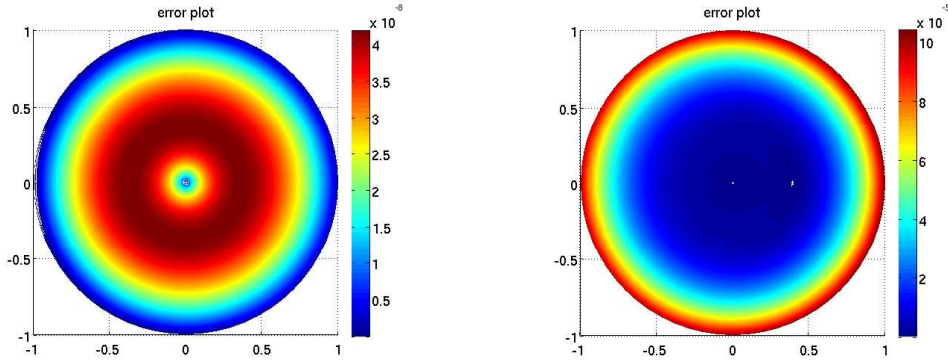
136

Figure 10.12: The graph depicts the absolute error for (D4) problem with $f(z) = \frac{45}{16}z^{\frac{-1}{2}}\bar{z}^{\frac{1}{2}} + \frac{45 \cdot 16}{21}z^{\frac{1}{2}}\bar{z}^{\frac{5}{2}}$, $N = 64, M = 512$ for the double Poisson method and the direct method respectively using Euler-Maclaurin formula. As the table suggests, the plots reflect the bounds for error in **D** at $N = 64, M = 512$. This is a color plot in screen.

are shown in Fig. 10.13. We note here a quadratic convergence in the both the methods owing to the logarithmic singularity involved in the '0'th coefficient. The order of accuracy in the $|| \cdot ||_\infty$ norm is shown in Fig. 10.14.

We now focus on (D1) and (D3) problems.

Example 7. We consider the following biharmonic problem on (D3) biharmonic problem.

$$f(z) = 72z\bar{z}^2$$
$$h_0 = \bar{z}$$
$$h_1 = 7\bar{z}$$

We test the performance of the function $f(z) = 72z\bar{z}^2$ using the direct and the double Poisson method for the (D3) biharmonic problem, the Table. 10.12 shows relative

137

Table 10.11: Relative error for $\omega(z) = z^3 \bar{z} \cos^2 \theta + z^{7/2} z^{5/2} \sin \theta$ using Euler-Maclaurin formula.

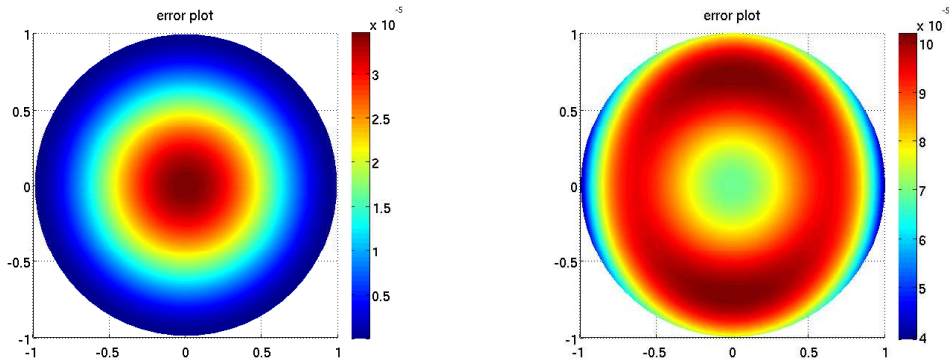| M	Direct Method			Double Poisson Method		
	$\|\|\cdot\|\|_\infty$	order	T_{dir}	$\|\|\cdot\|\|_\infty$	order	T_{doub}
16	3.5×10^{-1}	0	0.48	2.9×10^{-2}	0	0.27
32	9.5×10^{-2}	1.9	0.54	7.2×10^{-3}	2.0	0.33
64	2.4×10^{-2}	2.0	0.61	1.8×10^{-3}	2.0	0.42
128	6.1×10^{-3}	2.0	0.81	4.4×10^{-4}	2.0	0.63
256	1.5×10^{-3}	2.0	1.2	1.1×10^{-4}	2.0	1.01
512	3.7×10^{-4}	2.0	1.88	2.7×10^{-5}	2.0	1.57

Figure 10.13: The graph depicts the absolute error for (D2) problem with the solution $\omega(z) = z^3 \bar{z} \cos^2 \theta + z^{7/2} z^{5/2} \sin \theta$, $N = 64, M = 512$ in the direct and the Double Poisson method respectively using Euler-Maclaurin formula. As the table suggests, the plots reflect the bounds for error in $\mathbf{D}$ at $N = 64, M = 512$. This is a color plot in screen.
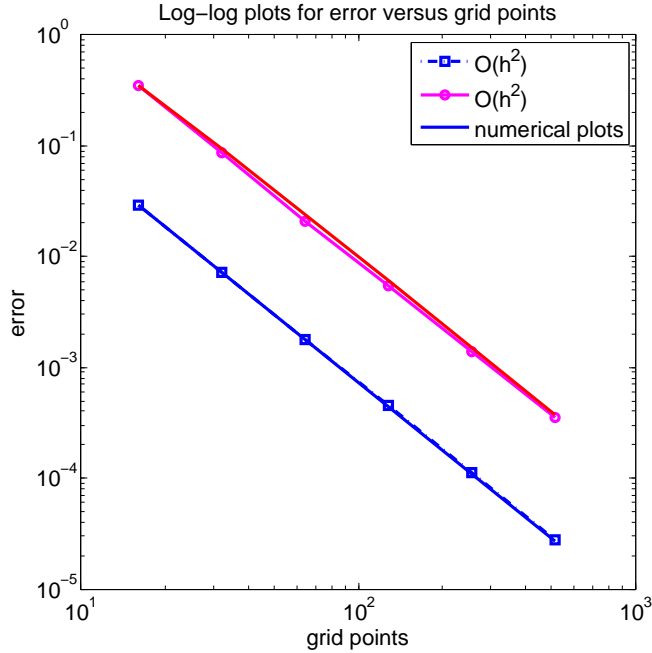
Figure 10.14: The order of accuracy is plotted here for the direct and the double Poisson method using Euler-Maclaurin formula for $\omega(z) = z^3\bar{z}\cos^2\theta + z^{7/2}z^{5/2}\sin\theta$. $\mathcal{O}(h^2)$ for direct method and $\mathcal{O}(h^2)$ convergence for double Poisson method in $||\cdot||_\infty$ norm are noted as the mesh is refined. This is a color plot in screen.

error for different values of M and $N = 64$. Using the Euler-Maclaurin formula, we notice that a second order convergence of error for the direct method and an almost fourth order convergence for the double Poisson method is shown in Fig. 10.15. The table also depicts the CPU time taken for the computation.

Several more computations of (D3) problems has been demonstrated in the steady state flow problems later.

Example 8. We now test the performance of the (D1) problem with $f(z) = 12\bar{z}+i12z$ and note the relative errors for different values of M and fixed $N = 64$ in Table. 10.13.

Table 10.12: Relative error for $f(z) = 72z\bar{z}^2$ using Euler-Maclaurin expansion.

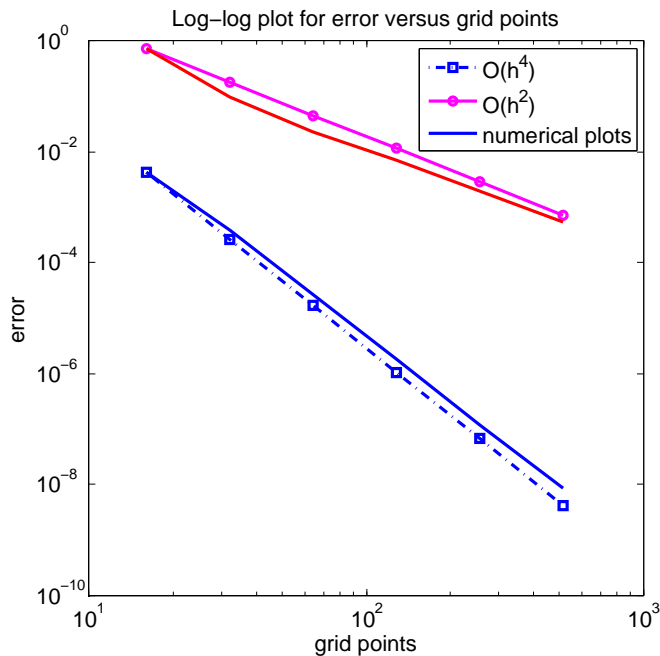| M	Direct Method			Double Poisson method		
	$\|\cdot\|_\infty$	order	T_{dir}	$\|\cdot\|_\infty$	order	T_{doub}
16	7.5×10^{-1}	0	0.50	4.3×10^{-3}	0	0.27
32	9.8×10^{-2}	2.9	0.64	3.8×10^{-4}	3.5	0.36
64	2.3×10^{-2}	2	0.85	2.6×10^{-5}	3.8	0.45
128	7.3×10^{-3}	1.7	1.27	1.8×10^{-6}	3.8	0.63
256	2.01×10^{-3}	1.9	2.19	1.3×10^{-7}	3.7	1.03
512	5.4×10^{-4}	1.9	3.83	8.4×10^{-9}	3.9	1.78

Figure 10.15: The order of accuracy is plotted here for the direct and the double Poisson method using Euler-Maclaurin formula for $f(z) = 72z\bar{z}^2$ on (D3) biharmonic problem. $\mathcal{O}(h^2)$ for direct method and $\mathcal{O}(h^4)$ convergence for double Poisson method in $\|\cdot\|_\infty$ norm are noted as the mesh is refined.

Table 10.13: Relative error for $f(z) = 12\bar{z} + i12z$ using Euler-Maclaurin formula.

	Direct Method			Double Poisson method		
M	$\|\cdot\|_\infty$	order	T_{dir}	$\|\cdot\|_\infty$	order	T_{doub}
16	3.3×10^{-2}	0	0.52	1.2×10^{-3}	0	0.31
32	6.8×10^{-3}	2.3	0.61	6.9×10^{-5}	4.1	0.38
64	3.1×10^{-3}	1.1	0.85	4.8×10^{-6}	3.9	0.52
128	9.1×10^{-4}	1.8	1.27	3.4×10^{-7}	3.8	0.81
256	2.1×10^{-4}	2.1	2.18	2.1×10^{-8}	4.0	1.36
512	5.7×10^{-5}	1.9	3.80	1.7×10^{-9}	3.6	2.60

We observe a second order convergence for Trapezoidal method and a fourth order convergence using Euler-Maclaurin for the double Poisson method. CPU timings are also shown in the Table. 10.13. The error plots for different values of M are shown in Fig. 10.16 and the order of accuracy is shown in Fig. 10.17.

$$
\begin{aligned}
f(z) &= 12z\bar{z} + i12z \\
h_0 &= z + i\bar{z} \\
h_1 &= 3 + 2iz
\end{aligned}
$$

Next we consider another example of (D1) biharmonic problem.

Example 9. We implement a (D1) biharmonic problem given by

$$
\begin{aligned}
f(z) &= \frac{45}{16} z^{\frac{-1}{2}} \bar{z}^{\frac{1}{2}} + \frac{45 \cdot 16}{21} z^{\frac{1}{2}} \bar{z}^{\frac{5}{2}} \\
h_0 &= \bar{z}^2 + z. \\
h_1 &= \frac{9}{2}\bar{z} + \frac{5}{2}.
\end{aligned}
$$

We observe the relative error in Table.10.14 for different values of M and fixed $N = 64$. We observe a second order convergence for Trapezoidal rule and an almost
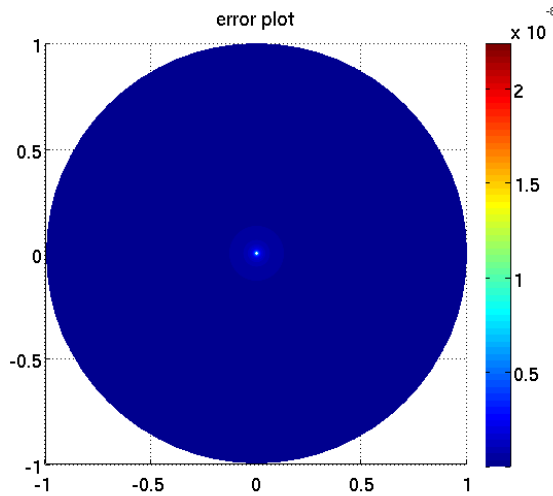
141

Figure 10.16: The graph depicts the error plot for $f(z) = 12\bar{z} + i12z$, $N = 64, M = 512$ on (D1) biharmonic problem in the double Poisson method using Euler-Maclaurin formula. As the table suggests, the plots reflect the bounds for error in $\mathbf{D}$ at $N = 64, M = 512$.

fourth order convergence for the decomposition method, both using Euler-Maclaurin formula. The error plot is shown in Fig. 10.18 and the order of accuracy is shown in Fig. 10.19.

10.1.1 Annular Domain

We now focus on problems in an annular domain $\mathbf{\Omega} = \{z \in \mathbb{R}^2 : R_1 < |z| < R_2\}$ with (D2) and (D4) biharmonic boundary value problems. We set $\mathbf{\Omega_1} =$
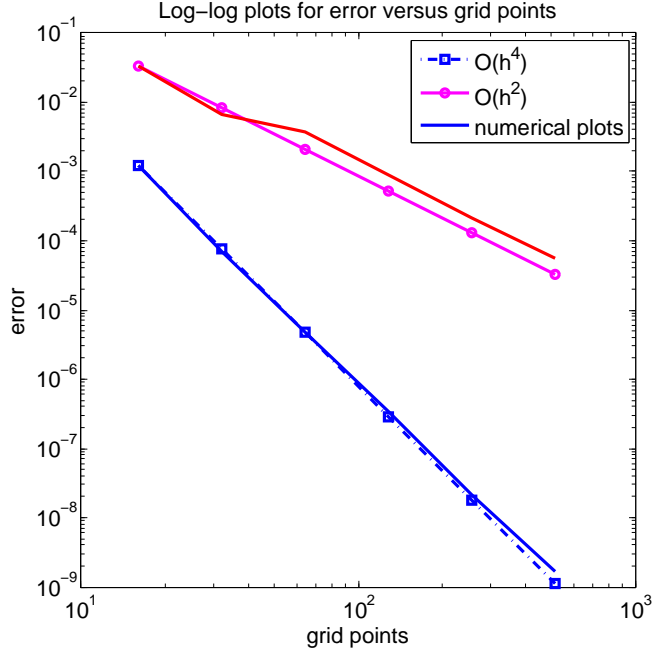
Figure 10.17: The order of accuracy is plotted here for the direct and the double Poisson method using Euler-Maclaurin formula for $f(z) = 12\bar{z} + i12z$ on (D3) biharmonic problem. $\mathcal{O}(h^2)$ for direct method and $\mathcal{O}(h^4)$ convergence for double Poisson method in $|| \cdot ||_\infty$ norm are noted as the mesh is refined.

$z \in \mathbb{R}^2 : |z| < R_1$ and $\mathbf{\Omega_2} = z \in \mathbb{R}^2 : |z| < R_2$.

Example 10. We consider the following (D2) and (D4) problem respectively in $\mathbf{\Omega}$.

$$f(z) = 12\bar{z} + i12z$$

$$\begin{cases} h_0 = (R_1)^5 e^{-i\theta} + i(R_1)^5 e^{-i\theta} & \text{on} \quad \partial\mathbf{\Omega_1} \\ h_0 = (R_2)^5 e^{-i\theta} + i(R_2)^5 e^{-i\theta} & \text{on} \quad \partial\mathbf{\Omega_2} \end{cases} \tag{D2}$$

143

Table 10.14: Relative error for $f(z) = \frac{45}{16}z^{\frac{-1}{2}}\bar{z}^{\frac{1}{2}} + \frac{45\cdot16}{21}z^{\frac{1}{2}}\bar{z}^{\frac{5}{2}}$ using Euler-Maclaurin expansion.

	Direct Method			Double Poisson Method		
M	$\|\cdot\|_\infty$	order	T_{dir}	$\|\cdot\|_\infty$	order	T_{doub}
16	2.3×10^{-2}	0	0.51	1.2×10^{-3}	0	0.29
32	6.02×10^{-3}	1.9	0.63	1.1×10^{-4}	3.4	0.34
64	1.6×10^{-3}	1.9	0.86	9.3×10^{-6}	3.6	0.47
128	4.8×10^{-4}	1.7	1.29	7.9×10^{-7}	3.6	0.64
256	1.2×10^{-4}	2.0	2.17	7.3×10^{-8}	3.4	1.05
512	3.4×10^{-5}	1.8	3.82	7.3×10^{-9}	3.3	1.81

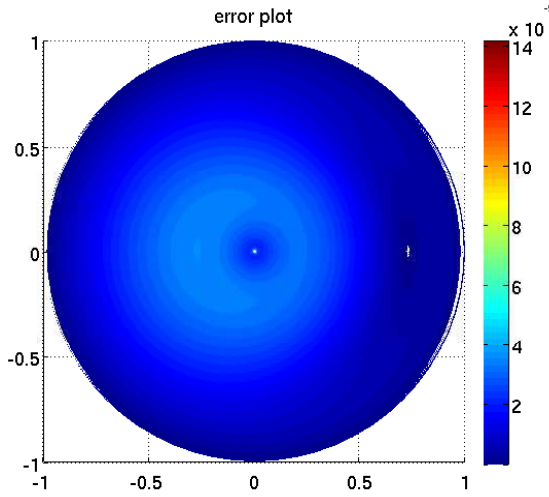

Figure 10.18: The graph depicts the error plot for $f(z) = \frac{45}{16}z^{\frac{-1}{2}}\bar{z}^{\frac{1}{2}} + \frac{45\cdot16}{21}z^{\frac{1}{2}}\bar{z}^{\frac{5}{2}}$, $N = 64, M = 512$ on (D1) biharmonic problem in the double Poisson method using Euler-Maclaurin expansion. As the table suggests, the plots reflect the bounds for error in $\mathbf{D}$ at $N = 64, M = 512$.

$$\begin{cases} h_2 & = 6(R_1)^3 e^{-i\theta} + 6i(R_1)^3 e^{-i\theta} \qquad \text{on} \quad \partial\Omega_1 \\ h_2 & = 6(R_2)^2 e^{-i\theta} + 6i(R_2)^2 e^{-i\theta} \qquad \text{on} \quad \partial\Omega_2 \end{cases} \qquad (\text{D2})$$

$$\begin{cases} h_0 & = (R_1)^5 e^{-i\theta} + i(R_1)^5 e^{-i\theta} \qquad \text{on} \quad \partial\Omega_1 \\ h_0 & = (R_2)^5 e^{-i\theta} + i(R_2)^5 e^{-i\theta} \qquad \text{on} \quad \partial\Omega_2 \end{cases} \qquad (\text{D4})$$
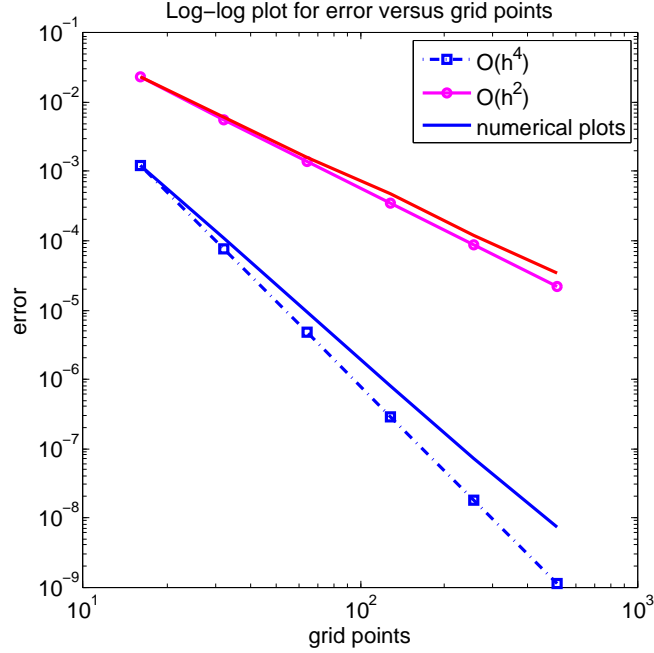
Figure 10.19: The order of accuracy is plotted here for the direct and the double Poisson method using Euler-Maclaurin formula for $f(z) = \frac{45}{16} z^{\frac{-1}{2}} \bar{z}^{\frac{1}{2}} + \frac{45 \cdot 16}{21} z^{\frac{1}{2}} \bar{z}^{\frac{5}{2}}$ on (D3) biharmonic problem. $\mathcal{O}(h^2)$ for direct method and $\mathcal{O}(h^4)$ convergence for double Poisson method in $|| \cdot ||_\infty$ norm are noted as the mesh is refined.

$$\begin{cases} h_2 & = -18(R_1)^2 e^{-i\theta} - 18i(R_1)^2 e^{-i\theta} \qquad \text{on} \quad \partial\boldsymbol{\Omega_1} \\ h_2 & = 18(R_2)^2 e^{-i\theta} + 18i(R_2)^2 e^{-i\theta} \qquad \text{on} \quad \partial\boldsymbol{\Omega_2} \end{cases} \tag{D4}$$

Taking $R_1 = 3/4, R_2 = 1$ the performance of the algorithm using the Trapezoidal rule is shown in the Tables. 10.15, 10.16. We obtain here quadratic convergence using the Trapezoidal rule and this is reflected in the Tables.10.15, 10.16. CPU timings and the order of accuracy are also observed.

145

Table 10.15: Relative error for $f(z) = 12\bar{z} + i12z$ in (D2) problem using Trapezoidal rule.

M	$\|\cdot\|_\infty$	order	T_{doub}
Relative error for $f(z) = 12\bar{z} + i12z$ in a (D2) problem.			
17	3.01×10^{-5}	0	0.18
33	7.8×10^{-6}	2.0	0.21
65	1.9×10^{-6}	2.0	0.27
129	5.01×10^{-7}	1.9	0.46
265	1.2×10^{-7}	2.1	0.74
513	3.2×10^{-8}	1.9	1.35

Table 10.16: Relative error for $f(z) = 12\bar{z} + i12z$ in (D4) problem.

M	$\|\cdot\|_\infty$	order	T_{doub}
Relative error of (D2) biharmonic problem.			
17	2.8×10^{-3}	0	0.21
33	9.37×10^{-4}	1.5	0.27
65	2.65×10^{-4}	1.8	0.38
129	7.04×10^{-5}	1.9	0.62
265	1.81×10^{-5}	1.9	1.2
513	4.6×10^{-6}	1.9	2.1

Example 11. We consider the second (D2) and (D4) problems in $\mathbf{\Omega}$.

$$f(z) \;=\; 72\bar{z}^2 z$$

$$\begin{cases} h_0 \;=\; (R_1)^7 e^{-i\theta} + (R_1)^7 e^{-i\theta} & \text{on} \quad \partial\mathbf{\Omega_1} \\ h_0 \;=\; (R_2)^7 e^{-i\theta} + (R_2)^7 e^{-i\theta} & \text{on} \quad \partial\mathbf{\Omega_2} \end{cases} \qquad \text{(D2)}$$

$$\begin{cases} h_2 \;=\; 12(R_1)^5 e^{-i\theta} + 12(R_1)^5 e^{-i\theta} & \text{on} \quad \partial\mathbf{\Omega_1} \\ h_2 \;=\; 12(R_2)^5 e^{-i\theta} + 12(R_2)^5 e^{-i\theta} & \text{on} \quad \partial\mathbf{\Omega_2} \end{cases} \qquad \text{(D2)}$$

$$\begin{cases} h_0 \;=\; (R_1)^7 e^{-i\theta} + i(R_1)^7 e^{-i\theta} & \text{on} \quad \partial\mathbf{\Omega_1} \\ h_0 \;=\; (R_2)^7 e^{-i\theta} + i(R_2)^7 e^{-i\theta} & \text{on} \quad \partial\mathbf{\Omega_2} \end{cases} \qquad \text{(D4)}$$

$$\begin{cases} h_2 \;=\; -60(R_1)^4 e^{-i\theta} - 60(R_1)^4 e^{-i\theta} & \text{on} \quad \partial\mathbf{\Omega_1} \\ h_2 \;=\; 60(R_2)^4 e^{-i\theta} + 60(R_2)^4 e^{-i\theta} & \text{on} \quad \partial\mathbf{\Omega_2} \end{cases} \qquad \text{(D4)}$$

Taking $R_1 = 3/4$, $R_2 = 1$ the performance of the algorithm using the Trapezoidal rule is shown in the following Tables. 10.17, 10.18. We obtain here quadratic convergence using the Trapezoidal rule and CPU timings for computations are observed. The actual and the numerical plots of the absolute values of the solution is shown in Fig. 10.20.

Example 12. We now consider the (D2) and (D4) problems respectively in $\mathbf{\Omega}$ with

$$f(z) \;=\; \frac{45}{16} z^{\frac{-1}{2}} \bar{z}^{\frac{1}{2}} + \frac{45 \cdot 16}{21} z^{\frac{1}{2}} \bar{z}^{\frac{5}{2}},$$

$$\begin{cases} h_0 \;=\; (R_1)^4 e^{-i\theta} + i(R_1)^7 e^{-i\theta} & \text{on} \quad \partial\mathbf{\Omega_1}, \\ h_0 \;=\; (R_2)^4 e^{-i\theta} + i(R_2)^7 e^{-i\theta} & \text{on} \quad \partial\mathbf{\Omega_2}, \end{cases} \qquad \text{(D2)}$$

147

Table 10.17: Relative error for $f(z) = 72\bar{z}^2 z$ using Trapezoidal rule on double Poisson method in a (D2) problem.

Relative error in (D2) problem with $f(z) = 72\bar{z}^2 z$.			
M	$\lVert \cdot \rVert_\infty$	order	T_{doub}
17	1.59×10^{-4}	0	0.19
33	4.13×10^{-5}	1.9	0.22
65	1.05×10^{-5}	1.9	0.28
129	2.66×10^{-6}	1.9	0.47
265	6.68×10^{-7}	1.9	0.75
513	1.67×10^{-7}	2	1.37

Table 10.18: Relative error for $f(z) = 72\bar{z}^2 z$ using Trapezoidal rule on double Poisson method for (D4) problem.

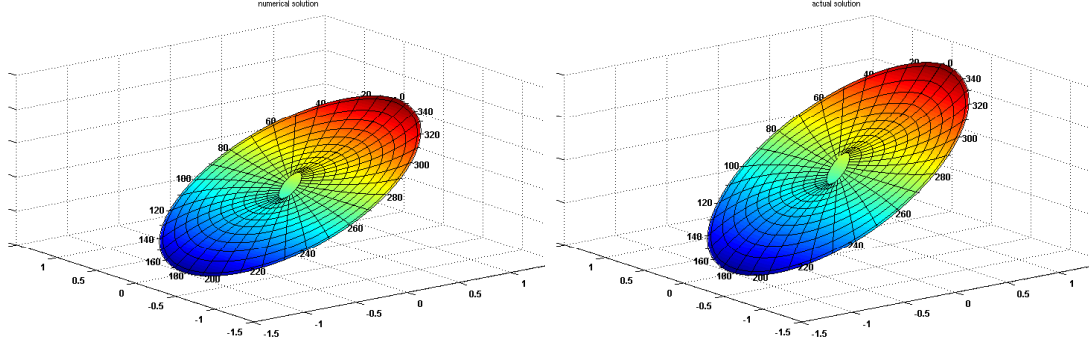| Relative error (D4) problem with $f(z) = 72\bar{z}^2 z$.			
M	$\lVert \cdot \rVert_\infty$	order	T_{doub}
17	1.59×10^{-4}	0	0.21
33	4.13×10^{-5}	1.9	0.28
65	1.05×10^{-5}	1.9	0.39
129	2.66×10^{-6}	1.9	0.61
265	6.68×10^{-7}	1.9	1.3
513	1.67×10^{-7}	1.9	2.2

Figure 10.20: The graph depicts the numerical solution and the actual solution plot respectively of $f(z) = 72\bar{z}^2 z$, $N = 64, M = 513$ for the (D2) biharmonic problem respectively using Trapezoidal expansion.

$$
\begin{cases}
h_2 & = \frac{15}{4}(R_1)^2 e^{-i\theta} + \frac{45}{4}(R_1)^5 e^{-2i\theta} \qquad \text{on} \quad \partial\mathbf{\Omega_1}, \\
h_2 & = \frac{15}{4}(R_2)^2 e^{-i\theta} + \frac{45}{4}(R_2)^5 e^{-2i\theta} \qquad \text{on} \quad \partial\mathbf{\Omega_2},
\end{cases} \tag{D2}
$$

$$
\begin{cases}
h_0 & = (R_1)^4 e^{-i\theta} + i(R_1)^7 e^{-i\theta} \qquad \text{on} \quad \partial\mathbf{\Omega_1}, \\
h_0 & = (R_2)^4 e^{-i\theta} + i(R_2)^7 e^{-i\theta} \qquad \text{on} \quad \partial\mathbf{\Omega_2},
\end{cases} \tag{D4}
$$

$$
\begin{cases}
h_2 & = -\frac{15}{2}(R_1) e^{-i\theta} - \frac{225}{4}(R_1)^4 e^{-2i\theta} \qquad \text{on} \quad \partial\mathbf{\Omega_1}, \\
h_2 & = -\frac{15}{2}(R_2) e^{-i\theta} - \frac{225}{4}(R_2)^4 e^{-2i\theta} \qquad \text{on} \quad \partial\mathbf{\Omega_2}.
\end{cases} \tag{D4}
$$

Taking $R_1 = 3/4, R_2 = 1$ the performance of the algorithm using the Trapezoidal rule is shown in the Tables. 10.19, 10.20. We obtain here quadratic convergence using the Trapezoidal rule and CPU time is observed.

149

Table 10.19: Relative error for $f(z) = \frac{45}{16}z^{\frac{-1}{2}}\bar{z}^{\frac{1}{2}} + \frac{45\cdot16}{21}z^{\frac{1}{2}}\bar{z}^{\frac{5}{2}}$ using Trapezoidal rule for double Poisson method in a (D2) problem.

Relative error using double Poisson method in a (D2) problem			
M	$\lVert \cdot \rVert_\infty$	order	T_{doub}
17	5.99×10^{-5}	0	0.18
33	1.55×10^{-5}	1.9	0.23
65	3.95×10^{-6}	1.9	0.29
129	9.99×10^{-7}	1.9	0.45
265	2.51×10^{-7}	1.9	0.74
513	6.29×10^{-8}	1.9	1.35

Table 10.20: Relative error for $f(z) = \frac{45}{16}z^{\frac{-1}{2}}\bar{z}^{\frac{1}{2}} + \frac{45\cdot16}{21}z^{\frac{1}{2}}\bar{z}^{\frac{5}{2}}$ using Trapezoidal rule for double Poisson method on (D4) problem.

double Poisson method on (D4) problem.			
M	$\lVert \cdot \rVert_\infty$	order	T_{doub}
17	1.59×10^{-4}	0	0.22
33	4.13×10^{-5}	1.9	0.28
65	1.05×10^{-5}	1.9	0.37
129	2.66×10^{-6}	1.9	0.63
265	6.68×10^{-7}	1.9	1.5
513	1.67×10^{-7}	2	2.3

10.1.2   Steady Flow

Now we consider several examples of incompressible flows at steady state with low and moderate Reynolds numbers within circular cylinder of unit radius. The main thrust of this application in this section lies in the implementation of our fast algorithms hence we have worked on flows with low and moderate Reynolds numbers. This numerical scheme is unstable for flows with higher Reynolds number. As in [33] we consider first, flows generated by rotation of part of the circumference. The Reynolds number R of the flow here is defined by the radius 'r' of the cylinder and the speed U of the rotation of the part of the circumference. This Reynolds number is then given by

$$R = \frac{Ur}{\nu} \tag{10.1}$$

where ν is the kinematic viscosity coefficient of the fluid. For studies on similar problem refer [30] and [36]. To solve this flow we make use of our fast algorithm for (D3) biharmonic problem. We consider here several examples of this type of flow see ([29], [33] , [24]).

Example 13. We first consider the following flow problem with smooth boundary data.

$$\psi_{z\bar{z}z\bar{z}} = -\frac{R}{16}J[\psi, \psi_{z\bar{z}}] \quad \text{in} \quad r < 1$$
$$\psi = 0 \quad \text{on} \quad r = 1$$
$$\frac{\partial \psi}{\partial r} = -\frac{1+\cos\theta}{2} \quad \text{on} \quad r = 1.$$

We employ the numerical methods as stated in the previous section and obtain the streamlines for different values of Reynolds number. The streamlines as shown in Fig. 10.21 with a 64×64 grid are in agreement as in [29]. Also the results were verified against the solution obtained from the solution of the (D3) biharmonic problem. The streamlines are plotted for $R = 0, 30, 64$ as shown in Fig. 10.21. This flow is

investigated for $0 \leq R \leq 64$.

Example 14. We consider another moving wall problem with the following smooth boundary condition (see [29]).

$$\psi = 0 \qquad \text{on} \quad r = 1$$
$$\frac{\partial \psi}{\partial r} = -\frac{1 + 2\cos\theta}{3} \qquad \text{on} \quad r = 1.$$

The streamlines for this flow is plotted $R = 5$ and $R = 40$ shown in Fig. 10.22. The number of iterations is respectively given by $1, 30$ with CPU time taken 31.19 for $R = 40$. The streamlines shown in Fig. 10.22 are in agreement with [29] and the results can also be verified from the solution of the (D3) biharmonic problem. The flow pattern is not symmetric about the x axis and the vortex center is shifted to the direction of the flow.

Example 15. We consider the next flow problem with the following boundary condition (see([29], [24])) and obtain the streamline patterns for different values of Reynolds number.

$$\psi_{z\bar{z}z\bar{z}} = -\frac{R}{16}J[\psi, \psi_{z\bar{z}}] \qquad \text{in} \quad r < 1$$
$$\psi = 0 \qquad \text{on} \quad r = 1$$
$$\frac{\partial \psi}{\partial r} = -\cos\theta \qquad \text{on} \quad r = 1.$$

The streamline pattern for this flow for $R = 16, 45$ are shown in Fig. 10.23 and the vorticity for Reynolds number 15 and 30 are shown respectively in Fig. 10.24. We observe here a symmetrical flow on either side of the y axis. The number of iterations is 32 for $R = 40$ and a CPU time of 19.03 were required to compute the solution. This flow is investigated for $0 \leq R \leq 45$.
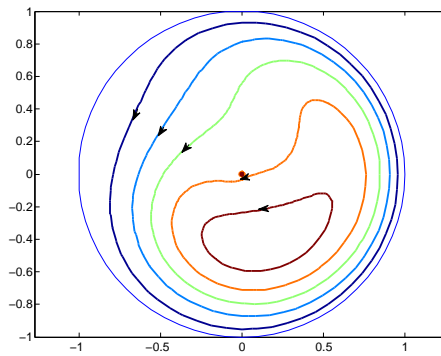
The next flow problem is given by the following boundary condition see ([29],
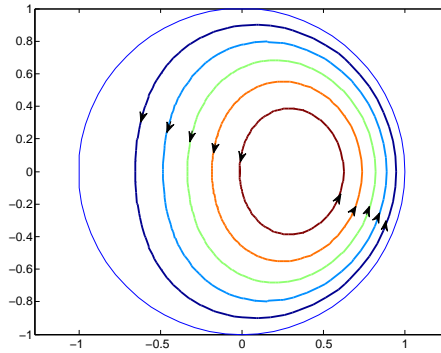
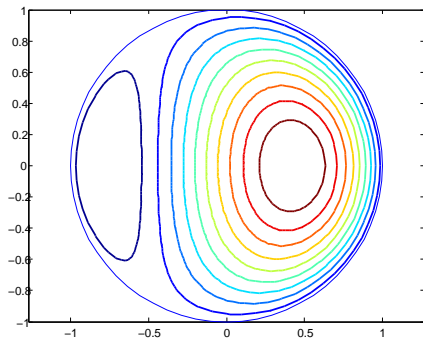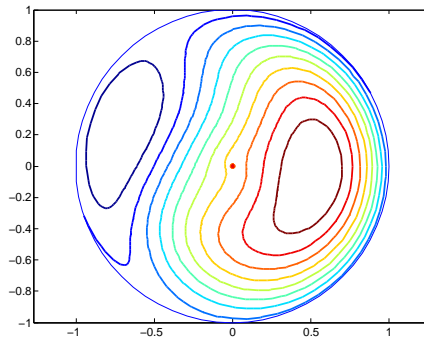(a) streamline patterns for R=0
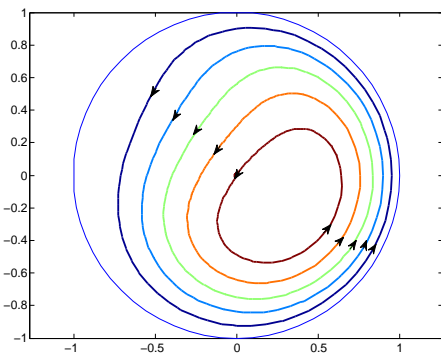
(b) streamline patterns for R=30

(c) streamline patterns for R=64

Figure 10.21: The streamline pattern computed for $\frac{\partial \psi}{\partial r} = -\frac{1+\cos\theta}{2}$, and parameter values of $N = 64, M = 64, R = 0, 30, 64$ respectively using the direct method of the algorithm in (D3) biharmonic problem.
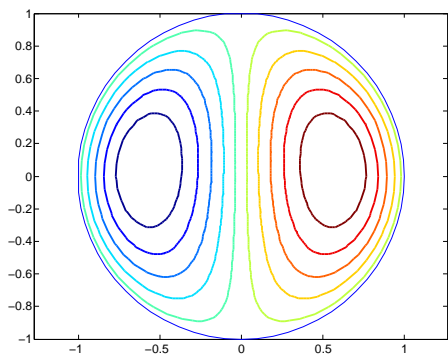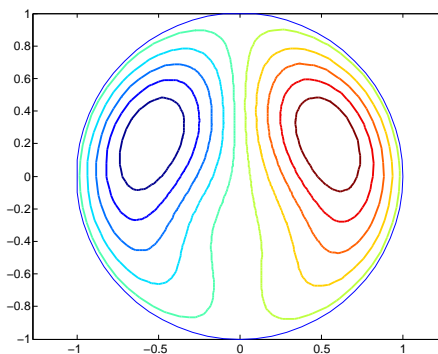
(a) streamline pattern for R=5   (b) streamline pattern for R=40

Figure 10.22: The streamline computed for $\frac{\partial \psi}{\partial r} = -\frac{1+2\cos\theta}{3}$, and parameter values of $N = 64, M = 64, R = 5(\text{left}), R = 40(\text{right})$ using the direct method of the algorithm in a (D3) problem.
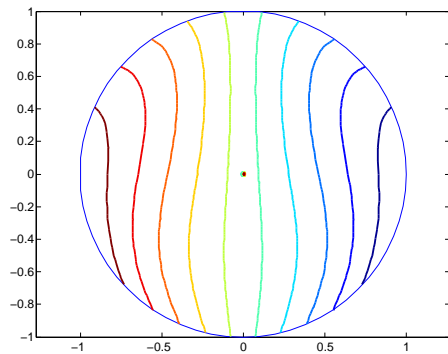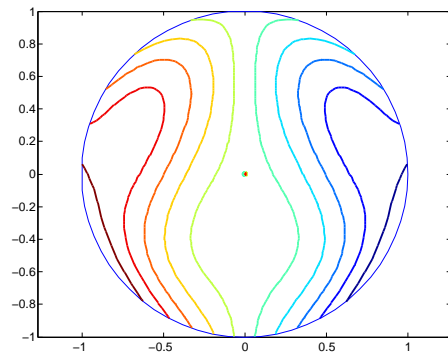

(a) streamline patterns for R=16   (b) streamline patterns for R=45

Figure 10.23: The streamlines computed for $\frac{\partial \psi}{\partial r} = -\cos\theta$, and parameter values of $N = 64, M = 64, R = 16(\text{left}), 45(\text{right})$ respectively using the direct method of the algorithm in (D3) biharmonic problem.

154

(a) vorticity patterns for R=15

(b) vorticity patterns for R=30

Figure 10.24: The vorticity pattern computed for $\frac{\partial \psi}{\partial r} = -\cos\theta$, and parameter values of $N = 64, M = 64, R = 15(\text{left}), 30(\text{right})$ respectively using the direct method of the algorithm in (D3) biharmonic problem.

[24]).

Example 16.

$$\psi = 0 \qquad \text{on} \quad r = 1$$

$$\frac{\partial \psi}{\partial r} = -\cos\theta\sin\theta \qquad \text{on} \quad r = 1.$$

We plot the streamlines and vorticity pattern for $R = 10, 80, 150.$ as in Fig. 10.25, 10.26 respectively. We see symmetrical streamlines in the four quadrants of the axes owing to the four times velocity change in the velocity in θ direction. The number of iterations taken for $R = 10, 80, 150$ are $4, 20$ and 26 respectively with the CPU time of 27.03 for $R = 150$. Sharp change in the vorticity is observed with increasing Reynolds number and the plots agree with those obtained in [24]. This flow is investigated for $0 \leq R \leq 150$.

Now we consider the moving wall problem with discontinuous boundary condition and investigate the flow for low Reynolds number.

(a) streamline patterns for R=0
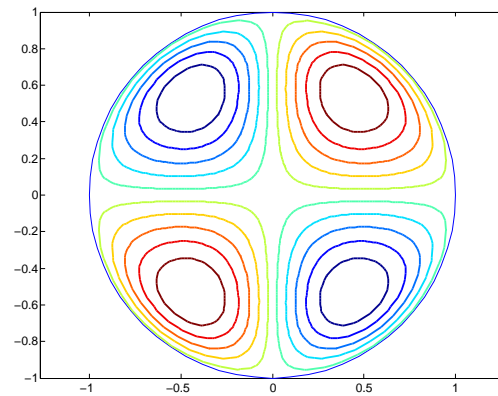
(b) streamline patterns for R=80
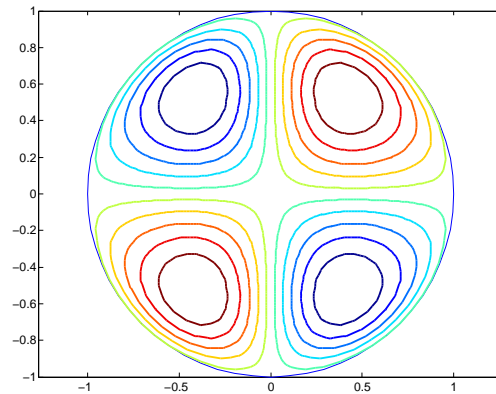
(c) streamline patterns for R=150

Figure 10.25: The streamlines computed for $\frac{\partial \psi}{\partial r} = -\cos\theta\sin\theta$, and parameter values of $N = 64, M = 64, R = 10, 80, 150$ respectively using the direct method of the algorithm in (D3) biharmonic problem.
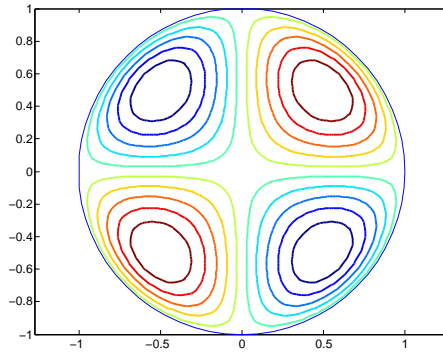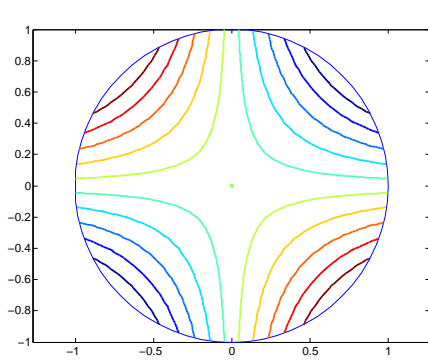
(a) vorticity patterns for R=10
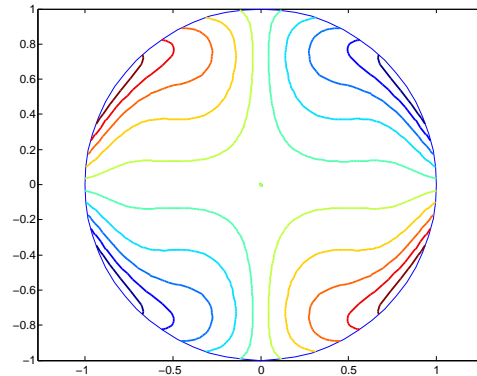
(b) vorticity patterns for R=80
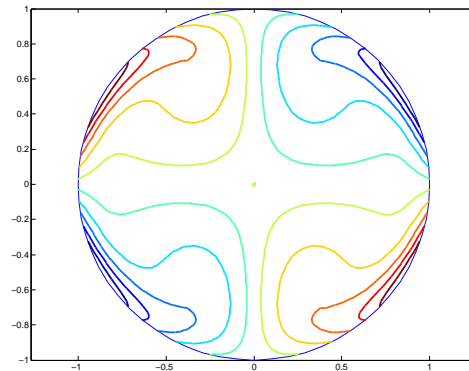
(c) vorticity patterns for R=150

Figure 10.26: The streamlines and the vorticity pattern are computed for the bondary condition $\frac{\partial \psi}{\partial r} = -\cos\theta\sin\theta$ and parameter values of $N = 64, M = 64, R = 10$ (left), 80 (right), 150 (middle) respectively using the direct method of the algorithm in (D3) biharmonic problem.

(a) streamline patterns for R=0   (b) streamline patterns for R=10

Figure 10.27: The streamlines computed for the discontinuous boundary data for parameter values of $N = 128, M = 129, R = 0(\text{left}), 10(\text{right})$ respectively using the direct method of the algorithm in (D3) biharmonic problem.

Example 17.

$$\psi = 0, \qquad r = 1$$

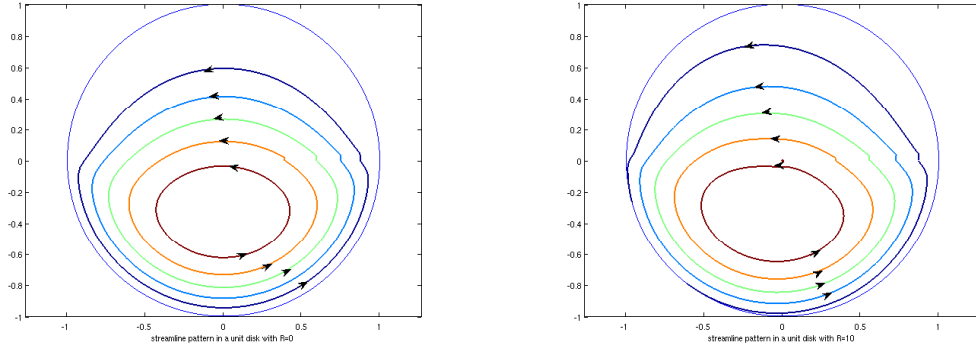$$\frac{\partial \psi}{\partial r} = \begin{cases} -1, & 0 \le \theta < \pi \\ 0, & \pi \le \theta < 2\pi \end{cases}$$

We investigate the flow for $0 \le R \le 20$ and we plot the streamlines for $R = 0, 10$ as in Fig. 10.27. We observe a non symmetric flow here and the center of the vortex is shifted to the direction of the flow. The number of iterations taken for $R = 0, 10$ are $1, 27$ with a CPU time of 96.05 The grid points were increased and we have used $M = 129, N = 128$. This problem was also studied by [33], [30] and our results are in agreement with them.

Next we investigate simple, slow, viscous outflow inflow problems [33]. We consider here the following boundary data. This problem is an example of the inflow-

158

outflow problems where ψ is specified along the boundary.

$$\frac{\partial \psi}{\partial r} = 0 \qquad 0 < \theta < 2\pi.$$

$$\psi = \begin{cases} 1 + \frac{(\theta - \alpha)}{\epsilon}, & \alpha - \epsilon < \theta < \alpha + \epsilon \\ 2, & \alpha + \epsilon < \theta < \beta - \epsilon \\ 1 + \frac{(\beta - \theta)}{\epsilon}, & \beta - \epsilon < \theta < \beta + \epsilon \\ 0, & \beta + \epsilon < \theta < 2\pi + \alpha - \epsilon. \end{cases}$$

We take $\alpha = 0, \epsilon = \frac{\pi}{32}, \beta = \pi$. The Reynolds number of the flow here is given by

$$R = \frac{U\epsilon}{\nu}.$$

where U is the speed, $U\epsilon$ the flow across the arc intercepted by ϵ. The streamline for the motions are plotted for very low Reynolds number as shown in Fig. 10.28. The number of iterations taken to compute the flow for $R = 0.02, 0.009$ are $20, 13$ with CPU time $15.3, 10.5$ respectively. This flow is studied by [20] and the results can also be verified from the exact solution of the (D3) biharmonic problem.
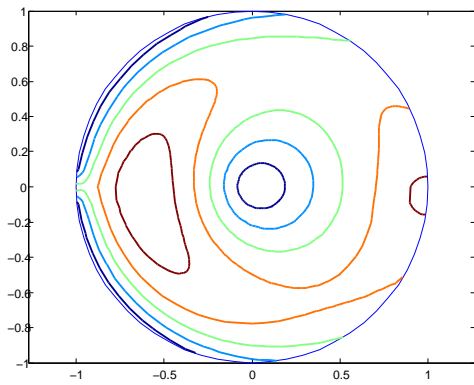
(a) streamline patterns for R=0.009
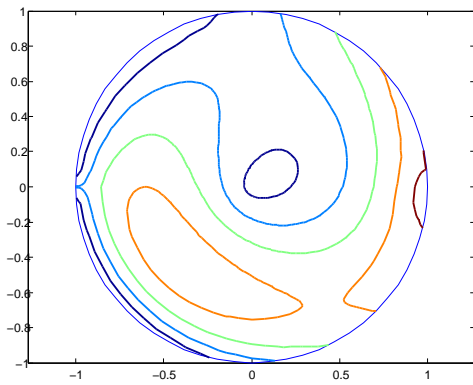
(b) streamline patterns for R=0.02

Figure 10.28: The streamlines computed for the discontinuous boundary data in the outflow inflow problem for parameter values of $N = 64, M = 65, R = 0.009, R = 0.02$ respectively using the direct method of the algorithm on (D3) problem.

11.   ERROR ESTIMATE FOR THE SINGULAR INTEGRALS

In this section, we provide an error estimate that results from the computation of the singular integrals $I_5(z)$ in step 3 of the fast algorithm of the direct method of the biharmonic problem in sec.(7.2.2).

Lemma 11.0.1. *For nonzero r and an analytic function f in $\mathbf{D}$, if each integral in step 3 of the fast algorithm in sec.(7.2.2), is computed with an error bounded by δ, then the resulting error ϵ to compute the singular integrals $(I_5^k(z), k = 1, 2, 3, 4)$ in the fast algorithm of the direct method is bounded by $\frac{4\delta(M-1)(K+4)}{K}$ where N is the total number of points in the azimuthal direction, M is the total number of points in the radial direction and $K = \frac{N}{2}$.*

We provide some notations here before going to the proof.

$$\epsilon_{1n,1}^{i,i+1} = \text{error in computing the integral} \int_{r_i}^{r_{i+1}} f_n(\rho) \left(\frac{R}{\rho}\right)^n \rho d\rho,$$

$$\epsilon_{2n,1}^{i,i+1} = \text{error in computing the integral} \int_{r_i}^{r_{i+1}} f_n(\rho) \left(\frac{\rho}{R}\right)^n \rho d\rho,$$

$$\epsilon_{20,1}^{i,i+1} = \text{error in computing the integral} \int_{r_i}^{r_{i+1}} f_0(\rho) \rho \log \rho d\rho,$$

$$\epsilon_{1n,2}^{i,i+1} = \text{error in computing the integral} \int_{r_i}^{r_{i+1}} f_n(\rho) \left(\frac{R}{\rho}\right)^n \rho^3 d\rho,$$

$$\epsilon_{2n,2}^{i,i+1} = \text{error in computing the integral} \int_{r_i}^{r_{i+1}} f_n(\rho) \left(\frac{\rho}{R}\right)^n \rho^3 d\rho,$$

$$\epsilon_{20,2}^{i,i+1} = \text{error in computing the integral} \int_{r_i}^{r_{i+1}} f_0(\rho)\rho^3 \log \rho d\rho,$$

$$\epsilon_{1n+1,3}^{i,i+1} = \text{error in computing the integral} \int_{r_i}^{r_{i+1}} f_{n-1}(\rho) \left(\frac{R}{\rho}\right)^n \rho^2 d\rho,$$

$$\epsilon_{2n+1,3}^{i,i+1} = \text{error in computing the integral} \int_{r_i}^{r_{i+1}} f_{n-1}(\rho) \left(\frac{\rho}{R}\right)^n \rho^2 d\rho,$$

$$\epsilon_{2-1,3}^{i,i+1} = \text{error in computing the integral} \int_{r_i}^{r_{i+1}} f_{-1}(\rho)\rho^2 \log \rho d\rho,$$

$$\epsilon_{1n-1,4}^{i,i+1} = \text{error in computing the integral} \int_{r_i}^{r_{i+1}} f_{n+1}(\rho) \left(\frac{R}{\rho}\right)^n \rho^2 d\rho,$$

$$\epsilon_{2n-1,4}^{i,i+1} = \text{error in computing the integral} \int_{r_i}^{r_{i+1}} f_{n+1}(\rho) \left(\frac{\rho}{R}\right)^n \rho^2 d\rho,$$

$$\epsilon_{21,4}^{i,i+1} = \text{error in computing the integral} \int_{r_i}^{r_{i+1}} f_1(\rho)\rho^2 \log \rho d\rho,$$

$$\left(A_{n,k}^{i,i+1}\right)_{app} = \text{the approximate value of} \quad A_{n,k}^{i,i+1}$$

$$\left(B_{n,k}^{i,i+1}\right)_{app} = \text{the approximate value of} \quad B_{n,k}^{i,i+1}$$

It is trivial to show the following relations from the recursive relations obtained in Section.6. For similar relation see [12].

$$p_{1n}^{(1)}(r_l) = -\sum_{i=2}^{l} \left(\frac{r_i}{r_l}\right)^n B_{n,1}^{i-1,i},$$

$$p_{2n}^{(1)}(r_l) = -\sum_{i=l}^{M-1} \left(\frac{r_l}{r_i}\right)^n A_{n,1}^{i,i+1},$$

162

$$s_{1n}^{(1)}(r_l) = \sum_{i=2}^{l} \left(\frac{r_l}{r_i}\right)^n A_{n,1}^{i-1,i},$$

$$s_{2n}^{(1)}(r_l) = \sum_{i=l}^{M-1} \left(\frac{r_i}{r_l}\right)^n B_{n,1}^{i,i+1},$$

$$t_{10}^{(1)}(r_l) = -\sum_{i=l}^{M-1} A_{0,1}^{i-1,i},$$

$$t_{20}^{(1)}(r_l) = -\sum_{i=l}^{M-1} B_{0,1}^{i,i+1},$$

$$p_{1n}^{(2)}(r_l) = -\sum_{i=2}^{l} \left(\frac{r_i}{r_l}\right)^n B_{n,2}^{i-1,i},$$

$$p_{2n}^{(2)}(r_l) = -\sum_{i=l}^{M-1} \left(\frac{r_l}{r_i}\right)^n A_{n,2}^{i,i+1},$$

$$s_{1n}^{(2)}(r_l) = \sum_{i=2}^{l} \left(\frac{r_l}{r_i}\right)^n A_{n,2}^{i-1,i},$$

$$s_{2n}^{(2)}(r_l) = \sum_{i=l}^{M-1} \left(\frac{r_i}{r_l}\right)^n B_{n,2}^{i,i+1},$$

$$t_{10}^{(2)}(r_l) = \sum_{i=l}^{M-1} A_{0,2}^{i-1,i},$$

$$t_{20}^{(2)}(r_l) = \sum_{i=l}^{M-1} B_{0,2}^{i,i+1},$$

$$p_{1n-1}^{(3)}(r_l) = \sum_{i=2}^{l} \left(\frac{r_i}{r_l}\right)^n B_{n-1,3}^{i-1,i},$$

$$p_{2n-1}^{(3)}(r_l) = \sum_{i=l}^{M-1} \left(\frac{r_l}{r_i}\right)^n A_{n-1,3}^{i,i+1},$$

$$s^{(3)}_{1n-1}(r_l) = -\sum_{i=2}^{l} \left(\frac{r_l}{r_i}\right)^n A^{i-1,i}_{n-1,3},$$

$$s^{(3)}_{2n-1}(r_l) = -\sum_{i=l}^{M-1} \left(\frac{r_i}{r_l}\right)^n B^{i,i+1}_{n-1,3},$$

$$t^{(3)}_{1-1}(r_l) = -\sum_{i=l}^{M-1} A^{i-1,i}_{-1,3},$$

$$t^{(3)}_{2-1}(r_l) = -\sum_{i=l}^{M-1} B^{i,i+1}_{-1,3},$$

$$p^{(4)}_{1n+1}(r_l) = \sum_{i=2}^{l} \left(\frac{r_i}{r_l}\right)^n B^{i-1,i}_{n+1,4},$$

$$p^{(4)}_{2n+1}(r_l) = \sum_{i=l}^{M-1} \left(\frac{r_i}{r_l}\right)^n A^{i,i+1}_{n+1,4},$$

$$s^{(4)}_{1n+1}(r_l) = -\sum_{i=2}^{l} \left(\frac{r_l}{r_i}\right)^n A^{i-1,i}_{n+1,4},$$

$$s^{(4)}_{2n+1}(r_l) = -\sum_{i=l}^{M-1} \left(\frac{r_i}{r_l}\right)^n B^{i,i+1}_{n+1,3},$$

$$t^{(4)}_{11}(r_l) = -\sum_{i=l}^{M-1} A^{i-1,i}_{1,4},$$

$$t^{4}_{21}(r_l) = -\sum_{i=l}^{M-1} B^{i,i+1}_{1,4}.$$

Now we show here, the proof for the lemma.

Proof. We consider the integral $I_5(r_l e^{\frac{2\pi i j}{N}})$ for $l \neq 1, r \neq 0, j = 1, 2....N$. Notice that for $l = M$ and $m = 1, 2, 3, 4$ we have $p^{(m)}_{2n}(r_M) = 0, s^{(m)}_{2n}(r_M) = 0, t^{(m)}_{20}(r_M) = 0$.

Thus,

$$
I_5(r_l e^{\frac{2\pi ij}{N}}) = \sum_{n=-K+1}^{K} \left(r_l^2 I_{5,n}^1(r_l) + I_{5,n}^2(r_l) + r_l I_{5,n}^3(r_l) + r_l I_{5,n}^4(r_l) \right) e^{\frac{2\pi nij}{N}}
$$

$$
= \sum_{n=-K+1}^{K} \left(r_l^2 (p_{1n}^{(1)}(r_l) + p_{2n}^{(1)}(r_l) + s_{1n}^{(1)}(r_l) + s_{2n}^{(1)}(r_l) + \log r_l t_{10}^{(1)}(r_l) \right.
$$

$$
+ t_{20}^{(1)}(r_l)) + p_{1n}^{(2)}(r_l) + p_{2n}^{(2)}(r_l) + s_{1n}^{(2)}(r_l) + s_{2n}^{(2)}(r_l) + \log r_1 t_{10}^{(2)}(r_l) + t_{20}^{(2)}(r_l)
$$

$$
+ r_l((p_{1n-1}^{(3)}(r_l) + p_{2n-1}^{(3)}(r_l) + s_{1n-1}^{(3)}(r_l) + s_{2n-1}^{(3)}(r_l) + \log r_l t_{10}^{(3)}(r_l)
$$

$$
+ t_{20}^{(3)}(r_l)) + r_l((p_{1n+1}^{(4)}(r_l) + p_{2n+1}^{(4)}(r_l) + s_{1n+1}^{(4)}(r_l) + s_{2n+1}^{(4)}(r_l)
$$

$$
\left. + \log r_l t_{10}^{(4)}(r_l) + t_{20}^{(4)}(r_l)) \right) e^{\frac{2\pi nij}{N}}
$$

$$
= \sum_{n=1}^{K} r_l^2 \left(-\sum_{i=2}^{l} \left(\frac{r_i}{r_l} \right)^n [(B_{n,1}^{i-1,i})_{app} + \frac{2}{n} \epsilon_{2n,1}^{i-1,i}]) \right) e^{\frac{2\pi nij}{N}}
$$

$$
+ \sum_{n=1}^{K} r_l^2 \left(-\sum_{i=l}^{M-1} \left(\frac{r_i}{r_l} \right)^n [(A_{n,1}^{i,i+1})_{app} + \frac{2}{n} \epsilon_{1n,1}^{i,i+1}]) \right) e^{\frac{2\pi nij}{N}}
$$

$$
+ \sum_{n=1}^{K} \left(-\sum_{i=2}^{l} \left(\frac{r_i}{r_l} \right)^n [(B_{n,2}^{i-1,i})_{app} + \frac{2}{n} \epsilon_{2n,2}^{i-1,i}] \right) e^{\frac{2\pi nij}{N}}
$$

$$
+ \sum_{n=1}^{K} \left(-\sum_{i=l}^{M-1} \left(\frac{r_l}{r_i} \right)^n [(A_{n,2}^{i,i+1})_{app} + \frac{2}{n} \epsilon_{1n,2}^{i,i+1}] \right) e^{\frac{2\pi nij}{N}}
$$

$$
+ \sum_{n=1}^{K} r_l \left(\sum_{i=2}^{l} \left(\frac{r_i}{r_l} \right)^n [(B_{n-1,3}^{i-1,i})_{app} + \frac{2}{n} \epsilon_{2n-1,3}^{i-1,i}] \right) e^{\frac{2\pi nij}{N}}
$$

$$
+ \sum_{n=1}^{K} r_l \left(\sum_{i=l}^{M-1} \left(\frac{r_l}{r_i} \right)^n [(A_{n-1,3}^{i,i+1})_{app} + \frac{2}{n} \epsilon_{2n-1,3}^{i,i+1}] \right) e^{\frac{2\pi nij}{N}}
$$

$$
+ \sum_{n=1}^{K} r_l \left(\sum_{i=2}^{l} \left(\frac{r_i}{r_l} \right)^n [(B_{n+1,4}^{i-1,i})_{app} + \frac{2}{n} \epsilon_{2n+1,4}^{i-1,i}] \right) e^{\frac{2\pi nij}{N}}
$$

$$
+ \sum_{n=1}^{K} r_l \left(\sum_{i=l}^{M-1} \left(\frac{r_l}{r_i} \right)^n [(A_{n+1,4}^{i,i+1})_{app} + \frac{2}{n} \epsilon_{2n+1,4}^{i,i+1}] \right) e^{\frac{2\pi nij}{N}}
$$

$$
+ \sum_{n=-K+1}^{-1} r_l^2 \left(\sum_{i=2}^{l} \left(\frac{r_l}{r_i} \right)^n [(A_{n,1}^{i-1,i})_{app} + \frac{2}{n} \epsilon_{1n,1}^{i-1,i}] \right) e^{\frac{2\pi nij}{N}}
$$

165

$$+ \sum_{n=-K+1}^{-1} r_l^2 \left(\sum_{i=l}^{M-1} \left(\frac{r_i}{r_l} \right)^n \left[(B_{n,1}^{i,i+1})_{app} + \frac{2}{n} \epsilon_{2n,1}^{i,i+1} \right] \right) e^{\frac{2\pi n i j}{N}}$$

$$+ \sum_{n=-K+1}^{-1} \left(\sum_{i=2}^{l} \left(\frac{r_l}{r_i} \right)^n \left[(A_{n,2}^{i-1,i})_{app} + \frac{2}{n} \epsilon_{1n,2}^{i-1,i} \right] \right) e^{\frac{2\pi n i j}{N}}$$

$$+ \sum_{n=-K+1}^{-1} \left(\sum_{i=l}^{M-1} \left(\frac{r_i}{r_l} \right)^n \left[(B_{n,2}^{i,i+1})_{app} + \frac{2}{n} \epsilon_{2n,2}^{i,i+1} \right] \right) e^{\frac{2\pi n i j}{N}}$$

$$+ \sum_{n=-K+1}^{-1} r_l \left(- \sum_{i=2}^{l} \left(\frac{r_l}{r_i} \right)^n \left[(A_{n-1,3}^{i-1,i})_{app} + \frac{2}{n} \epsilon_{1n-1,3}^{i-1,i} \right] \right) e^{\frac{2\pi n i j}{N}}$$

$$+ \sum_{n=-K+1}^{-1} r_l \left(- \sum_{i=l}^{M-1} \left(\frac{r_i}{r_l} \right)^n \left[(B_{n-1,3}^{i,i+1})_{app} + \frac{2}{n} \epsilon_{2n-1,3}^{i,i+1} \right] \right) e^{\frac{2\pi n i j}{N}}$$

$$+ \sum_{n=-K+1}^{-1} r_l \left(- \sum_{i=2}^{l} \left(\frac{r_l}{r_i} \right)^n \left[(A_{n+1,4}^{i-1,i})_{app} + \frac{2}{n} \epsilon_{1n+1,4}^{i-1,i} \right] \right) e^{\frac{2\pi n i j}{N}}$$

$$+ \sum_{n=-K+1}^{-1} r_l \left(- \sum_{i=l}^{M-1} \left(\frac{r_i}{r_l} \right)^n \left[(B_{n+1,4}^{i,i+1})_{app} + \frac{2}{n} \epsilon_{2n+1,4}^{i,i+1} \right] \right) e^{\frac{2\pi n i j}{N}}$$

$$+ \sum_{i=2}^{l} r_l^2 \log r_l \left[(A_{0,1}^{i-1,i})_{app} + \epsilon_{10,1}^{i-1,i} \right] + \sum_{i=l}^{M-1} r_l^2 \left[(B_{0,1}^{i,i+1})_{app} + \epsilon_{20,1}^{i,i+1} \right]$$

$$+ \sum_{i=2}^{l} \log r_l \left[(A_{0,2}^{i-1,i})_{app} + \epsilon_{10,2}^{i-1,i} \right] + \sum_{i=l}^{M-1} \left[(B_{0,2}^{i,i+1})_{app} + \epsilon_{20,2}^{i,i+1} \right]$$

$$- \sum_{i=2}^{l} r_l \log r_l \left[(A_{-1,3}^{i-1,i})_{app} + \epsilon_{1-1,3}^{i-1,i} \right] - \sum_{i=l}^{M-1} r_l \left[(B_{-1,3}^{i,i+1})_{app} + \epsilon_{2-1,3}^{i,i+1} \right]$$

$$- \sum_{i=2}^{l} r_l \log r_l \left[(A_{1,4}^{i-1,i})_{app} + \epsilon_{11,4}^{i-1,i} \right] - \sum_{i=l}^{M-1} r_l \left[(B_{1,4}^{i,i+1})_{app} + \epsilon_{21,4}^{i,i+1} \right].$$

$$
\begin{aligned}
Error(\epsilon) \;\leq\; & \sum_{n=1}^{K}\frac{2r_l^2}{n}\sum_{i=2}^{l}\left(\frac{r_i}{r_l}\right)^n|\epsilon_{2n,1}^{i-1,i}| + \sum_{n=1}^{K}\frac{2r_l^2}{n}\sum_{i=l}^{M-1}\left(\frac{r_l}{r_i}\right)^n|\epsilon_{1n,1}^{i,i+1}| \\
& +\sum_{n=1}^{K}\frac{2}{n}\sum_{i=2}^{l}\left(\frac{r_i}{r_l}\right)^n|\epsilon_{2n,2}^{i-1,i}| + \sum_{n=1}^{K}\frac{2}{n}\sum_{i=l}^{M-1}\left(\frac{r_l}{r_i}\right)^n|\epsilon_{1n,2}^{i,i+1}| \\
& +\sum_{n=1}^{K}\frac{2r_l}{n}\sum_{i=2}^{l}\left(\frac{r_i}{r_l}\right)^n|\epsilon_{2n-1,3}^{i-1,i}| + \sum_{n=1}^{K}\frac{2r_l}{n}\sum_{i=l}^{M-1}\left(\frac{r_l}{r_i}\right)^n|\epsilon_{1n-1,3}^{i,i+1}| \\
& +\sum_{n=1}^{K}\frac{2r_l}{n}\sum_{i=2}^{l}\left(\frac{r_i}{r_l}\right)^n|\epsilon_{2n+1,4}^{i-1,i}| + \sum_{n=1}^{K}\frac{2r_l}{n}\sum_{i=l}^{M-1}\left(\frac{r_l}{r_i}\right)^n|\epsilon_{1n+1,4}^{i,i+1}| \\
& +\sum_{n=-K+1}^{-1}\frac{2r_l^2}{n}\sum_{i=2}^{l}\left(\frac{r_l}{r_i}\right)^n|\epsilon_{1n,1}^{i-1,i}| + \sum_{n=-K+1}^{-1}\frac{2r_l^2}{n}\sum_{i=l}^{M-1}\left(\frac{r_i}{r_l}\right)^n|\epsilon_{2n,1}^{i,i+1}| \\
& +\sum_{n=-K+1}^{-1}\frac{2}{n}\sum_{i=2}^{l}\left(\frac{r_l}{r_i}\right)^n|\epsilon_{1n,2}^{i-1,i}| + \sum_{n=-K+1}^{-1}\frac{2}{n}\sum_{i=l}^{M-1}\left(\frac{r_i}{r_l}\right)^n|\epsilon_{2n,2}^{i,i+1}| \\
& +\sum_{n=-K+1}^{-1}\frac{2r_l}{n}\sum_{i=2}^{l}\left(\frac{r_l}{r_i}\right)^n|\epsilon_{1n-1,3}^{i-1,i}| + \sum_{n=-K+1}^{-1}\frac{2r_l}{n}\sum_{i=l}^{M-1}\left(\frac{r_i}{r_l}\right)^n|\epsilon_{2n-1,3}^{i,i+1}| \\
& +\sum_{n=-K+1}^{-1}\frac{2r_l}{n}\sum_{i=2}^{l}\left(\frac{r_l}{r_i}\right)^n|\epsilon_{1n+1,4}^{i-1,i}| + \sum_{n=-K+1}^{-1}\frac{2r_l}{n}\sum_{i=l}^{M-1}\left(\frac{r_i}{r_l}\right)^n|\epsilon_{2n+1,4}^{i,i+1}| \\
& +\sum_{i=2}^{l}r_l^2\log r_l|\epsilon_{10,1}^{i-1,i}| + \sum_{i=2}^{l}r_l^2|\epsilon_{20,1}^{i,i+1}| + \sum_{i=2}^{l}\log r_l|\epsilon_{10,2}^{i-1,i}| + \sum_{i=l}^{M-1}|\epsilon_{20,2}^{i,i+1}| \\
& +\sum_{i=2}^{l}r_l\log r_l|\epsilon_{1-1,3}^{i,i+1}| + \sum_{i=l}^{M-1}r_l|\epsilon_{2-1,3}^{i,i+1}| \sum_{i=2}^{l}r_l\log r_l|\epsilon_{11,4}^{i,i+1}| + \sum_{i=l}^{M-1}r_l|\epsilon_{21,4}^{i,i+1}|.
\end{aligned}
$$

We have for $2 \leq i \leq l, r_i \leq r_l$ and for $l \leq i \leq M-1, r_l \leq r_i$. If each integral is computed with an error bounded by δ where

$$
\begin{aligned}
\delta \;=\; \max_{i,n,\rho} \big\{ & |\epsilon_{10,1}^{i-1,i}|, |\epsilon_{20,1}^{i,i+1}|, |\epsilon_{2n,1}^{i-1,i}|, |\epsilon_{1n,1}^{i,i+1}|, |\epsilon_{2n,1}^{i,i+1}|, |\epsilon_{1n,1}^{i-1,i}|, |\epsilon_{10,2}^{i-1,i}|, |\epsilon_{20,1}^{i,i+1}|, \\
& |\epsilon_{2n,2}^{i-1,i}|, |\epsilon_{1n,2}^{i,i+1}|, |\epsilon_{2n,2}^{i,i+1}|, |\epsilon_{1n,2}^{i-1,i}|, |\epsilon_{1-1,3}^{i-1,i}|, |\epsilon_{2-1,3}^{i-1,i}|, |\epsilon_{2n-1,3}^{i-1,i}|, |\epsilon_{1n-1,3}^{i,i+1}|, |\epsilon_{2n-1,3}^{i,i+1}|, \\
& |\epsilon_{1n-1,3}^{i-1,i}|, |\epsilon_{11,4}^{i-1,i}|, |\epsilon_{21,4}^{i-1,i}|, |\epsilon_{2n+1,4}^{i,i+1}|, |\epsilon_{2n+1,4}^{i,i+1}|, |\epsilon_{1n+1,4}^{i-1,i}|, \big\}
\end{aligned}
$$

then

$$
\begin{aligned}
Error(\epsilon) \;\leq\; & \sum_{n=1}^{K}\frac{4\delta r_M^2}{n}(M-1)+\sum_{n=1}^{K}\frac{4\delta}{n}(M-1)\sum_{n=1}^{K}\frac{8\delta r_M}{n}(M-1)\\
& +\sum_{n=-K+1}^{-1}\frac{4\delta r_M^2}{n}(M-1)+\sum_{n=-K+1}^{-1}\frac{4\delta}{n}(M-1)\\
& +\sum_{n=-K+1}^{-1}\frac{8\delta r_M}{n}(M-1)+4\delta(M-1)\\
=\; & 4\delta(M-1)+16\delta(M-1)\left(\sum_{n=1}^{K}\frac{1}{n}-\sum_{n=1}^{K-1}\frac{1}{n}\right)\\
=\; & \frac{4\delta(M-1)(K+4)}{K}.
\end{aligned}
$$

$\square$

We note that for $l=M$,

$p_{2n}^{(1)}(r_M)=0, p_{2n}^{(2)}(r_M)=0, p_{2n-1}^{(3)}(r_M)=0, p_{2n+1}^{(4)}(r_M)=0, s_{2n}^{(1)}(r_M)=0, s_{2n}^{(2)}(r_M)=0, s_{2n-1}^{(3)}(r_M)=0, s_{2n+1}^{(4)}(r_M)=0, t_{20}^{(1)}(r_M)=0, t_{20}^{(2)}(r_M)=0, t_{21}^{(3)}(r_M)=0, t_{2-1}^{(4)}(r_M)=0.$

It can be similarly shown that for $l=M$,

$$
Error \;\leq\; \frac{8\delta(M-1)}{K}.
$$

We focus on the Trapezoidal rule and the Simpson rule to implement the error estimate in various test examples.

Note. In the case of Trapezoidal rule the error bound δ is given by

$$
\begin{aligned}
\delta \;=\; & \max_{i,n,\rho} \frac{\Delta^3 r}{12} \left\{ \frac{\partial^2}{\partial \rho^2}\left(\rho f_n(\rho)\left(\frac{r_{i+1}}{\rho}\right)^n\right), \frac{\partial^2}{\partial \rho^2}\left(\rho f_n(\rho)\left(\frac{\rho}{r_i}\right)^n\right), \right. \\
& \frac{\partial^2}{\partial \rho^2}\left(\rho \log \rho f_0(\rho)\right), \frac{\partial^2}{\partial \rho^2}\left(\rho^3 f_n(\rho)\left(\frac{r_{i+1}}{\rho}\right)^n\right), \frac{\partial^2}{\partial \rho^2}\left(\rho^3 f_n(\rho)\left(\frac{\rho}{r_i}\right)^n\right), \\
& \frac{\partial^2}{\partial \rho^2}\left(\rho^3 \log \rho f_0(\rho)\right), \frac{\partial^2}{\partial \rho^2}\left(\rho^2 f_{n-1}(\rho)\left(\frac{r_{i+1}}{\rho}\right)^n\right), \frac{\partial^2}{\partial \rho^2}\left(\rho^2 f_{n-1}(\rho)\left(\frac{\rho}{r_i}\right)^n\right), \\
& \frac{\partial^2}{\partial \rho^2}\left(\rho^3 \log \rho f_{-1}(\rho)\right), \frac{\partial^2}{\partial \rho^2}\left(\rho^2 f_{n+1}(\rho)\left(\frac{r_{i+1}}{\rho}\right)^n\right), \frac{\partial^2}{\partial \rho^2}\left(\rho^2 f_{n+1}(\rho)\left(\frac{\rho}{r_i}\right)^n\right), \\
& \left. \frac{\partial^2}{\partial \rho^2}\left(\rho^3 \log \rho f_1(\rho)\right) \right\}.
\end{aligned}
$$

The error bound δ in the case of Simpson rule is given by

$$
\begin{aligned}
\delta \;=\; & \max_{i,n,\rho} \frac{\Delta^5 r}{90} \left\{ \frac{\partial^4}{\partial \rho^4}\left(\rho f_n(\rho)\left(\frac{r_{i+1}}{\rho}\right)^n\right), \frac{\partial^4}{\partial \rho^4}\left(\rho f_n(\rho)\left(\frac{\rho}{r_i}\right)^n\right), \right. \\
& \frac{\partial^4}{\partial \rho^4}\left(\rho \log \rho f_0(\rho)\right), \frac{\partial^4}{\partial \rho^4}\partial \rho^2\left(\rho^3 f_n(\rho)\left(\frac{r_{i+1}}{\rho}\right)^n\right), \frac{\partial^4}{\partial \rho^4}\left(\rho^3 f_n(\rho)\left(\frac{\rho}{r_i}\right)^n\right), \\
& \frac{\partial^4}{\partial \rho^4}\left(\rho^3 \log \rho f_0(\rho)\right), \frac{\partial^4}{\partial \rho^4}\left(\rho^2 f_{n-1}(\rho)\left(\frac{r_{i+1}}{\rho}\right)^n\right), \frac{\partial^4}{\partial \rho^4}\left(\rho^2 f_{n-1}(\rho)\left(\frac{\rho}{r_i}\right)^n\right), \\
& \frac{\partial^4}{\partial \rho^4}\left(\rho^3 \log \rho f_{-1}(\rho)\right), \frac{\partial^4}{\partial \rho^4}\left(\rho^2 f_{n+1}(\rho)\left(\frac{r_{i+1}}{\rho}\right)^n\right), \frac{\partial^4}{\partial \rho^4}\left(\rho^2 f_{n+1}(\rho)\left(\frac{\rho}{r_i}\right)^n\right), \\
& \left. \frac{\partial^4}{\partial \rho^4}\left(\rho^3 \log \rho f_1(\rho)\right) \right\}.
\end{aligned}
$$

11.1 Examples

Several problems are tested to determine the bounds of M, the number of circles required to obtain a desired accuracy. We here consider the error estimates for the following functions.

Problem 1. We consider the function $f(z) = 12\bar{z}$. Here

$$f_n(\rho) = \begin{cases} 12\rho & \text{if } n = -1 \\ 0 & \text{if } n \neq -1. \end{cases}$$

For Trapezoidal rule the error bound δ is

$$\begin{aligned}
\delta &= \max_{i,n,\rho} \frac{\Delta^3 r}{12} \left\{ \frac{\partial^2}{\partial \rho^2} \left(\frac{12\rho^3}{r_{i+1}} \right), \frac{\partial^2}{\partial \rho^2} \left(12 r_i \rho \right), \frac{\partial^2}{\partial \rho^2} \left(\frac{12\rho^5}{r_{i+1}} \right), \frac{\partial^2}{\partial \rho^2} \left(12 r_i \rho^2 \right), \right. \\
&\qquad \left. \frac{\partial^2}{\partial \rho^2} \left(12 \rho^3 \right), \frac{\partial^2}{\partial \rho^2} \left(12 \rho^4 \log \rho \right), \frac{\partial^2}{\partial \rho^2} \left(\frac{12\rho^5}{r_{i+1}^2} \right), \frac{\partial^2}{\partial \rho^2} \left(12 r_i^2 \rho \right), \right\} \\
&= 20 \Delta^3 r.
\end{aligned}$$

Now if the error $(\epsilon) = .001$ and K is given we see from our analysis that

$$(M - 1) \geq \frac{\epsilon K}{80 \Delta^3 r (K + 4)}.$$

Hence we obtain the following which agrees with our computation result in Fig.11.1. We notice that the dominant parameter is the number of circles M and the variation in the estimate occurs when we increase the number of circles and it improves the accuracy of the integration

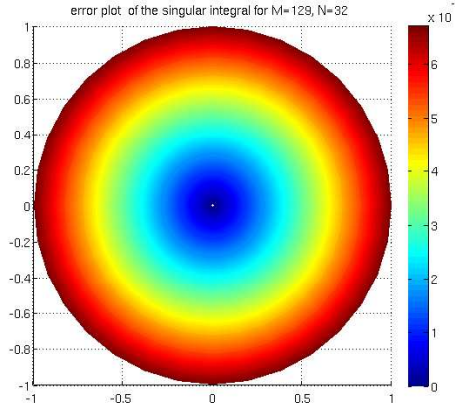$$\begin{aligned}
M &\leq 317 \quad \text{for N=32} \\
M &\leq 301 \quad \text{for N=64} \\
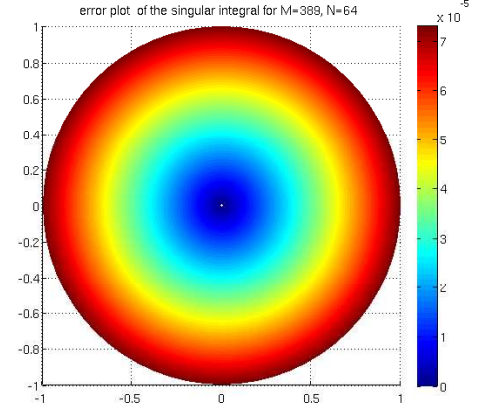M &\leq 293 \quad \text{for N=128} \\
M &\leq 288 \quad \text{for N=256}
\end{aligned}$$

For error $(\epsilon) = .0001$ and K given we see

$$M \leq 397 \quad \text{for N=64}$$

(a) error plot of singular integrals   (b) error plot of singular integrals

Figure 11.1: The graph depicts the error plot of the singular integrals for $f = 12\bar{z}$, with parameters $N = 32, 64, M = 129, 389$ respectively using the trapezoidal rule.

The error bound δ in the case of Simpson rule is given by

$$
\begin{aligned}
\delta &= \max_{i,n,\rho} \frac{\Delta^5 r}{90} \left\{ \frac{\partial^4}{\partial \rho^4} \left(\left(\frac{12\rho^5}{r_{i+1}} \right)^n \right) \frac{\partial^4}{\partial \rho^4} \left(12\rho^4 \log \rho \right) \right\} \\
&= 16\Delta^5 r.
\end{aligned}
$$

Now using the estimate we obtain the following bounds for M which agrees with the computation in Fig.11.2

$$
\begin{aligned}
(M - 1) &\geq \frac{\epsilon K}{4\Delta^5 r (K + 4)} \\
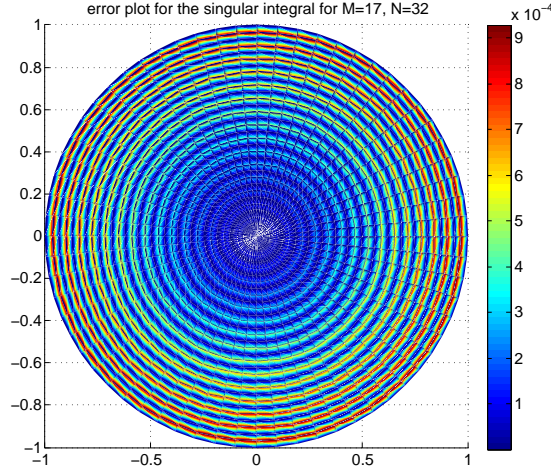\Rightarrow M &\leq 17 \quad \text{for} \quad K = 16.
\end{aligned}
$$

171

Figure 11.2: The graph depicts the error plot of the singular integrals for $f = 12\bar{z}$, with parameters $N = 32, M = 17$ using Simpson rule.

Problem 2. We next consider the function $f(z) = z^2\bar{z}$. The error bound for δ in the case of trapezoidal rule is given by

$$
\begin{aligned}
\delta \;\leq\; & \max_{i,n,\rho} \frac{\Delta^3 r}{12} \left\{ \frac{\partial^2}{\partial\rho^2}\left(\frac{\rho^4 r_i}{\rho}\right), \frac{\partial^2}{\partial\rho^2}\left(\frac{\rho}{r_{i+1}}\rho^4\right), \frac{\partial^2}{\partial\rho^2}\left(\frac{\rho^7}{r_{i+1}}\right), \frac{\partial^2}{\partial\rho^2}\left(r_i\rho^5\right), \right. \\
& \left. \frac{\partial^2}{\partial\rho^2}\left(\rho^5\right), \frac{\partial^2}{\partial\rho^2}\left(\frac{\rho^7}{r_{i+1}^2}\right), \frac{\partial^2}{\partial\rho^2}\left(\frac{\rho^7}{r_{i+1}}\right), \frac{\partial^2}{\partial\rho^2}\left(r_i^2\rho^3\right), \right\} \\
\leq\; & \frac{42}{12}\Delta^3 r.
\end{aligned}
$$

Now if the error $(\epsilon) = .0001$ and K is given we see from our analysis that

$$
\begin{aligned}
(M-1) \;\geq\; & \frac{12\epsilon K}{42\Delta^3 r(K+4)} \\
\Rightarrow M \;\leq\; & 397 \quad \text{for} \quad K = 32.
\end{aligned}
$$

172

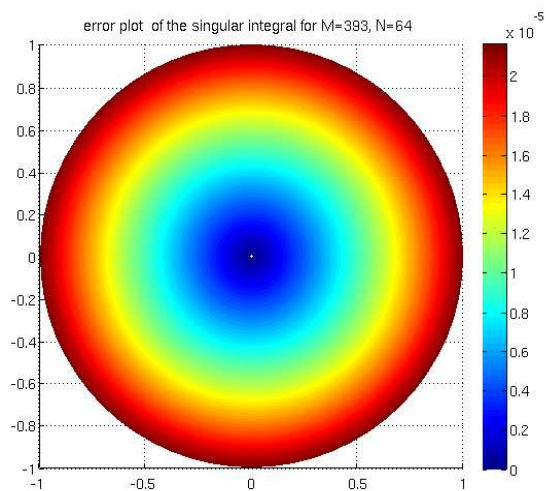It is in agreement with our computation result in Fig.11.3.

Figure 11.3: The graph depicts the error plot of the singular integrals for $f = z^2 \bar{z}$, $N = 32, M = 393$ using Trapezoidal rule.

12. CONCLUSION AND FUTURE WORK

We have developed several FFT and recursive-relation-based accurate and fast algorithms for the Poisson and biharmonic problems in a unit disc in the complex plane using the direct method and the double Poisson method. We performed numerical implementation and application of the fast methods on several test problems. The direct method when compared with the double Poisson method give better accuracy for the homogeneous problems. However for nonhomogeneous problems, the double Poisson method achieved better accuracy when compared to the direct method. The loss of order of accuracy in the direct method seems to come from the discretization near the origin in the four singular integrals when compared with the two singular integrals in the double Poisson method. This problem can be overcome and we are working on it. Both the methods have asymptotic computational complexity of the order $\mathcal{O}(\log \mathcal{N})$ per degree of freedom.

These algorithms also serve as important tools to solve steady, incompressible flow problems with low to moderate Reynolds number within circular cylinders. However our future plan is to use these fast algorithms for flows with high Reynolds number. Future work includes development of fast algorithms for the variable coefficient diffusion equation and investigate non-homogeneous Poisson problem with singularity imposed on the source term.

REFERENCES

[1] Z. AbdulHadi, Y. Abu Muhanna, and S. Khuri. On some properties of solutions of the biharmonic equation. *Appl. Math. Comput.*, 177(1):346–351, 2006.

[2] H. Begehr. Boundary value problems for the complex Poisson equation. In *AMADE: Analytic methods of analysis and differential equations, 2006, edited by A. A. Kilbas and S. V. Rogosin*, pages 9–26. Camb. Sci. Publ., Cambridge, U.K, 2008.

[3] H. Begehr and T. Vaitekhovich. Iterated Dirichlet problem for the higher order Poisson equation. *Matematiche (Catania)*, 63(1):139–154, 2008.

[4] Heinrich Begehr. Boundary value problems in complex analysis. II. *Bol. Asoc. Mat. Venez.*, 12(2):217–250, 2005.

[5] Heinrich Begehr. Boundary value problems in complex analysis. II. *Bol. Asoc. Mat. Venez.*, 12(2):217–250, 2005.

[6] Heinrich Begehr. Dirichlet problems for the biharmonic equation. *Gen. Math.*, 13(2):65–72, 2005.

[7] Heinrich Begehr. Biharmonic Green functions. *Matematiche (Catania)*, 61(2):395–409 (2007), 2006.

[8] Heinrich Begehr. Six biharmonic Dirichlet problems in complex analysis. In *Function spaces in complex and Clifford analysis, edited by Le Hung Son and Wolfgang Tutschke*, pages 243–252. Natl. Univ. Publ. Hanoi, Hanoi, 2008.

[9] Heinrich Begehr. Iterated polyharmonic Green functions for plane domains. *Acta Math. Vietnam.*, 36(2):169–181, 2011.

[10] Leonardo Borges and Prabir Daripa. A parallel version of a fast algorithm for singular integral transforms. *Numer. Algorithms*, 23(1):71–96, 2000.

[11] Leonardo Borges and Prabir Daripa. A parallel version of a fast algorithm for singular integral transforms. *Numer. Algorithms*, 23(1):71–96, 2000.

[12] Leonardo Borges and Prabir Daripa. A fast parallel algorithm for the Poisson equation on a disk. *J. Comput. Phys.*, 169(1):151–192, 2001.

[13] D. Braess and P. Peisker. On the numerical solution of the biharmonic equation and the role of squaring matrices for preconditioning. *IMA J. Numer. Anal.*, 6(4):393–404, 1986.

[14] Xiao-liang Cheng, Weimin Han, and Hong-ci Huang. Some mixed finite element methods for biharmonic equation. *J. Comput. Appl. Math.*, 126(1-2):91–109, 2000.

[15] Prabir Daripa. A fast algorithm to solve nonhomogeneous Cauchy-Riemann equations in the complex plane. *SIAM J. Sci. Statist. Comput.*, 13(6):1418–1432, 1992.

[16] Prabir Daripa. A fast algorithm to solve the Beltrami equation with applications to quasiconformal mappings. *J. Comput. Phys.*, 106(2):355–365, 1993.

[17] Prabir Daripa. A brief review of some application driven fast algorithms for elliptic partial differential equations. *Cent. Eur. J. Math.*, 10(1):204–216, 2012.

[18] Prabir Daripa and Daoud Mashat. Singular integral transforms and fast numerical algorithms. *Numer. Algorithms*, 18(2):133–157, 1998.

[19] Ranjan K. Dash and Prabir Daripa. Analytical and numerical studies of a singularly perturbed Boussinesq equation. *Appl. Math. Comput.*, 126(1):1–30, 2002.

[20] S. C.R. Dennis. Numerical methods in fluid dynamics. *In Proc. 4th Int. Conf. on Numerical Methods in Fluid Dyn.*, 4(0):138–143, 1974.

[21] P. Farkas. Mathematical foundation for fast algorithms for the biharmonic equation. *Thesis.*, 1(1):1–72, 1989.

[22] Anne Greenbaum, Leslie Greengard, and Anita Mayo. On the numerical solution of the biharmonic equation in the plane. *Phys. D*, 60(1-4):216–225, 1992. Experimental mathematics: computational issues in nonlinear science (Los Alamos, NM, 1991).

[23] Michael D. Greenberg. *Application of Green's functions in science and engineering.* Prentice-Hall, Berlin, 1971. Green's function.

[24] Leslie Greengard and Mary Catherine Kropinski. An integral equation approach to the incompressible Navier-Stokes equations in two dimensions. *SIAM J. Sci. Comput.*, 20(1):318–336, 1998.

[25] Leslie Greengard, Mary Catherine Kropinski, and Anita Mayo. Integral equation methods for Stokes flow and isotropic elasticity in the plane. *J. Comput. Phys.*, 125(2):403–414, 1996.

[26] Weizhang. Huang and Tang Tao. Steady motion of a viscous fluid inside a circular boundary. *J. Numer. Methods Fluids.*, 0(0):submitted, 1995.

[27] Sharad Kapur and Vladimir Rokhlin. High-order corrected trapezoidal quadrature rules for singular functions. *SIAM J. Numer. Anal.*, 34(4):1331–1356, 1997.

[28] M. C. A. Kropinski. Integral equation methods for particle simulations in creeping flows. *Comput. Math. Appl.*, 38(5-6):67–87, 1999.

[29] K. Kuwahara and I.Imai. Steady viscous flow within a circular boundary. *Phys. Fluids.*, 12(2):94–101, 1969.

[30] D.G. Mabey. Fluid dynamics. *J.Roy. Aero.Soc*, 61(2):181–198, 1957.

[31] Anita Mayo. The rapid evaluation of volume integrals of potential theory on general regions. *J. Comput. Phys.*, 100(2):236–245, 1992.

[32] S.G. Mikhlin. Integral equations. *Peragmon Press.*, 1(1):1–300, 1957.

[33] R.D. Mills. Computing internal viscous flow problems for the circle by integral methods. *J. Fluid Mech.*, 79(3):609–624, 1977.

[34] Peter Monk. A mixed finite element method for the biharmonic equation. *SIAM J. Numer. Anal.*, 24(4):737–749, 1987.

[35] P. Peisker. On the numerical solution of the first biharmonic equation. *RAIRO Modél. Math. Anal. Numér.*, 22(4):655–676, 1988.

[36] Lord. Rayleigh. Fluid dynamics. *Phil.Mag*, 5(5):354–363, 1893.

[37] V. Rokhlin. End-point corrected trapezoidal quadrature rules for singular functions. *Comput. Math. Appl.*, 20(7):51–62, 1990.

[38] A. P. S. Selvadurai. *Partial differential equations in mechanics. 2.* Springer-Verlag, Berlin, 2000. The biharmonic equation, Poisson's equation.

[39] Avram Sidi and Moshe Israeli. Quadrature methods for periodic singular and weakly singular Fredholm integral equations. *J. Sci. Comput.*, 3(2):201–231, 1988.